NASA Contractor Report 182298

Time-Dependent Computational Studies of Flames in Microgravity

Elaine S. Oran and K. Kailasanath
Naval Research Laboratory
Washington, D.C.

June 1989

Prepared for
Lewis Research Center
Under Purchase Order C-80001-G

National Aeronautics and
Space Administration

CONTENTS

ABSTRACT

This report describes the research performed at the Center for Reactive Flow and Dynamical Systems in the Laboratory for Computational Physics and Fluid Dynamics, at the Naval Research Laboratory, in support of the NASA Microgravity Science and Applications Program. The primary focus of this research was on investigating fundamental questions concerning the propagation and extinction of premixed flames in earth gravity and in microgravity environments.

Our approach was to use detailed time-dependent, multispecies, numerical models as tools to simulate flames in different gravity environments. The models include a detailed chemical kinetics mechanism consisting of elementary reactions among the eight reactive species involved in hydrogen combustion, coupled to algorithms for convection, thermal conduction, viscosity, molecular and thermal diffusion, and external forces. The external force, gravity, can be put in any direction relative to flame propagation and can have a range of values.

A combination of one-dimensional and two-dimensional simulations has been used to investigate the effects of curvature and dilution on ignition and propagation of flames, to help resolve fundamental questions on the existence of flammability limits when there are no external losses or buoyancy forces in the system, to understand the mechanism leading to cellular instability, and to study the effects of gravity on the transition to cellular structure. These studies have shown that a flame in a microgravity environment can be extinguished without external losses and that the mechanism leading to cellular structure is not preferential diffusion but a thermo-diffusive instability. The simulations have also lead to a better understanding of the interactions between buoyancy forces and the processes leading to thermo-diffusive instability. When a flame which exhibits a cellular structure in a zero-gravity environment is subjected to earth gravity, it evolves into either a bubble rising upwards in a tube or a flame oscillating between convex and concave curvatures in the case of downward propagation. The effect of gravity is minimal on flames in mixtures which are far from flammability limits.

INTRODUCTION

In this report we describe the research performed at the Naval Research Laboratory in support of the NASA Microgravity Science and Applications Program over the period December 1985—December 1988. This work has been performed at the Center for Reactive Flow and Dynamical Systems in the Naval Research Laboratory by Drs. Gopal Patnaik, K. Kailasanath and Elaine Oran.The emphasis of our research has been on investigating fundamental combustion questions concerning the propagation and extinction of gas-phase flames in microgravity and earth-gravity environments. Our approach to resolving these fundamental questions has been to use detailed time-dependent, multispecies numerical models to perform carefully designed computational experiments. The basic questions we have addressed, a general description of the numerical approach, and a summary of the results are described in this introduction. More detailed discussions are presented in the next two sections and in the appendices to this report.

It is well known from flammability studies in normal earth gravity that a flame propagating upward in a tube propagates in a wider range of mixture stoichiometries and dilutions than a flame propagating downward. This means that the apparent flammability limits of upward-propagating flames are broader than those of downward-propagating flames. Various explanations for this phenomena are based on factors such as buoyancy forces, preferential diffusion, flame chemistry, conductive and radiative heat losses, the aerodynamics of burnt gases, and flame stretch [1-6] . One certainty is that gravitational acceleration (buoyancy) is very important and may also be interacting with and influencing other physical processes. Furthermore, the microgravity experiments in the NASA drop tower [7] and Lear-jets [8] have shown that instabilities often occur in the propagation of flames near the flammability limits.

A systematic study which isolates the various processes that could lead to flame extinction is needed to gain a better understanding of flammability limits in general and more specifically, the role of gravity on flame propagation and extinction. Numerical simulations, in which the various physical and chemical processes can be independently controlled, can significantly advance our understanding of flame instabilities in a microgravity environment and flammability limits on earth and in a microgravity environment. In the past three years, we have addressed a number of basic questions aimed at resolving some of the important aspects of flame structure and propagation.

There are still many questions left unanswered and, as such, this final report is also a progress report on a continuing investigation.

The basic questions we have adddressed are: the effects of curvature and dilution on ignition and propagation of flames, the existence of flammability limits in the absence of external losses or buoyancy forces in the system, the mechanisms leading to cellular instability, and the effects of gravity on flame instabilities. These studies have shown that a flame in a microgravity environment can be extinguished without external losses and that the mechanism leading to cellular structure is not preferential diffusion but is a thermo-diffusive instability. Furthermore, the simulations have also lead to a better understanding of the interactions between gravity induced flame dynamics and the intrinsic processes involved in flame propagation. When a flame which exhibits a cellular structure in a zero-gravity environment is subjected to earth gravity, it evolves into either a bubble rising upwards in a tube or a flame oscillating between convex and concave curvatures in the case of downward propagation. The simulations have also shown that the effect of gravity is minimal on flames in mixtures which are far from flammability limits.

In the research described here, we have used both one-dimensional and two-dimensional numerical simulations to systematically isolate and evaluate the importance of various processes that might be controlling the dynamics of flames, particularly near the flammability limits, and to evaluate the relative importance of these processes in normal gravity and microgravity. Both the numerical models are time-dependent and solve the multispecies coupled partial differential reactive-flow equations. These models include a detailed chemical kinetics mechanism coupled to algorithms for convection, thermal conduction, viscosity, molecular diffusion, thermal diffusion, and external forces. The external force, gravity, can be in any direction relative to flame propagation and can have a range of values. Energy sources and sinks may also be prescribed as a function of time. The one-dimensional model was developed before this NASA project began, but the two-dimensional model was developed during the past two years. The development of the two-dimensional model was supported primarily by ONR/NRL funding, and it has been applied to study the evolution of multidimensional flame structure in support of the NASA Microgravity Science and Applications Program. The models are described in greater detail in the next section.

COMPUTATIONAL TOOLS

Two computational models developed at NRL, FLIC2D and FLAME1D, have been used to study the propagation and extinction of premixed gaseous flames. FLIC2D has been used to study the tendency of hydrogen-air mixtures to show cellular instability [9] and more recently to model diffusion flames [10]. Many submodels in FLIC2D are based on FLAME1D, a one-dimensional, time-dependent Lagrangian model which has been tested extensively and applied to various studies of flame phenomena including calculations of burning velocities [11,12], minimum ignition energies and quenching distances [12,13], effects of curvature and dilution [14], and flammability limits [15]. For completeness, both models are described below.

FLAME1D

This is a time-dependent model [12] which solves the compressible, conservation equations for mass, momentum and energy [16,17] in one spatial dimension. Since it was developed specifically to study the initiation, propagation, and quenching of laminar flames, it consists of algorithms for modelling convection, detailed chemical kinetics and energy release, thermal conduction, molecular and thermal diffusion of the individual species, and various energy deposition mechanisms. The model has a modular form and the algorithms representing the various chemical and physical processes are combined using an asymptotic timestep-split approach in which the individual processes are integrated separately and then coupled together [17,18]. The model also permits a variety of initial and boundary conditions.

The convective transport terms in the equations are solved by the algorithm ADINC, a Lagrangian convection algorithm which solves implicitly for the pressures [19]. Since ADINC communicates compression and expansion across the system implicitly, it overcomes the Courant time-step limit. Since it is Lagrangian, it can maintain steep gradients computationally without numerical diffusion for a long period of time. This is important in flame calculations where the diffusive transport of material and energy can govern the system evolution and therefore must be calculated accurately. An adaptive regridding algorithm has been developed to add and delete computational cells. For the flame calculation, cells are added in the region ahead of the flame so that the front always propagates into a finely zoned region. Cells are removed behind the flame where the gradients are very shallow.

The chemical interactions are described by a set of nonlinear coupled ordinary differential equations. This set of equations may be stiff when there are large differences in the time constants associated with different chemical reactions, and are invariably stiff for combustion problems. These equations are solved using VSAIM, a fully vectorized version of the selected asymptotic integration method CHEMEQ [20,21]. In VSAIM, the stiff equations are identified and solved using a very stable asymptotic method while the remaining equations are solved using a standard classical method.

The diffusive transport processes considered in this model are molecular diffusion, thermal conduction and thermal diffusion. These processes are crucial to the description of flame phenomena since they are the mechanisms by which heat and reactive species are transported ahead to the unburned gas. An iterative algorithm, DFLUX, is used to obtain the diffusion velocities without the cost of performing matrix inversions [17,22]. This method has been vectorized and is substantially faster than matrix inversions when four or more species are involved.

Problems can be set up in either planar, cylindrical, or spherical coordinates as well as a variable power series coordinates which can model one-dimensional nozzle-like geometries. The model can also be configured with either an open or closed boundary at one end. The open boundary simulates an unconfined system.

FLIC2D

FLIC2D is a time-dependent, Eulerian, implicit, compressible, two-dimensional flame model. In FLAME1D, a Lagrangian method was chosen for convective transport because eliminating the advection term in effect means eliminating numerical diffusion from the calculation. Extending, this Lagrangian approach to multidimensions would be extremely difficult and expensive, requiring many years of algorithm development and testing. Therefore, we felt that we would have more success in multidimensions with an Eulerian method. However, most Eulerian methods are either more numerically diffusive than what is acceptable in a flame model, or they are explicit and hence extremely inefficient at the very low velocities associated with laminar flames. To circumvent these numerical problems, we developed BIC-FCT, the Barely Implicit Correction to Flux-Corrected Transport [23,24]. BIC-FCT combines an explicit high-order, nonlinear FCT method [25,26] with an implicit correction process. This combination maintains high-order accuracy and yet removes the timestep limit imposed by the speed of sound. By using FCT for the explicit step, BIC-FCT is accurate enough

to compute with sharp gradients without overshoots and undershoots. Thus spurious numerical oscillations that would lead to unphysical chemical reactions do not occur. The development of this new algorithm has made it possible to model multidimensional flames in detail. However, because there is always some residual numerical diffusion, even in high-order Eulerian algorithms, we need to monitor calculations to ensure that numerical diffusion never becomes larger than the physical diffusion processes we need to resolve.

In generalizing the flame model to two-dimensions, simplifications were made in the diffusive transport calculations in order to reduce the cost of computations. In FLIC2D, thermal conductivity of the individual species is modeled by a polynomial fit in temperature to existing experimental data. Individual conductivities are then averaged using a mixture rule [12,27] to get the thermal conductivity coefficient of the gas mixture. A similar process is used to obtain the mixture viscosity from individual viscosities. Heat and momentum diffusion are then calculated explicitly using these coefficients.

Mass diffusion also plays a major role in determining the properties of laminar flames. Binary mass-diffusion coefficients are represented by an exponential fit to experimental data, and the individual species-diffusion coefficients are obtained by applying mixture rules [12].The individual species-diffusion velocities are determined explicitly by applying Fick's law followed by a correction procedure to ensure zero net flux [27]. This procedure is equivalent to using the iterative algorithm DFLUX [22] (used in FLAME1D) to second order.

The chemical reaction-rate equations are modelled and solved as before using a vectorized version of CHEMEQ, an integrator for stiff ordinary differential equations [21]. Because of the complexity of the reaction scheme and the large number of computational cells in a two-dimensional calculation, the solution of the chemical rate equations takes a large fraction of the total computational time. A special version of CHEMEQ called TBA was developed to exploit the special hardware features of the CRAY X-MP.

As in the one-dimensional code, all of the chemical and physical processes are solved sequentially and then coupled asymptotically by timestep splitting [17,18]. This modular approach greatly simplifies the model and makes it easier to test and change the model. Individual modules were tested against known analytic and other previously

verified numerical solutions. One-dimensional predictions of the complete model were compared to those from the Lagrangian model FLAME1D which has been benchmarked extensively against theory and experiment.

In summary, all of the chemical and diffusive-transport algorithms are essentially the same in FLIC2D as in FLAME1D. Thus given the input data concerning the species, their transport coefficients, and the reactions among the species, either the one- or two-dimensional model can be run. The major differences between the two models are in the costs of running them and the algorithm chosen for convective transport. In general, we use the results of one-dimensional calculations as initial conditions for the two-dimensional calculations in order to reduce the cost of computations. The two-dimensional flame model is discussed in greater detail in Appendix A.

SUMMARY OF RESEARCH

The thrust of the work during the past three years was two-fold. The first part was to study the propagation and extinction of flames using FLAME1D, the time-dependent, one-dimensional flame model. The second was to develop and use a multidimensional flame model, FLIC2D, to study mechanisms leading to cellular flame instability and the effects of gravity on the multidimensional structure of flames. Both models use a detailed set of chemical kinetics of all the species involved in hydrogen combustion as well as multi-species difffusion and thermal conduction.

Effects of Curvature and Dilution on Flame Propagation

We studied the effects of curvature and dilution on zero-gravity flame propagation in hydrogen-oxygen-nitrogen mixtures using the time-dependent, one-dimensional, Lagrangian flame model, FLAME1D. We performed a systematic study in which we varied both dilution and geometry. First, we considered the propagation of a spherical flame in a stoichiometric hydrogen-air mixture (2:1:4). We then increased the amount of nitrogen dilution and simulated spherical flames in hydrogen-oxygen-nitrogen mixtures in the ratios 2:1:7, 2:1:10, 2:1:11, 2:1:13 and 2:1:15 . We finally studied the propagation of cylindrical and planar flames in the same mixtures.

We found that in a stoichiometric hydrogen-air mixture, the velocity of a spherical flame first decreases with increasing radii until it reaches a minimum value, and then it increases. For large radii, the burning velocity approaches the planar burning velocity. With increasing dilution, the same trends were observed. Furthermore, the burning velocity of both spherical and planar flames decreases with increasing dilution.

These observations lead to the conclusion that a flame can be extinguished with less dilution in one geometry than in another. Specifically, we showed that a 2:1:13/hydrogen-oxygen-nitrogen mixture does not support a self-sustained spherical flame, although it does support cylindrical and planar flames. These observations have been explained on the basis of preferential diffusion, flame stretch, and chemical kinetics. These observations are also in qualitative agreement with experimental observations in both zero and one gravity. Detailed comparisons with experimental data are not possible because the actual flames near this extinction limit are unstable and multidimensional.

We are currently extending this work to fuel-lean and fuel-rich mixtures. Preliminary results indicate that the same trends are observed in fuel-rich mixtures as in stoichiometric mixtures discussed above. However, in fuel-lean mixtures, we expect the flame velocity to first increase with increasing radii and then to decrease to the planar burning velocity for large radii. This might result in mixtures which burn for some time and then extinguish for large radii where the burning velocity drops. Such behavior is characteristic of the "self-extinguishing" flames observed in the NASA drop tower [7]. In the actual experiment, heat loss might play an important role [28]. Furthermore, lean hydrogen-air mixtures are prone to cellular instabilities. Therefore, detailed study of flame propagation in such mixtures must be done with a multidimensional model.

A paper describing our work in this area in greater detail is enclosed as Appendix B.

Flame Propagation and Extinction in Fuel-Rich Mixtures

Microgravity flames in fuel-rich hydrogen-air mixtures appear to be stable and nearly one-dimensional. Therefore, we can study the extinction process and flammability limits by simulating the propagation of planar flames in fuel-rich hydrogen-air mixtures at zero gravity. We found that the burning velocity and flame temperature monotonically decreased with increasing fuel concentration. With further increase in the fuel-concentration, the temperature of the burning mixture does not seem to be high enough to sustain a steadily propagating flame. For temperatures of about 950 K, the endothermic radical-producing reactions take up more energy than what is produced by the exothermic reactions and hence a self-sustained flame is not observed. In a practical system, even minimal heat losses would ensure that an incipient flame is extinguished in such a fuel-rich mixture. The exact limit composition and temperature would vary from one experimental set-up to another. This work is described in greater detail in Appendix C.

Simulations of Cellular Flames

After testing the FLIC2D code, we used it to simulate unsteady nonplanar flames and the mechanisms leading to cellular structure. The first calculation modelled a flame in a fuel-lean mixture of hydrogen-oxygen-nitrogen in the ratio of 1.5:1:10. A multidimensional flame is observed in this mixture in the experiments of Mitani and Williams [29]. The numerical simulations showed that in this mixture, a one-dimensional planar

flame is unstable because perturbing the flame leads to a multidimensional structure resembling that of a cellular flame.

A similar calculation was performed for a fuel-rich mixture of hydrogen-oxygen-nitrogen in the ratio, 3:1:16. Flames in this mixture are stable in the experiments of Mitani and Williams [29], and also in our calculations. In this case, an initial perturbation is quickly damped, restoring the flame profile to its one-dimensional shape.

We then performed additional simulations to determine the mechanism controlling the instability. There are two possible mechanisms that can lead to cellular instability. One mechanism is the preferential diffusion of one reactant over another due to its higher diffusivity. For example, in a hydrogen-oxygen-nitrogen mixture, hydrogen diffuses much faster than oxygen or nitrogen. Another mechanism is the differences in the rate at which mass and heat diffuse (diffusional-thermal theory). In the third calculation, the mass diffusivity of hydrogen was set equal to oxygen. This eliminates the preferential diffusion effect, and means that the light fuel will not move fast compared to the other reactant. If the mechanism of instability were preferential diffusion, the lean flame would be stable. This is in fact the result: with this change of relative diffusivities, the lean flame was stable in the calculation.

This result supports both the preferential diffusion theory and the diffusional-thermal theory. A further calculation was performed in which the mass diffusivity of oxygen was set equal to that of hydrogen. In this case, the flame was unstable, which disagrees with the prediction of preferential diffusion. However, the diffusional-thermal theory does predict that this flame is unstable. Thus for these hydrogen flames studied, the results agree with the predictions of the diffusional-thermal theory and not the preferential diffusion theory. These simulations provide an example of the use of numerical simulations in identifying the controlling instability when more than one mechanism is plausible. A paper describing detailed numerical simulations of cellular flames is attached to this report as appendix D.

Effects of Gravity on Cellular Flames

We have studied the effects of gravity on flame structure by comparing simulations of zero-gravity flames to upward- and downward-propagating flames. These simulations show that the effects of gravity become greater as the lean flammability limit is approached. For example, in a 1.5:1:10/hydrogen-oxygen-nitrogen mixture, gravity plays

only a secondary role in determining the multidimensional structure of the flame. However, in a 1:1:10 mixture, an upward-propagating flame is highly curved and evolves into a bubble that rises upwards in the tube. The zero-gravity flame shows a cellular structure. The structure of the downward-propagating flame oscillates in time exhibiting both concave and convex curvatures towards the unburnt mixture. These observations have been explained on the basis of an interaction between the processes leading to Rayleigh-Taylor instability and the cellular instability. The simulations also suggest that cellular instability grows more rapidly than Rayleigh-Taylor instability. A paper describing this work in greater detail is included as appendix E.

A list of papers and presentations related to the work described above are given below.

Journal Articles and Meeting Proceedings

Effects of Curvature and Dilution on Unsteady Flame Propagation, K. Kailasanath and E.S. Oran, in Dynamics of Reactive Systems, I. Flames and Configurations, *Prog. Aero. Astro.* 105, AIAA, 1986.

A Barely Implicit Correction for Flux-Corrected Transport, G. Patnaik, R.H. Guirguis, J.P. Boris, and E.S. Oran, *J. Comput. Phys.*, 71, 1-20 (1987).

An Implicit Flux-Corrected Transport Scheme for Low Speed Flow, G. Patnaik, J.P. Boris, R.H. Guirguis, and E.S. Oran, AIAA 25th Aerospace Sciences Meeting, Paper No. AIAA-87-0482, AIAA, NY.

Time-Dependent Simulations of Laminar Flames in Hydrogen-Air Mixtures, K. Kailasanath and E.S. Oran, in *Complex Chemical Reaction Systems,* Eds., J. Warnatz and W. Jager , Springer-Verlag, Heidelberg, 1987.

Numerical Modelling of Unsteady Laminar Flames, K. Kailasanath, E.S. Oran and J.P. Boris, to appear as Chapter 3 in *Physics, Chemistry and the Modelling of Flames* by R. Fristrom, Johns Hopkins University Press, 1988.

Simulations of Flames near the Rich Flammability Limit of Hydrogen-Air Mixtures, K. Kailasanath and E.S. Oran, in preparation for submission to *Combustion and Flame,* 1989.

Detailed Numerical Simulations of Cellular Flames , G. Patnaik, K. Kailasanath, K. J. Laskey, and E. S. Oran, to be published in the *Proceedings of the 22th Symposium (International) on Combustion*, Seattle, WA., August, 1988.

FLIC: A Detailed Two-dimensional, Flame Model, G. Patnaik, K. J. Laskey, K. Kailasanath, E.S. Oran and T.A. Brun, to be published as Naval Research Laboratory Memorandum Report, 1989.

Meeting Presentations

Effects of Geometry and Diffusive Transport on Premixed, Laminar Flame Propagation, K. Kailasanath, E.S. Oran and G. Patnaik, 1985 Fall Technical Meeting of the Eastern Section of the Combustion Institute, Philadelphia, November, 1985.

Effects of Fluctuations on Chemically Reacting Systems and the Generation of Turbulence, E. S. Oran, invited talk presented at the Workshop on Flame Structure, Novosibirsk, USSR, July, 1986.

Ignition Studies of a Dilute, Stoichiometric Mixture of Hydrogen, Oxygen and Nitrogen, S. Kurban Ghafil, C. Brochet, K. Kailasanath, and E. Oran, *Poster Presentation at the 21th Symposium (International) on Combustion*, Munich, Germany, August, 1986.

Time-Dependent Simulations of Laminar Flames in Hydrogen-Air Mixtures, K. Kailasanath and E.S. Oran, Second Workshop on Modelling of Complex Reaction Systems, Heidelberg, Germany, August, 1986.

Application of an Implicit Flux-Corrected Transport Scheme to Combustion Modeling, G. Patnaik, K. Kailasanath, and E. Oran, 1986 Fall Technical Meeting of the Eastern Section of the Combustion Institute, San Juan, PR, December, 1986.

An Implicit Flux-Corrected Transport Scheme for Low Speed Flow, G. Patnaik, J.P. Boris, R.H. Guirguis, and E.S. Oran, AIAA Paper 87-0482, 25th Aerospace Sciences Meeting, AIAA, Reno, January, 1987.

Some Challenges in the Numerical Simulation of Laminar and Turbulent Flames, Elaine S. Oran, Princeton University, March, 1987

Numerical Calculations of Combustion Flows, Elaine S. Oran, University of California, San Diego, November, 1987.

Detailed Numerical Simulations of Lean Flame Structure, G. Patnaik, K. Kailasanath, K. J. Laskey, and E. S. Oran, 1987 Fall Technical Meeting of the Eastern Section of the Combustion Institute, Gaithersburg, MD, November, 1987.

Numerical Simulations of Cellular Structure in Hydrogen Flames, G. Patnaik, K. Kailasanath, K. J. Laskey, and E. S. Oran, Presented at the 3rd Workshop on

Numerical Methods in Laminar Flame Propagation, Leeds, England, April, 1988.

Numerical Simulation of Complex Fluid Systems, Elaine S. Oran, George Washington University, Washington, DC, April, 1988.

Future Trends in Numerical Simulations of Reacting Flows, Elaine S. Oran, 12th International Association for Mathematics and Computers in Simulation (IMACS) World Congress, Paris, France, July, 1988.

Detailed Numerical Simulations of Cellular Flames , G. Patnaik, K. Kailasanath, K. J. Laskey, and E. S. Oran, *presented at the 22th Symposium (International) on Combustion*, Seattle, WA., August, 1988.

Effect of Gravity on Multi-Dimensional Laminar Premixed Flame Structure, K. Kailasanath, G. Patnaik and E. S. Oran, *presented at the 39th International Astronautical Congress* , Bangalore, India, October, 1988.

New Directions in Computing Reacting Flows, Elaine S. Oran, Symposium on Advances and Trends in Computational Structural Mechanics and Fluid Dynamics, Washington, DC, October, 1988.

Numerical Simulations of Unsteady, Unstable Flames, E.S. Oran, G. Patnaik, K. Kailasanath, and K. Laskey, American Physical Society, Division of Fluid Dynamics, November, 1988.

The Current Status of CFD in Combustion Modeling, E. S. Oran, invited talk to be presented at the 1988 Fall Technical Meeting of the Eastern Section of the Combustion Institute, Clearwater, FL, December, 1988.

FUTURE DIRECTIONS

The calculations discussed above have lead to a better understanding of the structure and propagation of flames. We now understand the reasons for some of the observed differences in the structure of upward and downward propagating flames. However, we need to do further simulations to completely describe upward and downward propagating flames in the standard flammability limit tube and to determine flammability limits. An important factor that has not been considered in the above simulations is the effect of losses due to heat conduction to walls and due to radiation. Furthermore flames near the flammability limits are actually three-dimensional. In principle, FLIC can be extended to perform calculations in a three-dimensional geometry. Currently, a major limiting factor is the cost of such computations.

The solution of the chemical rate equations takes a significant portion (60 - 70 %) of the computer time because of the large number of species and the large number of rate equations involved in a mechanism consisting of elementary reactions. The problem becomes even more expensive in hydrocarbon fuels, starting with the simplest, methane. One approach to reducing the cost of multidimensional flame simulations is to use a greatly simplified reaction mechanism. However, a satisfactory simplified reaction mechanism does not exist currently, even for methane. Although, we have reduced a 108 reaction-rate mechanism for methane to about 50 rates [30], this is still too expensive to use in a multidimensional flame calculation. Currently there are many ongoing efforts to find ways of easing the burden of integrating full chemical reaction-rate mechanisms [31,32]. Using such simplified approaches in FLIC2D is straightforward and will enable us to simulate multidimensional flames in hydrocarbon mixtures.

Another approach to reducing the cost of chemistry calculations is to develop faster chemical integration algorithms. We are continually finding ways to make the algorithms we use faster. In addition, there are some new approaches to sorting stiff equations [33] which are promising. However, it is unlikely that reducing the computer time required by using faster algorithms alone will be sufficient to allow us to perform calculations of complex hydrocarbon flames in the near future.

The flame calculations performed to date with FLIC2D are in a two-dimensional cartesian coordinate system. With this version of the code we have been able to simulate the cellular structure of flames in a channel. Extensions to an axisymmetric geometry are straightforward. The axisymmetric version of the code will be used to simulate flame

propagation in cylindrical tubes. This will enable us to simulate new modes of flame instability. Calculations in an axisymmetric geometry using simplified and appropriate chemistry need to be done before full three-dimensional simulations of flames in tubes are performed.

REFERENCES

1. Lovachev, L.A., *Combust. Sci. Tech.* 21: 209–224 (1979).
2. Hertzberg, M., The Flammability limits of Gases, Vapors and Dust: Theory and Experiment, in **Fuel Air Explosions**, p. 3, University of Waterloo Press, 1982.
3. Ishizuka, S. and Law, C.K., *Nineteenth Symposium (Intl.) on Combustion*, pp. 327–335, The Combustion Institute, 1982.
4. Jarosinski, J., Strehlow, R.A. and Azarbarzin, A., *Nineteenth Symposium (Intl.) on Combustion*, pp. 1549–1557, The Combustion Institute, 1982.
5. Berlad, A.L., and Joshi, N.D., Gravitational Effects on the Extinction Conditions for Premixed Flames, presented at the 35th I.A.F. Congress, October 1984.
6. Jarosinski, J., *Prog. Energy Combust. Sci.*, 12: 81-116 (1986).
7. Ronney, P.D., Effect of Gravity on Laminar Premixed Gas Combustion II. — Ignition and Extinction Phenomena, *Combust. Flame.* 62: 121-133 (1985).
8. Strehlow, R.A., Work presented at the NASA Microgravity Combustion Science Working Group Meeting, NASA-LRC, Cleveland, Ohio, Oct. 1984. also Strehlow, R.A., Noe, K.A., and Wherley, B.L., The Effect of Gravity on Premixed Flame Propagation and Extinction in a Vertical Standard Flammability Tube, *Proceedings of the 21st Symposium (International) on Combustion,* The Combustion Institute, Pittsburg, PA., 1988.
9. Patnaik, G., Kailasanath, K., Laskey, K.J., and Oran, E.S., Detailed Numerical Simulations of Cellular Flames, to be published in *Proceedings of the 22th Symposium (International) on Combustion*, Seattle, WA., August, 1988.
10. Laskey, K., *Numerical Study of Diffusion and Premixed Jet Flames*, Ph.D. Thesis, Carnegie Mellon University, 1988, (in preparation).
11. Kailasanath, K., Oran, E.S., and Boris, J.P., Time-dependent simulation of flames in hydrogen-oxygen-nitrogen mixtures, in **Numerical Methods in Laminar Flame Propagation**, p. 152, Friedr. Vieweg and Sohn, Wiesbaden, 1982.
12. Kailasanath, K., Oran, E.S., and Boris, J.P., *A One-Dimensional Time-Dependent Model for Flame Initiation, Propagation and Quenching*, NRL Memorandum Report No. 4910, Washington, D.C., 1982.
13. Kailasanath, K., Oran, E.S., and Boris, J.P.,*Combust. Flame.* 47: 173–190 (1982).
14. Kailasanath, K., and Oran, E.S., *Prog. Aero. and Astro.* 105, Part 1, 167-179, 1986.

15. Kailasanath, K., and Oran, E.S., Time-Dependent Simulations of Laminar Flames in Hydrogen-Air Mixtures, *Proceedings of the 2nd Workshop on Modelling of Chemical Reaction Systems*, Heidelberg, West Germany, August, 1986; also Naval Research Laboratory Memorandum Report 5965, Washington D.C. 1987.

16. Williams, F.A., **Combustion Theory**, The Benjamin/Cummings Publishing Company, Menlo Park, CA, 1985.

17. Oran, E.S., and Boris, J.P., *Prog. Energy Comb. Sci.* 7: 1–71 (1981).

18. Oran, E.S., and Boris, J.P., **Numerical Simulation of Reactive Flow**, Elsevier, New York, 1987.

19. Boris, J.P., *ADINC: An Implicit Lagrangian Hydrodynamics Code*, NRL Memorandum Report 4022, Naval Research Laboratory, Washington, D.C., 1979.

20. Young, T.R., and Boris, J.P., *J. Phys. Chem.* 81: 2424–2427 (1977).

21. Young, T.R., *CHEMEQ - A Subroutine for Solving Stiff Ordinary Differential Equations*, NRL Memorandum Report 4091, Naval Research Laboratory, Washington, D.C., 1980.

22. Jones, W.W., and Boris, J.P., *Comp. Chem.* 5: 139–146 (1981).

23. Patnaik, G., Boris, J.P., Guirguis, R.H., and Oran, E.S., An Implicit Flux-Corrected Transport Scheme for Low Speed Flow, AIAA 25th Aerospace Sciences Meeting, Paper No. AIAA-87-0482, AIAA, NY.

24. Patnaik, G., Guirguis, R.H., Boris, J.P., and Oran, E.S., *J. Comput. Phys.* 71: 1-20 (1987).

25. Boris, J.P., *Flux-Corrected Transport Modules for Solving Generalized Continuity Equations*, NRL Memorandum Report 3237, Naval Research Laboratory, Washington, D.C., 1976.

26. Boris, J.P., and Book, D.L., **Methods of Computational Physics**, Vol. 16, Chapter 11, Academic Press, New York, 1976.

27. Kee, R. J., Dixon-Lewis, G., Warnatz, J., Coltrin, M.E. and Miller, J. A., *A FORTRAN Computer Code Package for the Evaluation of Gas-Phase Multi-Component Transport Properties*, Sandia National Laboratories Report SAND86-8246, 1986.

28. Ronney, P. D. (Princeton University), Private communication, 1988. (Data on propagation and extinction of hydrogen-oxygen-nitrogen flames in microgravity)

29 Mitani, T., and Williams F.A., *Combust. Flame.* 39: 169–190 (1980).

30. Frenklach, M., Kailasanath, K., and Oran, E.S., *Prog. Aero. and Astro.* 105, Part

2, 365-376, 1986.

31. Paczko, G., Lefdal, P.M., and Peters, N., Reduced Reaction Schemes for Methane, Methanol and Propane Flames, *Proceedings of the 21st Symposium (International) on Combustion,* The Combustion Institute, Pittsburg, PA., 1988.
32. Frenklach, M., (Penn. State University), Private Communication, 1988.
33. Lam, S.H. and Goussis, D.A., Basic Theory and Demonstration of Computational Singular Perturbation for Stiff Equations, presented at the *12th IMACS World Congress on Scientific Computation,* Paris, France, July 1988.

Appendix A

FLIC : A Detailed Two-dimensional Flame Model

FLIC — A Detailed, Two-Dimensional Flame Model

G. Patnaik,[1] K. J. Laskey,[2] K. Kailasanath,
E. S. Oran, and T. A. Brun[3]

Laboratory for Computational Physics
and Fluid Dynamics
Naval Research Laboratory
Washington D.C. 20375

[1]Berkeley Research Associates, Springfield, VA
[2]Carnegie-Mellon University, Pittsburgh, PA
[3]Harvard University, Cambridge, MA

Abstract

This report describes ***FLIC***, a detailed, two-dimensional model for flames. In order to describe a flame in enough detail to simulate its initiation, propagation, and extinction, ***FLIC*** combines algorithms for subsonic convective transport with buoyancy, detailed chemical reaction processes, and diffusive transport processes such as molecular diffusion, thermal conduction, and viscosity. Several new numerical techniques had to be developed specifically for multi-dimensional flame modelling, and these are highlighted in this report. The numerical implementation of the flame model is described here, and a typical application is provided for illustration. ***FLIC*** is currently the state-of-the-art in detailed two-dimensional, time dependent flame models.

Contents

1. Introduction

This report describes the new computer code ***FL***ame with ***I***mplicit ***C***onvection (***FLIC***), a two-dimensional time-dependent program developed specifically to compute and study the behavior of flames and other subsonic chemically reactive flows. In order to describe a flame in enough detail to simulate its initiation, propagation, and extinction, ***FLIC*** combines algorithms for subsonic convective transport with buoyancy, detailed chemical reaction processes, and diffusive transport processes such as molecular diffusion, thermal conduction, and viscosity. Currently, we have not included algorithms for radiation transport or thermal diffusion, although these important processes can, in principle, be added in the same modular fashion as those physical processes that have been included.

FLIC solves the reactive-flow conservation equations for density, ρ, momentum, $\rho\vec{V}$, energy, E, and number densities of the individual species, n_k, $k = 1, ..., n_{sp}$, according to:

$$\frac{\partial \rho}{\partial t} + \nabla \cdot \left(\rho \vec{\mathbf{V}}\right) = 0, \tag{1.1}$$

$$\frac{\partial \rho \vec{V}}{\partial t} + \nabla \cdot \left(\rho \vec{V} \vec{\mathbf{V}}\right) = -\nabla P + \vec{F} - \nabla \times \mu \nabla \times \vec{V} + \nabla \left(\frac{4}{3} \mu \nabla \cdot \vec{V}\right), \tag{1.2}$$

$$\frac{\partial E}{\partial t} + \nabla \cdot \left(E \vec{\mathbf{V}}\right) = -\nabla \cdot \left(P \vec{\mathbf{V}}\right) + \nabla \cdot (\kappa \nabla T) - \sum_{k=1}^{n_{sp}} \nabla \cdot \left(n_k h_k \vec{V}_k\right) + \sum_{r=1}^{n_r} Q_r, \tag{1.3}$$

$$\frac{\partial n_k}{\partial t} + \nabla \cdot \left(n_k \vec{\mathbf{V}}\right) = -\nabla \cdot \left(n_k \vec{V}_k\right) + w_k. \tag{1.4}$$

Here $\vec{V}$ is the fluid velocity, P is the pressure, μ is the coefficient of shear viscosity, $\vec{F}$ is a body force, κ is the thermal conductivity of the mixture of gases, h_k is the enthalpy of species k, $\vec{V}_k$ is the diffusion velocity of species k, Q_r is the heat

released from reaction r, and w_k is production of species k by chemical reaction. These equations are solved assuming that the individual species are ideal gases obeying the thermal equation of state,

$$P_k = n_k kT\,, \tag{1.5}$$

and that the differential relation between internal energy u and pressure P is given by

$$\delta u = \frac{\delta P}{\gamma - 1}\,, \tag{1.6}$$

where γ, the ratio of specific heats of the mixture, is a function of its temperature and composition.

FLIC solves these equations in two dimensions for low-velocity compressible flow such that the Mach number is less than 0.1. Depending on specified initial and boundary conditions, the flames modeled can be either premixed or diffusion flames in either planar or axisymmetric geometries.

To date, ***FLIC*** has been applied to the study of the cellular instability near the flammability limits of a premixed flame in a gas containing hydrogen, oxygen, and nitrogen flame [1]. Cellular flames are formed when the mass diffusion of the deficient reactant overwhelms the stabilizing influence of heat conduction [2,3]. For hydrogen flames, this behavior is seen close to the extinction limit [4] when the flame is thick and temperatures are low. The fluid velocity is usually low, typically less than 20 cm/s in the burned region. Radiation effects are not important because the flame is not luminous and absorbing species, such as CO_2 found in hydrocarbon flames, are absent. A brief summary of this work is given in section 6.

1.1 Algorithm Development and Implementation

Producing a code that describes low-speed flames required the development of several new numerical methods as well as finding new ways to implement existing algorithms. For example, a new multidimensional, low-speed convection algorithm had to be developed. An important requirement of any convection algorithm is that the numerical diffusion not be larger than the physical diffusion processes that must be resolved. The FCT method [5,6] meets this criterion, but it is inherently

an explicit method; so that the small timesteps it requires makes it inefficient for low-speed flows. The BIC-FCT method [7] was developed specifically to combine the accuracy of FCT with the efficiency of an implicit method for low-speed flows. BIC-FCT allows timesteps up to a hundred times larger than FCT and yet the calculation time of one BIC-FCT timestep is approximately equal to the calculation time of one timestep in the standard FCT module. Section 2 describes BIC-FCT in detail.

To solve the detailed combustion equations for hydrogen-oxygen chemistry involves solving coupled nonlinear ordinary differential equations for eight species and 48 chemical reactions representing the conversion of chemical species and chemical energy release into the system. This is the most expensive part of a reactive flow calculation because it requires integrating the set of equations at each computational cell for each timestep. The characteristic times of these differential equations vary by orders of magnitude, resulting in a set of very "stiff" equations. Then, because the cost of the calculation is approximately linear with the number of computational cells, the computational cost can be extreme in multidimensional computations. ***FLIC*** handles the cost of integrating ODEs in two ways: one, by not integrating the chemical reaction equations where there is nothing or essentially nothing happening, the other is by optimizing the integration procedure. We are using the CHEMEQ [8,9] method to solve stiff sets of ordinary differential equations, but in the TBA implementation that is fully optimized for the CRAY X-MP computer. TBA, described in section 3, allows speeds of up to 50 percent over VSAIM, the multidimensional implementation of CHEMEQ used to date.

Thermo-physical properties of the individual species and the mixture are required throughout the computation. These properties are modelled with high-order curve fits to values derived from more accurate calculations. The individual properties are combined where needed to obtain mixture properties through mixing rules. This simplified method is highy efficient yet sufficiently accurate. Section 4 describes the numerical solution of the diffusive transport processes.

The submodels representing the various physical processes are in independent modules that are coupled together. Several modifications have been made to the usual timestep splitting method in order to increase the stability limits and improve the efficiency of ***FLIC***. Section 5 describes the details of these improvements.

1.2 Comparison with FLAME1D

FLAME1D is a one-dimensional program used extensively to study the properties of the ignition and extinction of hydrogen flames [10]. It is useful to compare ***FLIC*** to FLAME1D because some FLAME1D algorithms are not obviously extendable to multidimensions and others are simply too expensive. The more important differences between these codes are described here.

1. ***FLIC*** uses an Eulerian representation of the convective transport instead of a Lagrangian representation. Specifically, ADINC, the one-dimensional Lagrangian algorithm [11] used in FLAME1D, is replaced by BIC-FCT [7], a very accurate multidimensional implicit Eulerian algorithm. A Lagrangian formulation, though preferable, is exceedingly difficult in multidimensions. However, unlike ADINC, BIC-FCT can be readily used to describe two-dimensional or three-dimensional flows.

2. Although the basic CHEMEQ algorithm is used in both codes, the VSAIM implementation used in FLAME1D was replaced by the TBA implementation. This algorithm is optimized for the CRAY X-MP, and can be retrofitted into CRAY versions of FLAME1D.

3. Another expensive part of the flame calculation is determining the amount that individual species diffuse. In FLAME1D, we used an iterative matrix expansion algorithm [12] that produces the diffusion flux of a species to arbitrary order, although we generally used it only up to second order. In ***FLIC***, we use a simpler technique which first evaluates a Fickian flux and then makes a correction. This approach is equivalent to the first order of the matrix expansion, cannot be made higher order, but it is computationally less intensive and certainly adequate for the flame problems treated to date.

4. In FLAME1D, thermal conduction is computed directly from expressions for the individual thermal conductivities of the species derived from molecular theory. In ***FLIC***, we use curve fits and mixture rules which has been benchmarked against the more exact calculations used in FLAME1D.

5. Whereas FLAME1D did not include algorithms for either viscosity or gravity, both of these effects are included in ***FLIC***.

6. At the moment, FLAME1D has a more flexible gridding algorithm. Because the basic convection algorithm in FLAME1D was Lagrangian, relatively non-diffusive cell splitting and merging routines are used to refine or coarsen the grid. The result is a rather general gridding capability. The general approach to adaptive gridding must be different in a multidimensional Eulerian code, and this is now being developed for ***FLIC***.

2. Convection

In this chapter, we describe the fluid convection algorithm, BIC-FCT, how it is used in ***FLIC***, and how the gravitational acceleration term is included. In detailed flame simulations that must resolve the individual species diffusion, the numerical diffusion that results from solving the convection equations numerically must be small enough so that we can resolve the physical diffusion processes. For high-speed flows, the Eulerian explicit monotone methods such as FCT [13] or most of the TVD [14] methods achieve this goal, and some even allow variable-order accuracy. Unfortunately, the timestep required by explicit methods must be small enough to resolve the sound waves in the system, otherwise the numerical method is unstable. There is little or no penalty paid for this small timestep in high-speed flow in which the physical phenomena evolve fast, but for low-speed flows, explicit methods are very inefficient and expensive. For example, resolving a microsecond of physical time with a timestep of 10^{-8} s requires 100 timesteps, but resolving one second requires 10^8 timesteps. For many low-speed flows this temporal accuracy is unnecessary; we need only to be able to resolve a millisecond of physical time with 100 timesteps. For this reason, implicit methods that allow large timesteps are usually used for calculations of low-speed flows.

One often-considered approach to eliminating numerical diffusion is to use Lagrangian methods, in which diffusion is totally absent by definition. We have found that this approach works well in one dimension, but there are a number of serious problems in multi-dimensions [15]. In complex flows, the multidimensional Lagrangian grid becomes distorted to the point where nearest neighbors are no longer connected by grid lines, a situation that leads to extremely inaccurate calculations. Eventually grid lines can even cross, which makes the solution unstable. Such problems are often avoided by a regridding procedure that actually adds diffusion to

the solution, or by using dynamically restructuring grid such as in SPLISH [16], which adds complexity. Except in one dimension, it has not yet been shown that Lagrangian methods are to be preferred because of the geometric complexities that arise.

Most common methods for solving convection problems use algorithms that produce ripples near steep gradients such as in a flame or shock front. The first high-order, nonlinear, monotone algorithm, Flux-Corrected Transport (FCT) [13], was designed to prevent these ripples by maintaining local positivity near steep gradients while keeping a high order of accuracy elsewhere. Other nonlinear methods have been reviewed by Woodward and Collela [14]. Although these methods are explicit, there are recent reports on implicit, nonlinear methods [17,18]. A major problem with applying these implicit methods to low-speed flows is that they are expensive even though they can be very accurate.

The Barely Implicit Correction to Flux-Corrected Transport, BIC-FCT [7], was designed to overcome the problem of numerical diffusion in low-velocity implicit methods. BIC-FCT combines an explicit high-order, nonlinear FCT method [5,6] with an implicit correction process. This method removes the timestep limit imposed by the speed of sound on explicit methods, retains the accuracy required to resolve the detailed features of the flow, and keeps the computational cost as low as possible.

2.1 The BIC-FCT Algorithm

BIC-FCT is based on an approach suggested by Casulli and Greenspan [19], who showed that it is not necessary to treat all of the terms in the gas-dynamic equations implicitly to be able to use longer timesteps than those dictated by explicit stability limits. Only those explicit terms which force a timestep limit due to the sound speed have to be treated implicitly. In a pure convection problem, the timestep is still limited by the fluid velocity, but for the low Mach number flow in flames, this results in a hundredfold increase in the timestep. The term "Barely Implicit Correction" emphasizes that only the minimal number of terms in the conservation equations are treated implicitly.

BIC-FCT solves the convective portion of the Navier-Stokes equations:

$$\frac{\partial \rho}{\partial t} + \nabla \cdot \left(\rho \vec{\mathbf{V}}\right) = 0 , \tag{2.1}$$

$$\frac{\partial \rho \vec{V}}{\partial t} + \nabla \cdot \left(\rho \vec{V} \vec{\mathbf{V}}\right) = -\nabla P + \vec{F} , \tag{2.2}$$

$$\frac{\partial E}{\partial t} + \nabla \cdot \left(E \vec{\mathbf{V}}\right) = -\nabla \cdot \left(P \vec{\mathbf{V}}\right) + S , \tag{2.3}$$

$$\frac{\partial n_k}{\partial t} + \nabla \cdot \left(n_k \vec{\mathbf{V}}\right) = 0 . \tag{2.4}$$

where $\vec{F}$ is a body force, usually gravity, and S is used to couple in the contributions to the change in energy due to other processes as discussed in chapter 5. In addition, note that convection of species is done at the same time.

BIC-FCT takes a predictor-corrector approach. The first explicit step uses FCT and a large timestep governed by a CFL condition on the fluid velocity,

$$\frac{\rho' - \rho^o}{\Delta t} = -\nabla \cdot \left(\rho^o \vec{V}^o\right), \tag{2.5}$$

$$\frac{\rho' \vec{V}' - \rho^o \vec{V}^o}{\Delta t} = -\nabla \cdot \left(\rho^o \vec{V}^o \vec{V}^o\right) - \nabla P^o, \tag{2.6}$$

$$\frac{E' - E^o}{\Delta t} = -\nabla \cdot (E^o + P^o) \left[\omega \vec{V}' + (1-\omega)\vec{V}^o\right] + S, \tag{2.7}$$

where the implicitness parameter $0.5 \leq \omega \leq 1.0$. This produces the intermediate values denoted by primes.

The second step is an implicit correction requiring the solution of one elliptic equation for the pressure correction, $\delta P \equiv \omega(P^n - P^o)$:

$$\frac{\delta P}{(\gamma - 1)\omega \Delta t} - \omega \Delta t \nabla \cdot \left(\frac{E^o + P^o}{\rho'} \nabla \delta P\right) = \frac{E' - E^o}{\Delta t} - \frac{\rho' \vec{V'}^2 - \rho^o \vec{V^o}^2}{2\Delta t} \tag{2.8}$$

The elliptic equation (Eq. (2.8)) is solved by the multigrid method, MGRID [20]. This method is O(N) in both number of computations as well as storage. It is vectorized and extremely efficient on the CRAY X-MP. MGRID requires that the number of grid points in each direction be factorizible by a large power of two. While this has not proven to be very restrictive for ***FLIC***, it has been a problem in other applications. MGRID also has only a limited set of boundary conditions. Fortunately, the Neumann boundary conditions used in solving Eq. (2.8) has been implemented.

The final step is the correction of the provisional values for momentum, energy, and pressure:

$$\rho^n \vec{V}^n = -\Delta t \nabla \delta P + \rho' \vec{V}', \tag{2.9}$$

$$E^n = \frac{\delta P}{(\gamma - 1)\omega} + E^o, \tag{2.10}$$

$$P^n = \delta P + P^o. \tag{2.11}$$

Because BIC-FCT uses FCT for the explicit step, it has the high-order monotone properties that accurately treat sharp gradients. This accuracy combined with the savings that result from removing the sound-speed limitation on the timestep makes BIC-FCT a very cost effective convection algorithm. BIC-FCT takes about $15\mu s$ per point per computational timestep on the CRAY X-MP computer. This is as fast as the explicit FCT code currently in use. BIC-FCT has opened up the possibility of doing accurate, multidimensional, slow-flow calculations in which fluid expansion is important. Because the cost of BIC-FCT is modest even in two dimensions, reasonably detailed chemistry models as well as other physical processes can be included. Premixed flames, diffusion flames, and turbulent jet flames are some of the applications for which BIC-FCT is well suited.

2.2 Gravity

Buoyancy effects due to the force of gravity have been incorporated in ***FLIC***. The body force term $\vec{F}$ in Eq. (2.6) is used for this purpose and is given by

$$\vec{F} = \vec{g}(\rho - \rho_\infty) \tag{2.12}$$

where ρ_∞ is a suitable reference density, usually the cold ambient density. As currently implemented, the direction of the gravity vector is aligned with the flow direction, but this restriction can be removed trivially. Indeed, the gravity vector can be made time-dependent to simulate g-jitter in microgravity.

If the ambient density cannot be used, the hydrostatic head has to be included in its place. This second approach is not as suitable as the method given by Eq. (2.12) because of the need for very high precision calculations.

3. Chemistry

This chapter describes the integration package TBA that is used to solve the ordinary differential equations (ODE's) representing the chemical reactions and energy release. TBA is a fully vectorized FORTRAN subroutine for the CRAY X-MP. It is designed to replace VSAIM, the older vectorized version of CHEMEQ [8,9], an algorithm that solves a system of ODE's in a single computational cell. Both VSAIM and TBA are based on CHEMEQ and are designed to make the calculation of a large number of sets of ODE's more efficient. TBA is faster than VSAIM because it is designed to make specific use of the Cray X-MP's gather/scatter hardware and other capabilities.

The ODE's solved by these routines are of the form

$$\frac{dn_i}{dt} = F_i = Q_i - L_i n_i, \tag{3.1}$$

where n_i is the number density of species i, Q_i is the rate of formation of species i, and $L_i n_i$ is the rate of destruction of species i. Sometimes these equations can be solved by classical algorithms, sometimes they are stiff and need special techniques. TBA uses a different algorithm for each type of equation and gains efficiency by gathering all equations of a given type together and integrating them by groups.

A detailed hydrogen-oxygen reaction scheme has been implemented in ***FLIC***. This reaction scheme consists of forty-eight reversable reactions involving eight species. Nitrogen, acting as a diluent, is considered to be chemically inert. This reaction scheme, developed by Burks and Oran [21], has been used by Kailasanath *et al.* [22] in FLAME1D and is given in table 3.1. The total rate of formation and destruction of each species is obtained algebraically from the reaction rates of the individual chemical reactions and from the species concentrations. The reaction

rate for each chemical reaction r is assumed to follow the modified Arrhenius form:

$$k_r = AT^B e^{-C/T} \tag{3.2}$$

The computation of the rates in Eq. (3.2) is quite time consuming, mainly due to the calculation of the exponential term. Some time can be saved by computing the temperature dependence of the reaction rates only once per global timestep. The rates of formation and destruction of the species, which are also dependent on the species concentrations, is computed as often as needed by TBA, which updates them many times during each global timestep.

3.1 Numerical Method

TBA uses a second-order predictor-corrector method that is essentially the same numerical integration algorithm as CHEMEQ [9]. Normal ODE's are integrated using a simple classical scheme and stiff ODE's are integrated using an asymptotic method. Unlike CHEMEQ or VSAIM, TBA also recognizes equations that will approach equilibrium during the period of integration and handles them with a third scheme. TBA sorts the equations from every cell into one of three types — normal, stiff, or equilibrium, and then integrates all of the equations of each type together. A large number of cells are integrated simultaneously; as cells are completed, the results are returned to the control program and stored and data from new cells are read in and integrated.

The entire set of equations from each cell is integrated using the smallest timestep required by any equation in the set. The timestep is then increased or decreased based on the relative difference between the predictor and corrector stages. The predictor stages for the three types of equations are:

$$n_i' = n_i^o + \delta t F_i^o \ , \qquad \text{(Normal)} \tag{3.3}$$

$$n_i' = n_i^o + \frac{\delta t F_i^o}{1 + \delta t L_i^o} \ , \qquad \text{(Stiff)} \tag{3.4}$$

$$n_i' = Q_i / L_i \ . \qquad \text{(Equilibrium)} \tag{3.5}$$

The corrector stages are:

$$n_i^n = n_i^o + \frac{\delta t}{2} \left[F_i^o + F_i' \right] \ , \qquad \text{(Normal)} \tag{3.6}$$

Reaction Rate	A[a]	B	C[a]	Source
$H + HO \rightleftharpoons O + H_2$	1.40(−14)	1.00	3.50(+03)	[23]
	3.00(−14)	1.00	4.48(+03)	[23]
$H + HO_2 \rightleftharpoons H_2 + O_2$	4.20(−11)	0.00	3.50(+02)	[23]
	9.10(−11)	0.00	2.91(+04)	[23]
$H + HO_2 \rightleftharpoons HO + HO$	4.20(−10)	0.00	9.50(+02)	[23]
	2.00(−11)	0.00	2.02(+04)	[23]
$H + HO_2 \rightleftharpoons O + H_2O$	8.30(−11)	0.00	5.00(+02)	[24]
	1.75(−12)	0.45	2.84(+04)	$k_r = k_f/K_c$
$H + H_2O_2 \rightleftharpoons HO_2 + H_2$	2.80(−12)	0.00	1.90(+03)	[23]
	1.20(−12)	0.00	9.40(+03)	[23]
$H + H_2O_2 \rightleftharpoons HO + H_2O$	5.28(−10)	0.00	4.50(+03)	[23]
	3.99(−10)	0.00	4.05(+04)	$k_r = k_f/K_c$
$HO + H_2 \rightleftharpoons H + H_2O$	1.83(−15)	1.30	1.84(+03)	[25]
	1.79(−14)	1.20	9.61(+03)	[25]
$HO + HO \rightleftharpoons H_2 + O_2$	1.09(−13)	0.26	1.47(+04)	$k_f = k_r K_c$
	2.82(−11)	0.00	2.42(+04)	[26]
$HO + HO \rightleftharpoons O + H_2O$	1.00(−16)	1.30	0.00(+00)	[25]
	3.20(−15)	1.16	8.77(+03)	$k_r = k_f/K_c$
$HO + HO_2 \rightleftharpoons H_2O + O_2$	8.30(−11)	0.00	5.03(+02)	[27]
	2.38(−10)	0.17	3.69(+04)	$k_r = k_f/K_c$
$HO + H_2O_2 \rightleftharpoons HO_2 + H_2$	1.70(−11)	0.00	9.10(+02)	[23]
	4.70(−11)	0.00	1.65(+04)	[23]
$HO_2 + H_2 \rightleftharpoons HO + H_2O$	1.20(−12)	0.00	9.41(+03)	[26]
	1.33(−14)	0.43	3.62(+04)	$k_r = k_f/K_c$

Table 3.1 Chemical Reaction Rates for H_2-O_2 Combustion: $k_i = AT^B \exp(-C/T)$[b]

[a] Exponentials to the base 10 are given in parentheses: $1.00(-10) = 1.00 \times 10^{-10}$.

[b] Bimolecular reaction rate constants are in units of cm^3/ (molecule s).

Reaction Rate	A[a]	B	C[a]	Source
$HO_2 + HO_2 \rightleftharpoons H_2O_2 + O_2$	3.00(−11)	0.00	5.00(+02)	[24]
	1.57(−09)	−0.38	2.20(+04)	$k_r = k_f/K_c$
$O + HO \rightleftharpoons H + O_2$	2.72(−12)	0.28	−8.10(+01)	$k_f = k_r K_c$
	3.70(−10)	0.00	8.45(+03)	[23]
$O + HO_2 \rightleftharpoons HO + O_2$	8.32(−11)	0.00	5.03(+02)	[27]
	2.20(−11)	0.18	2.82(+04)	$k_r = k_f/K_c$
$O + H_2O_2 \rightleftharpoons H_2O + O_2$	1.40(−12)	0.00	2.12(+03)	[24]
	5.70(−14)	0.52	4.48(+04)	$k_r = k_f/K_c$
$O + H_2O_2 \rightleftharpoons HO + HO_2$	1.40(−12)	0.00	2.13(+03)	[24]
	2.07(−15)	0.64	8.23(+03)	$k_r = k_f/K_c$
$H + H + M \rightleftharpoons H_2 + M$	1.80(−30)	−1.00	0.00(+00)	[23]
	3.70(−10)	0.00	4.83(−04)	[23]
$H + HO + M \rightleftharpoons H_2O + M$	6.20(−26)	−2.00	0.00(+00)	[23]
	5.80(−09)	0.00	5.29(+04)	[23]
$H + O_2 + M \rightleftharpoons HO_2 + M$	4.14(−33)	0.00	−5.00(+02)	[23]
	3.50(−09)	0.00	2.30(+04)	[23]
$HO + HO + M \rightleftharpoons H_2O_2 + M$	2.50(−33)	0.00	−2.55(+03)	[23]
	2.00(−07)	0.00	2.29(+04)	[23]
$O + H + M \rightleftharpoons HO + M$	8.28(−29)	−1.00	0.00(+00)	[28]
	2.33(−10)	0.21	5.10(+04)	$k_r = k_f/K_c$
$O + HO + M \rightleftharpoons HO_2 + M$	2.80(−31)	0.00	0.00(+00)	[28]
	1.10(−04)	−0.43	3.22(+04)	$k_r = k_f/K_c$
$O + O + M \rightleftharpoons O_2 + M$	5.20(−35)	0.00	−9.00(+02)	[23]
	3.00(−06)	−1.00	5.94(+04)	[23]

Table 3.1 Continued Chemical Reaction Rates for H_2–O_2 Combustion: $k_i = AT^B \exp(-C/T)$[b]

[a] Exponentials to the base 10 are given in parentheses: $1.00(-10) = 1.00 \times 10^{-10}$.

[b] Bimolecular reaction rate constants are in units of cm^3/ (molecule s).

$$n_i^n = n_i^o + \frac{2\delta t\,[Q_i' - L_i^o n_i^o + F_i^o]}{4 + \delta t\,[L_i' + L_i^o]}\,, \qquad \text{(Stiff)} \tag{3.7}$$

$$n_i^n = \frac{2Q_i'}{L_i' + L_i^o}\,. \qquad \text{(Equilibrium)} \tag{3.8}$$

The original CHEMEQ report [9] describes the details of the timestep selection algorithm, stiffness criterion, and other important details. A detailed report on TBA [29] is currently under preparation.

3.2 Data-Handling Algorithm

TBA is designed to handle a large number of cells, each with an independent timestep. Thus, each cell is integrated with a different number of subcycles. Cells have to be constantly shuffled in and out of the integration routine. Whenever the integration of a cell is complete, it is put onto a list. At the end of the integration loop, this list is passed to another routine, CDATA, which stores the results and inserts new cells to be integrated into the places left by the completed cells. Towards the end of the integration procedure there are no additional cells to integrate and the arrays in the integrator will be only partially filled. When this occurs, we sort and move all completed cells to the ends of the arrays where they will not be integrated further. When the integration of the remaining cells is complete, all the data is written out in one operation. Thus we avoid both unnecessary shuffling and unnecessary calls to CDATA. The sort algorithm developed specificially for this application is O(N) and makes the minimum number of swaps. The sort is optimized by the use of CRAY assembly routines that make bitwise comparisons.

In the original VSAIM routine, all equations passed through one integration loop where they were tested for stiffness by `if` statements and either the stiff or normal calculations were performed. The CRAY X-MP vectorizes `if` statements by performing the calculations for both possibilities and then throwing away the results for the false condition, so this approach is wasteful. TBA creates index arrays for different types of equations and sets up a separate integration loop for each of the three types. This approach succeeds due to the speed of the CRAY X-MP gather/scatter hardware.

3.3 Programming Strategies

Many strategies or tricks were used to enhance the speed of TBA, most of which are in what is considered extremely poor programming style, but reflect certain idiosyncracies of CRAY programming in general. Some are documented in CRAY manuals, especially the *Optimization Guide* [30].

For example, many of the arrays are equivalenced as both one- and two-dimensional arrays. The CRAY will only vectorize the innermost nested loop, so wherever possible we looped over the one-dimensional equivalent array, to avoid an outer loop. Working space for TBA is supplied in a common block, as this proved substantially faster than passing it through the argument list in the calling sequence. Memory access is the bottleneck on the CRAY so scalar temporaries are used to reduce memory traffic. A full 50% speed up was achieved through their use. A power of two as the number of species results in memory conflicts that slow the program considerably. There are eight (2^3) chemical species in ***FLIC*** which would result in very poor performance. Thus a "dummy" species was put in, removing the memory conflict.

The following code fragment illustrates the importance of large vector lengths. Note that if the order of the loops were switched, the `if` could be taken out of the inner loop and the memory access made contiguous. However, a much shorter inner loop results, and the execution time is actually greater.

```
      do 250 i=1,numeqns
         do 240 j=1,numcells
            if (convchk(j)) then concent(i,j)=corr2d(i,j)
240      continue
250   continue
```

These sorts of tricks are higly specific to the CRAY X-MP computer and must be used to gain full advantage of its speed. Though TBA can be transported to other machines (it was developed on a VAX), it was written specifically for the CRAY X-MP with its gather/scatter hardware in mind.

4. Diffusive Transport Processes

The diffusive transport processes currently included in ***FLIC*** are molecular diffusion including the Dufour effect, thermal conduction, and viscosity, all processes that are crucial for describing flame structure. As yet, we have have not included the thermal effects on mass diffusion (thermal diffusion or the Soret effect), thermal dissipation due to viscosity, or radiation transport. Although it is a second-order effect, thermal diffusion may become important for near-limit flames and so should be included in the future. Thermal dissipation is negligible at the extremely low Mach numbers in the flows under consideration. Radiation effects are important in many flames, particularly hydrocarbon flames that form soot, but is not particularly important in hydrogen flames.

The differential equations describing these diffusive processes have been solved with a two-dimensional, explicit Eulerian scheme. Spatial derivatives have been approximated by central differences and a simple forward-Euler time marching scheme has been used for time advancement. This explicit method has a timestep limit roughly equal to the timestep required by BIC-FCT for the fluid convection. However, each diffusive transport process has its own stability condition, and on occasion it can require a timestep up to five times smaller. When this is the case, the approach we have taken is to subcycle the integration for that process. The alternate approach would be to use an implicit algorithm for selected terms, but this is generally more expensive than subcycling when fewer than ten subcycles are required.

4.1 Mass Diffusion

The part of the species conservation equations for species number density that describes mass diffusion are

$$\frac{\partial n_k}{\partial t} = -\nabla \cdot \left(n_k \vec{V}_k \right) \ , \quad n_k \ = \ 1, ...n_{sp} \ , \tag{4.1}$$

subject to the constraint

$$\sum_{k=1}^{n_{sp}} Y_k \vec{V}_k = 0 \ . \tag{4.2}$$

The effects of molecular diffusion in the energy equation (Dufour effect) appear as

$$\frac{\partial E}{\partial t} = -\nabla \cdot \left(\sum_{k=1}^{n_{sp}} n_k h_k \vec{V}_k \right) \ , \tag{4.3}$$

where h_k is the temperature-dependent enthalpy for each of the species. The values of $\{V_k\}$ are found by solving [31]

$$S_k = \sum_{\substack{j=1 \\ j \neq k}}^{n_{sp}} \frac{X_j X_k}{D_{kj}} (V_j - V_k) = \nabla X_k, \tag{4.4}$$

subject to

$$\sum_{k=1}^{n_{sp}} S_k = 0, \tag{4.5}$$

and Eq. (4.2), where X_k and Y_k are the mole and mass fractions of species k. The exact solution of this equation for the set $\{V_k\}$ can be obtained by solving the matrix equation implied by Eq. (4.4).

To avoid solving the full matrix equation at each location at each timestep, we find an approximation to the $\{V_k\}$ using Fick's Law and then correct this by the procedure described by Coffee and Heimerl [32] to ensure that the constraint Eq. (4.2) is met. The diffusion velocity according to Fick's law is

$$\widehat{V_k} = -\frac{1}{X_k} D_{km} \nabla X_k \ , \tag{4.6}$$

where D_{km} is the diffusion coefficient of species k in the mixture of gases. Equation 4.6 determines the diffusion velocities to within a constant. We then assume that a

constant $\vec{V}_c$ is added to all the raw diffusion velocities $\widehat{V}_k$ and require that the sum of the diffusion fluxes equal zero. Thus,

$$\sum_{k=1}^{n_{sp}} Y_k \vec{V}_k = \sum_{k=1}^{n_{sp}} Y_k \left(\widehat{V}_k + \vec{V}_c \right) = 0 \tag{4.7}$$

leads to

$$\vec{V}_c = - \sum_{k=1}^{n_{sp}} Y_k \widehat{V}_k \ . \tag{4.8}$$

The component of the corrected diffusion velocity defined by

$$\vec{V}_k = \widehat{V}_k + \vec{V}_c \tag{4.9}$$

is then used in Eq. (4.1).

The set of $\{V_k\}$ found in this way is algebraically equivalent to the first iteration of the DFLUX algorithm [12], an approach based on a matrix expansion that converges to arbitrary order. Values of $\{V_k\}$ obtained by the procedure described above were compared to the results of DFLUX to check their accuracy. The explicit finite differencing used to solve Eq. (4.1) has the numerical stability limit,

$$\max \left(D_{km} \Delta t / \Delta x^2 \right) < 1/2 \ .$$

Generally the mass-diffusion algorithm is subcycled within an overall timestep determined by the convection algorithm. However, the code is designed to decrease the overall timestep to below that required by the mass-diffusion stability limit if the number of subcycles required exceeds a specified maximum value. Subcycling becomes necessary when the temperature of the reacting flow becomes high and the diffusion coefficients increase accordingly.

Determining the diffusion velocities by Eq. (4.6) requires as input the set of diffusion coefficients of species k into the mixture, $\{D_{km}\}$. However, these quantities are difficult to obtain from first principles and are usually found by applying a mixture rule to the individual binary diffusion coefficients. Binary diffusion coefficients can be estimated theoretically [33] and sometimes measured experimentally [33,34]. Here we use the same approach as in FLAME1D (Kailasanath *et al.* [22]). Binary diffusion coefficients are expressed in the form

$$D_{kl} = \frac{A_{kl}}{n_{tot}} T^{B_{kl}} \tag{4.10}$$

	O	H_2	OH	H_2O	O_2	HO_2	H_2O_2	N_2
H	6.30(17)	8.29(17)	6.30(17)	6.70(17)	6.70(17)	6.70(17)	4.43(17)	6.10(17)
	7.28(-1)	7.28(-1)	7.28(-1)	7.28(-1)	7.32(-1)	7.32(-1)	7.28(-1)	7.32(-1)
O		3.61(17)	1.22(17)	2.73(17)	9.69(16)	9.69(16)	1.57(17)	9.69(16)
		7.32(-1)	7.74(-1)	6.32(-1)	7.74(-1)	7.74(-1)	6.32(-1)	7.74(-1)
H_2			3.49(17)	6.41(17)	3.06(17)	3.06(17)	4.02(17)	2.84(17)
			7.32(-1)	6.32(-1)	7.32(-1)	7.32(-1)	6.32(-1)	7.38(-1)
OH				2.73(17)	1.16(17)	9.69(16)	1.57(17)	9.69(16)
				6.32(-1)	7.24(-1)	7.74(-1)	6.32(-1)	7.74(-1)
H_2O					2.04(17)	2.04(17)	1.57(17)	1.89(17)
					6.32(-1)	6.32(-1)	6.32(-1)	6.32(-1)
O_2						8.74(17)	1.14(17)	8.29(16)
						7.24(-1)	6.32(-1)	7.24(-1)
HO_2							1.14(17)	8.85(16)
							6.32(-1)	7.74(-1)
H_2O_2								1.14(17)
								6.32(-1)

Table 4.1 Binary diffusion coefficients expressed in the form: $D_{jk} = A_{jk}\frac{T^{B_{jk}}}{N}$. For each pair of species, the upper term is A_{jk} and the lower term is B_{jk}, exponentials to the base 10 are given in parentheses.

where the sets $\{A_{kl}\}$ and $\{B_{kl}\}$ are tabulated [22] for each pair of species in the hydrogen–oxygen reaction system, and are given in table 4.1. These are then combined by a mixture rule [35,36]

$$D_{km} = \frac{1 - Y_k}{\sum_{\substack{l=1 \\ l \neq k}}^{n_{sp}} \frac{X_l}{D_{kl}}}, \tag{4.11}$$

which provides values of D_{km} to use in Eq. (4.6).

4.2 Thermal Conduction

The effects of thermal conduction are expressed in the energy equation as

$$\frac{\partial E}{\partial t} = -\nabla \cdot (\kappa \nabla T) \ , \tag{4.12}$$

where κ is the mixture thermal conductivity. Explicit finite differencing introduces a stability limit

$$\max\left(\kappa \Delta t / \rho c_p \Delta x^2\right) < 1/2 \ ,$$

where $\kappa/\rho c_p$ is the thermal diffusivity coefficient. Subcycling is used here in the same manner as it is for mass diffusion. However, this stability condition is less stringent than that for mass diffusion and typically only two or three subcycles are needed.

The mixture thermal conductivity κ is obtained by combining the thermal conductivities of the individual gases $\{\kappa_k\}$ that are in the mixture. The $\{\kappa_k\}$ are estimated theoretically and are a function of temperature. We have used the third-order polynomial fit in temperature determined by Laskey [37] and is presented in Table 4.2. The mixture thermal conductivity is then calculated using (Mathur *et al.* [38])

$$\kappa = \frac{1}{2}\left[\sum_{k=1}^{n_{sp}} X_k \kappa_k + \frac{1}{\sum_{k=1}^{n_{sp}} \frac{X_k}{\kappa_k}}\right] \ . \tag{4.13}$$

4.3 Viscosity

The viscosity terms in the Navier-Stokes equations are included in ***FLIC***. The stress-tensor term, which represents the effect of viscosity in the momentum conservation equations, is:

$$\frac{\partial \rho \vec{V}}{\partial t} = -\nabla \cdot \tau \ , \tag{4.14}$$

where

$$\tau = \left(\frac{2}{3}\mu - \lambda\right)\left(\nabla \cdot \vec{V}\right)\mathbf{I} - \mu\left[\left(\nabla \vec{V}\right) + \left(\nabla \vec{V}\right)^T\right] \ , \tag{4.15}$$

Species	A	B	C	D
H	4.710(3)	3.354(1)	-9.971(-3)	1.964(-6)
O	1.089(3)	1.038(1)	-3.739(-3)	8.251(-7)
H_2	6.306(3)	4.304(1)	-8.505(-3)	2.160(-6)
OH	1.679(3)	1.091(1)	-1.613(-3)	4.150(-7)
H_2O	-2.077(2)	1.603(1)	-7.932(-4)	1.530(-7)
O_2	3.862(2)	8.613(0)	-1.966(-3)	3.619(-7)
HO_2	1.576(2)	1.070(1)	-1.143(-3)	4.471(-8)
H_2O_2	-1.097(3)	9.895(0)	-1.779(-3)	1.396(-7)
N_2	7.024(2)	6.917(0)	-1.191(-3)	2.035(-7)

Table 4.2 Thermal conductivity of species $k, \kappa_k = A + BT + CT^2 + DT^3$, erg/cm-s-K. Exponentials to the base 10 are given in parentheses.

and μ is the dynamic viscosity coefficient. The quantity λ, the second coefficient of viscosity, is set to $-2/3\mu$. The stress tensor τ includes all the viscous terms which arise in the compressible Navier-Stokes equations.

Eq. (4.14) is solved explicitly in the same manner as the mass diffusion or thermal conduction equations. Thus there is a stability criterion given by

$$\max\left(\mu\Delta t/\rho\Delta x^2\right) < 1/2\,,$$

where μ/ρ is the kinematic viscosity. Subcycling is used so that the overall computational timestep is set by the convection stability limit and not by the viscosity stability limit. If the number of subcycles required for stability exceeds some maximum value, the global timestep is reduced. The viscous diffusion algorithm was tested using two test problems: 1) the boundary-layer growth over a flat plate parallel to the flow, and 2) the boundary-layer thickness on a flat plate normal to the flow (stagnation point flow).

For the parallel-plate test, the velocity profile of the parallel flow was initially uniform along the plate with a typical velocity profile that is valid for a boundary-layer thickness greater than three computational cells. This particular initialization was chosen because a physical boundary layer less than three cells wide would be

swamped by numerical diffusion from the FCT algorithm that creates a boundary layer at least this thick. Setting up the problem this way simulates the growth of a boundary layer away from the leading edge of the plate and minimizes any numerical effects on the solution. The result of this test is a boundary layer whose growth matches the Blasius solution.

The stagnation-flow test was initialized with a boundary layer of constant thickness and uniform velocity along the plate. Again, the initial boundary layer thickness was more than three cells to minimize numerical effects. The results showed the development of a constant-thickness boundary layer whose velocity profile very closely matched that predicted by theory.

For a gas containing a single species k, the dynamic viscosity μ_k can be otained from the kinetic theory of gases [33]. Over a suitable range of temperature, this can be expressed as a third-order polynomial in temperature. Laskey [37] has compared this polynomial fit, presented in Table 4.3, to the calculations and to tabulated values for the viscosity and found good agreement. The mixture dynamic viscosity is calculated using the expression (Wilke [39])

$$\mu = \sum_{k=1}^{n_{sp}} \frac{X_k \mu_k}{\sum_{j=1}^{n_{sp}} X_j \Phi_{kj}} , \tag{4.16}$$

where

$$\Phi_{kj} = \frac{1}{\sqrt{8}} \left(1 + \frac{M_k}{M_j}\right)^{-\frac{1}{2}} \left(1 + \left(\frac{\mu_k}{\mu_j}\right)^{\frac{1}{2}} \left(\frac{M_j}{M_k}\right)^{\frac{1}{4}}\right)^2 . \tag{4.17}$$

This mixture viscosity, μ, is used in the stress tensor (Eq. (4.15)) to model the viscous portion of the Navier-Stokes equations.

Species	A	B	C	D
H	1.516(-5)	1.074(-7)	-3.178(-11)	6.255(-15)
O	4.504(-5)	5.355(-7)	-1.811(-10)	3.740(-14)
H_2	2.802(-5)	2.236(-7)	-6.958(-11)	1.399(-14)
OH	5.630(-5)	5.193(-7)	-1.678(-10)	3.413(-14)
H_2O	-8.597(-6)	6.608(-7)	-2.305(-10)	4.601(-14)
O_2	4.930(-5)	5.861(-7)	-1.983(-10)	4.093(-14)
HO_2	5.006(-5)	5.952(-7)	-2.013(-10)	4.156(-14)
H_2O_2	-9.109(-6)	3.966(-7)	-1.345(-10)	2.623(-14)
N_2	5.302(-5)	4.596(-7)	-1.464(-10)	2.969(-14)

Table 4.3 Viscosity of species $k, \mu_k = A + BT + CT^2 + DT^3$,dyne-s/cm^2. Exponentials to the base 10 are given in parentheses.

5. Model Integration

The conservation equations contain terms representing convection, buoyancy, thermal conduction, molecular diffusion, viscous diffusion, and chemical reactions. The approach that ***FLIC*** uses is to determine a global timestep, solve equations representing the individual physical processes separately for that timestep, and then couple the solutions. The coupling procedure is a variation of the standard timestep splitting method of Yanenko [40] and described for reactive flows by Oran and Boris [15]Chapters 4 and 13.

The usual explicit timestep-splitting approach assumes that in some predetermined global timestep, the effect of all the physical processes can be evaluated as a running sum of the effects of individual processes. Each physical process is integrated independently using the results of the previous process as initial conditions. This method is correct in the limit of small timesteps and works well in a practical sense when the changes in the variables during the global timestep are small. Using this appproach, the global timestep is often limited to the smallest timestep required by the stability limits of the integration algorithms for the various processes. This is the approach we have used in a number of programs in which the convection is solved by an explicit integration procedure. The global timestep is usually determined by the CFL condition on the sum of the sound speed and the fluid velocity. The chemistry integration is subcycled in the global timestep. However, subcycling can sometimes be used for individual processes if changes in variables due to that particular process are not too large.

Figure 5.1 summarizes the integration process in a typical ***FLIC*** timestep. The global timestep is first estimated based on the stability requirements of the convection algorithm, BIC-FCT. Then it is compared with the stability requirements of the particular physical processes which are allowed to subcycle if necesary to

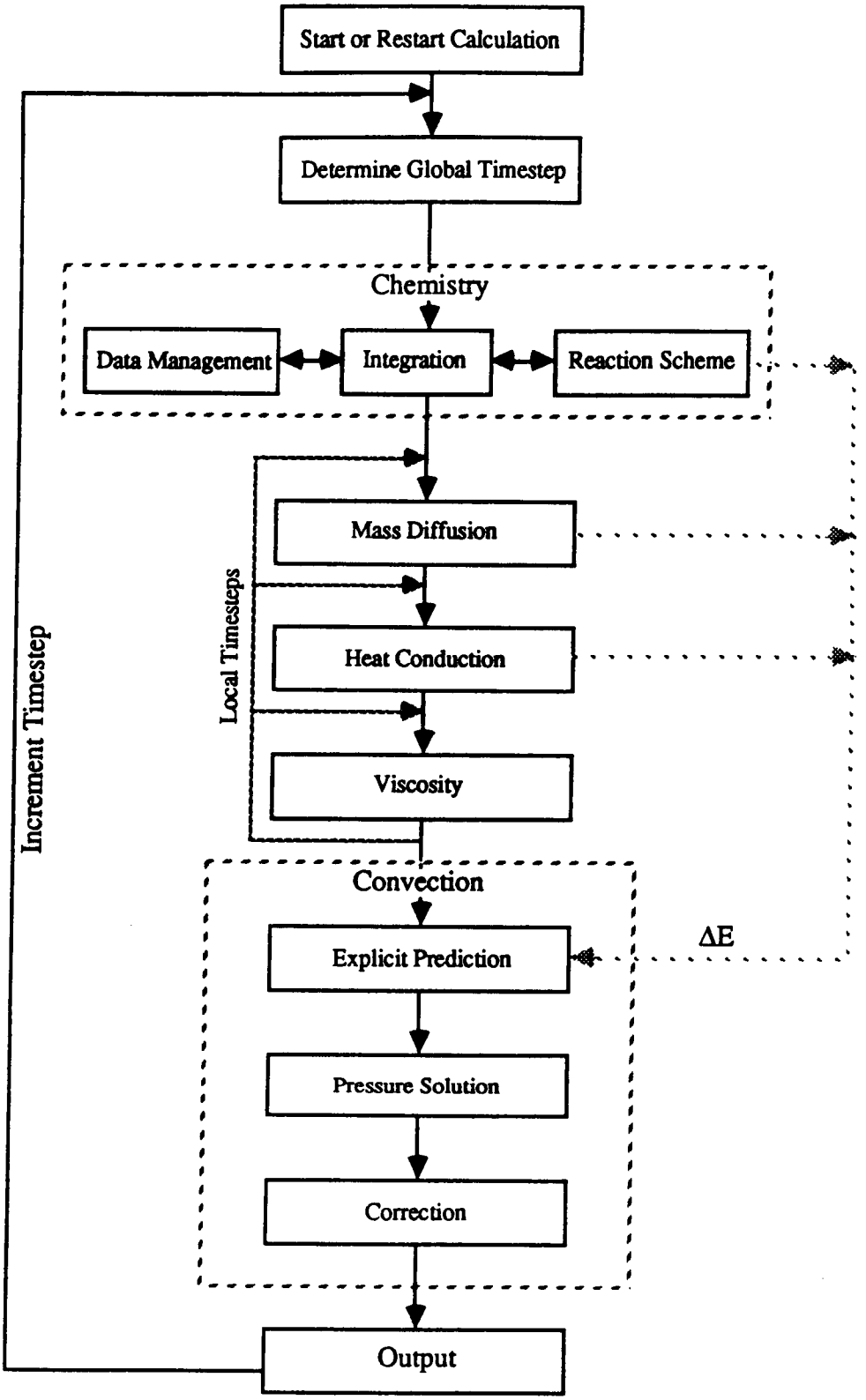

Figure 5.1 Flowchart of ***FLIC***, indicating interprocess communication.

ensure stability. The overall timestep must be decreased sometimes to ensure that a physical variable does not change too much during a timestep. The most obvious difference between the scheme shown in Fig. 5.1 and the standard timestep splitting approach is that changes in the internal energy caused by each process are evaluated and added up at the end of a global timestep. This energy change is then used by the BIC-FCT convection algorithm (see Eq. (2.7)). This approach is quite similar to that used in FLAME1D [22], however, now changes in the internal energy are accumulated instead of changes in the pressure. The ADINC method [11], used in FLAME1D, does not solve an energy equation, and thus the only way other processes can be coupled is through the pressure. The BIC-FCT scheme used by ***FLIC*** does not require that energy changes be applied only during the convection step; this is merely a convenience that allows for larger global timesteps due to tighter coupling.

Some of the individual process integrations in ***FLIC*** are subcycled within a global timestep, including the ordinary differential equations representing the chemical reactions and the diffusive terms such as molecular diffusion and thermal conduction. For example, the timestep limit imposed by some chemical reactions may be orders of magnitude lower than that required by other physical processes, and so the chemistry integration is subcycled. Subcycling is built into the chemistry integration in an extremely sophisticated manner [9], so that the maximum allowable timestep at each computational cell is used, completely independent of the timestep in other cells. The chemistry is integrated up to the overall timestep before it is coupled to the other processes. However, if the energy release in an overall timestep due to chemistry is too large (typically greater than 10%), then the overall timestep must be decreased. Mass diffusion and thermal conduction are also subcycled, but only up to five times. The accuracy of the solution is generally tested by performing a separate calculation with a smaller timestep and noting whether the solution has converged.

All dependent variables, except for internal energy, are updated after each process integration, but dependent variables are not updated during subcycling of a process. This leads to a considerable savings, especially during the chemistry integration, because the evaluation of the temperature exponentials in Arrhenius expressions is done only once per global timestep. On the other hand, the global timestep may have to be decreased if the dependent variables change too much.

One consequence of a source term in the energy equation is the possibility of "ripples" in the pressure, which then manifest themselves in other variables as well. These ripples arise if a strong source is localized to a region only a few cells wide. These ripples are insignificant in ***FLIC*** where the flame zone is well resolved, but can be significant in other applications [37]. One way to avoid the ripples is to use a high-frequency filter such as

$$P^{filtered} = P + \alpha \nabla^4 P,$$

where α is a small constant. Other filters, including another FCT step, can also be used.

The particular advantages to using timestep splitting are that we can write very modular programs in which the integration of each physical process can be carried out with an optimum method, debugging is simpler, and explicit subcycling can be used to keep the costs down. Implicit methods can be used to avoid subcycling, but are more expensive when compared to explicit methods subcycled only a few times. In ***FLIC***, only five subcycles are allowed for each of the diffusion processes. Chemistry, on the other hand, subcycles thousands of times. At this point, it is not entirely clear if the extreme simplicity of the CHEMEQ scheme [9] results in faster integration of the chemistry equations than a more complicated implicit scheme. Disadvantages of timestep splitting are that the coupling process can be complicated, the algorithms and the overall program are less stable, and the timestep must be carefully controlled. However, we have found that the benefits of modular and fast programs outweigh potential disadvantages. This is discussed in some detail by Oran and Boris [15], pages 131–133.

6. Applications

FLIC has been written in a general manner so that it can be applied to solve a variety of slowly evolving problems involving chemistry and diffusive transport processes. It has already been applied to the study of multidimensional flames in premixed gases [1,41,42] and co-flowing diffusion flames [37,43]. A specific application of the code to the study of cellular flames in hydrogen-oxygen-nitrogen mixtures is described below to show what is required to perform a calculation with the code and to interpret the output from the code. Then other applications of the code are briefly discussed to bring out the generality of ***FLIC***.

6.1 A Sample Calculation

Flames in lean hydrogen-oxygen-nitrogen mixtures are known to exhibit a multidimensional cellular structure. The cellular structure is the result of a thermo-diffusive instability of a planar flame in the same mixture. Below we demonstrate how FLIC can be used to simulate the transition from a planar flame to a multidimensional cellular flame in a zero-gravity environment.

We need as input to the model:

A chemical reaction scheme involving all the species of interest (table 3.1),
Molecular diffusion coefficients for each pair of species (table 4.1),
For each species:
Molecular weights,
Thermal conductivity (Table 4.2),
Viscosity (Table 4.3),

Heats of formation [22],

Enthalpy coefficients [22].

To complete the specification of the problem, we also need the initial and boundary conditions such as composition, pressure, and temperature, in addition to the physical and chemical parameters given above. Figure 6.1 describes the configuration studied and gives the boundary conditions of the computational domain. Unburnt gas flows in from the left, and reaction products of the flame front flow out at the right. If the inlet velocity equals the burning velocity of the flame, the flame is fixed in space yielding a steady solution. Thus, transient effects from ignition can be eliminated. The initial conditions for the two-dimensional calculations were taken from one-dimensional calculations that gave the conditions for steady, propagating flames. The two-dimensional computational domain for this simulation was 2.0 cm $\times$ 4.5 cm, resolved by a 56 $\times$ 96 variably spaced grid. Fine zones, 0.36 mm $\times$ 0.15 mm, were clustered around the flame front.

The initial conditions specify a planar flame in a fuel-lean hydrogen-oxygen mixture diluted with nitrogen, H_2:O_2:N_2/1.5:1:10, a flame that showed multidimensional structure in the experiments by Mitani and Williams [4]. In order to study the evolution to cellular structure, the initial conditions were perturbed by displacing the center portion of the planar flame in the direction of the flow. The evolution to cellular structure is obtained by studying the output from the simulations.

The output from the calculation consists of the spatial and temporal distribution of all the species involved as well as the fluid density, temperature, pressure, internal energy, and momenta. Display of the data is not done by ***FLIC***, but is instead done as a post-processing operation. This cuts down the length and complexity of the ***FLIC*** code. A very useful diagnostic is contour plots showing isotherms and species distributions. Diagnostics, such as color-flood plots, allow visual interpretation of the data.

Figure 6.2 shows a sequence of isotherms from the calculation. The isotherms show that the temperature increases in the center portion of the flame, convex to the flow, and decreases in the the two adjacent concave regions, indicating more vigorous reaction in the convex region. The atomic hydrogen concentration increases in the convex and decreases in the concave regions. Also, the burning velocity in the

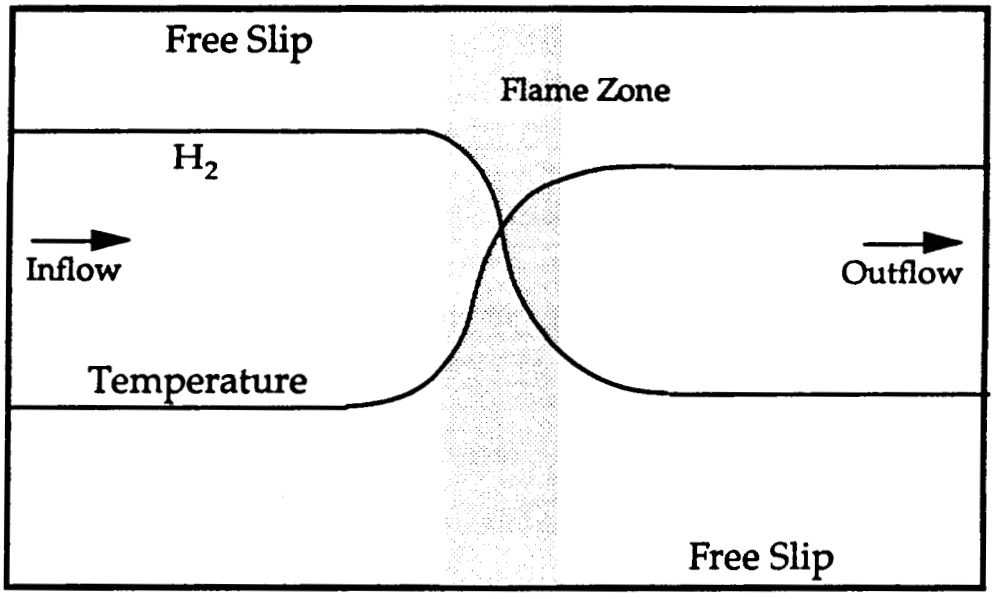

Figure 6.1 Initial and boundary conditions for the two-dimensional flame calculations.

convex region appears slightly higher than the burning velocity in a planar region, and the burning velocity in the concave regions were noticeably lower. Thus, this calculation shows that the planar lean one-dimensional hydrogen flame is unstable and evolves into a multidimensional flame having a cellular structure.

6.2 Applications of *FLIC*

The ***FLIC*** code has been used extensively to study the detailed evolution of cellular flames in premixed gases [1], to investigate the mechanisms which can lead to cellular structure [42], effects of gravity on flame structure and instabilities [41,42]. These studies have helped strengthen the prevailing theory of cellular instability and cast serious doubt on another theory which was also under consideration [1] ***FLIC*** has been geared primarily to these types of applications and several other related applications to premixed flames are planned for the near future.

FLIC can be converted to the study of diffusion flames extremely easily, and is begging for a suitable application in this area. A low-speed diffusion flame code [37,43] which has been used to study jet flames uses the same transport and diffusive packages as ***FLIC***. This code uses simplified chemistry, which was first calibrated by comparison to a detailed calculation with ***FLIC***.

6.3 Future Applications and Code Development

Calculations such as the one described earlier are time consuming (5 hours of CRAY X-MP time). There is interest to carry out these calculations in a larger domain for longer times. The cellular structure exhibited by flames is actually three-dimensional, so if these instabilities are to be studied fully, a three-dimensional version of ***FLIC*** is required. The computer time for these studies can quickly become intolerable; it is proposed to alleviate this by taking advantage of the multiprocessor architechure of the CRAY X-MP and the new Y-MP with its 16 processors. This will require some restructuring of the code and its algorithms to utilize microtasking appropriately. This restructuring may be simplified with the new "autotasking"

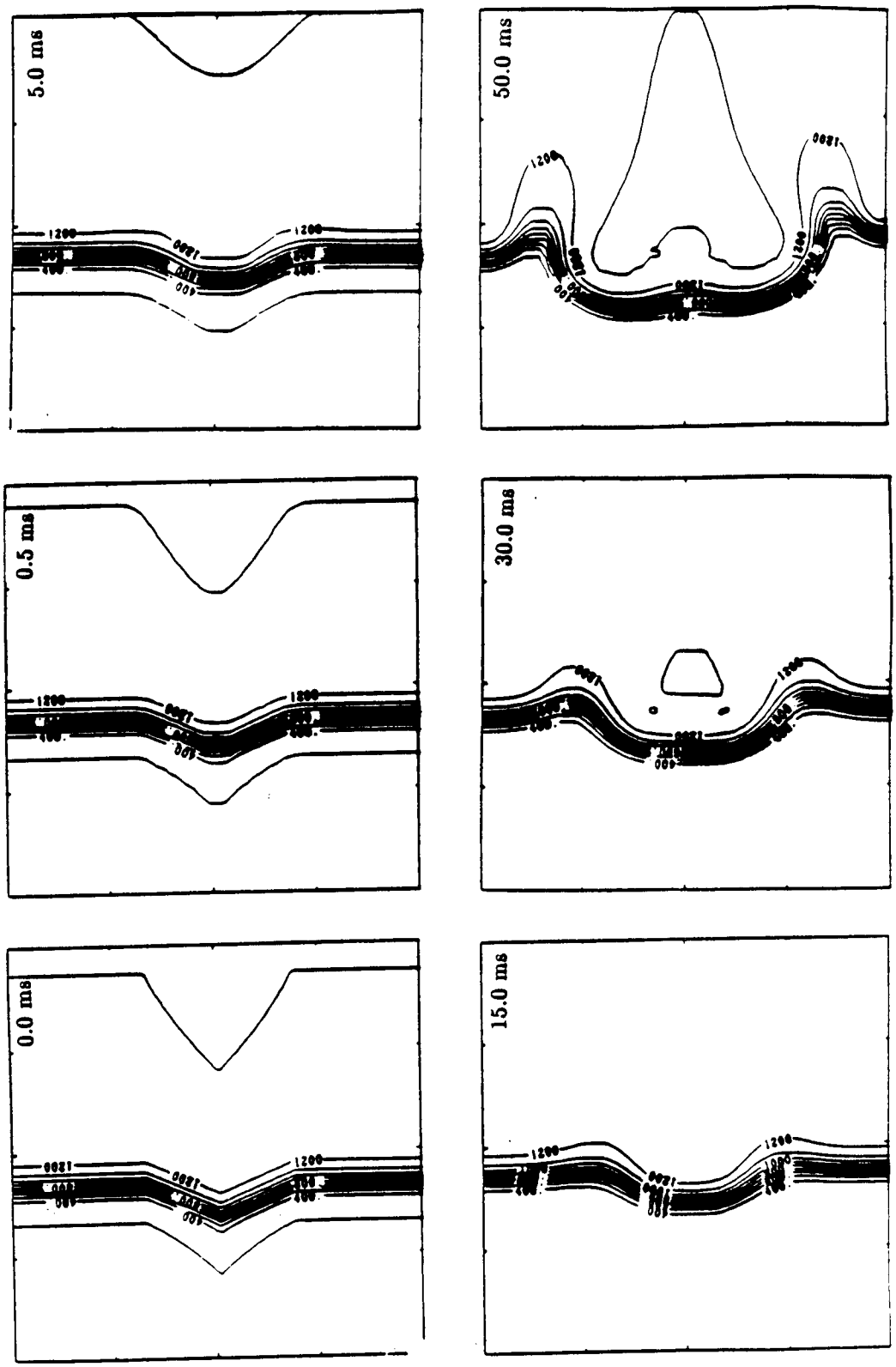

Figure 6.2 Evolution of isotherms in a fuel-lean hydrogen flame.

facility on the CRAY Y-MP.

One area of interest is the investigation of the behavior of flames near extinguishment. In particular, the prediction of flammability limits of flames in a flammability tube will provide a means for quantitative comparison with experiment. This complex task will require the addition of mechanisms which represent losses, including losses to the wall. The physics of the loss mechanisms of radicals to the walls is not yet fully understood. These additional mechanisms will need to be incorporated into ***FLIC***.

Detailed calculations will need to be performed for other more complex fuels of practical interest. The primary difficulty is in coping with the large number of species and chemical reactions that will be required for even the simplest hydrocarbon fuels. While the precise scaling of computer time with chemical complexity is not known, it is expected that the increase in the number of species will have the most dramatic effect. Thus, there is a need for reliable simplified chemistry models which have been first validated against a full model. It is anticipated that suitable simplified models for methane will become available soon. Radiation can not be neglected in hydrocarbon combustion. Thus a gas phase radiation model will have to be incorporated. Consideration of soot will have to wait until reliable models are available, which will not be in the near future.

All future applications are in areas that will require enormous amounts of computer time. One way to cut down on costs is to perform calculations only where they are strictly required. Calculations can be skipped in regions of low gradients, be it spatial or temporal gradients. This will require dynamic regridding or, more generally, re-discretization of the governing equations. A suitably efficient algorithm for this is essential, and its development is underway. Limitations and peculiarities of the target computer architecture will play a large role in determining the shape of these future versions of ***FLIC***.

Acknowledgments

This work was sponsored by NASA in the Microgravity Sciences Program and the Office of Naval Research through the Naval Research Laboratory. We also acknowledge some computational support from the Pittsburgh Supercomputing Center.

References

[1] G. Patnaik, K. Kailasanath, K. Laskey, and E. S. Oran. Detailed Numerical Simulations of Cellular Flames. In *Proceedings of the 22nd Symposium (International) on Combustion*, Pittsburgh, PA, 1989. The Combustion Institute.

[2] G. I. Barenblatt, Y. B. Zeldovich, and A. G. Istratov. On Diffusional Thermal Stability of Laminar Flame. *Zh. Prikl. Mekh. Tekh. Fiz.*, 4:21–26, 1962.

[3] G. I. Sivashinsky. Diffusional-Thermal Theory of Cellular Flames. *Combust. Sci. Tech.*, 15:137–146, 1977.

[4] T. Mitani and F. A. Williams. Studies of Cellular Flames in Hydrogen-Oxygen-Nitrogen Mixtures. *Combust. Flame.*, 39:169–190, 1980.

[5] J. P. Boris and D. L. Book. Solution of Convective Equations by the Method of Flux-Corrected Transport. In *Methods in Computational Physics*, volume 16, chapter 7, page 85. Academic Press, New York, 1976.

[6] J. P. Boris. Flux-Corrected Transport Modules for Solving Generalized Continuity Equations. Memorandum Report 3237, Naval Research Laboratory, 1976.

[7] G. Patnaik, R. H. Guirguis, J. P. Boris, and E. S. Oran. A Barely Implicit Correction for Flux-Corrected Transport. *J. Comput. Phys.*, 71:1–20, 1987.

[8] T. R. Young and J. P. Boris. A Numerical Technique For Solving Stiff Ordinary Differential Equations Associated with the Chemical Kinetics of Reactive Flow Problems. *J. Phys. Chem.*, 81:2424, 1977.

[9] T. R. Young. CHEMEQ — A Subroutine for Solving Stiff Ordinary Equations. Memorandum Report 4091, Naval Research Laboratory, 1980.

[10] K. Kailasanath and E. S. Oran. Time-Dependent Simulations of Laminar Flames in Hydrogen-Air Mixtures. Memorandum Report 5965, Naval Research Laboratory, 1987.

[11] J. P. Boris. ADINC: An Implicit Lagrangian Hydrodynamics Code. Memorandum Report 4022, Naval Research Laboratory, 1979.

[12] W. W. Jones and J. P. Boris. An Algorithm for Multispecies Diffusion Fluxes. *Comp. Chem.*, 5:139–146, 1981.

[13] J. P. Boris. A Fluid Transport Algorithm That Works. In *Computing as a Language of Physics*, pages 171–189. International Atomic Energy Agency, Vienna, 1971.

[14] P. Woodward and P. Colella. The Numerical Simulation of Two-Dimensional Fluid Flow with Strong Shocks. *J. Comp. Phys.*, 54:115–173, 1984.

[15] E. S. Oran and J. P. Boris. *Numerical Simulation of Reactive Flow.* Elsevier, New York, 1987.

[16] M. J. Fritts and J. P. Boris. The Lagrangian Solution of Transient Problems in Hydrodynamics Using a Triangular Mesh. *J. Comp. Phys.*, 31:173–215, 1979.

[17] B. A. Fryxell, P. R. Woodward, P. Colella, and K-H Winkler. An Implicit-Explicit Hybrid Method for Lagrangian Hydrodynamics. *J. Comput. Phys.*, 62, 1986.

[18] H. C. Yee and A. Harten. Implicit TVD Schemes for Hyperbolic Conservation Laws in Curvilinear Coordinates. In *AIAA 7th Computational Fluid Dynamics Conference*, pages 228–241, Washington, DC, 1985. AIAA.

[19] V. Casulli and D. Greenspan. Pressure Method for the Numerical Solution of Transient, Compressible Fluid Flows. *Int. J. Num. Methods Fluids*, 4:1001–1012, 1984.

[20] C. R. DeVore. Vectorization and Implementation of an Efficient Multigrid Algorithm for the Solution of Elliptic Partial Differential Equations. Memorandum Report 5504, Naval Research Laboratory, 1984.

[21] T. L. Burks and E. S. Oran. A Computational Study of the Chemical Kinetics of Hydrogen Combustion. Memorandum Report 4446, Naval Research Laboratory, 1981.

[22] K. Kailasanath, E. S. Oran, and J. P. Boris. A One-Dimensional Time-Dependent Model for Flame Initiation, Propagation, and Quenching. Memorandum Report 4910, Naval Research Laboratory, 1982.

[23] D. L. Baluch, D. D. Drysdale, D. G. Horne, and A. C. Lloyd. *Evaluated Kinetic Data for High Temperature Reactions*, volume 1. Butterworths, London, 1972.

[24] R. F. Hampson and D. Garvin. Chemical Kinetic and Photochemical Data for Modelling of Atmospheric Chemistry. NBS Technical Note 866, National Bureau of Standards, Washington, 1975.

[25] N. Cohen and K. R.. Westberg. Data Sheets. Technical report, The Aerospace Corporation, P. O. Box 92957, Los Angeles, CA, 1979.

[26] D. B. Olson and W. C. Gardiner Jr. An Evaluation of Methane Combustion Mechanisms. *J. Phy. Chem.*, 81:2514, 1977.

[27] A. C. Lloyd. Evaluated and Estimated Kinetic Data for Phase Reactions of the Hydroperoxyl Radical. *Int. J. Chem. Kinetics*, 6:169, 1974.

[28] G. S. Bahn. *Reaction Rate Compilation for H-O-N System.* Gordon and Breach, New York, 1968.

[29] T. A. Brun, T.R Young, and G. Patnaik. TBA — An Optimized Stiff ODE Solution Scheme. In preparation, 1989.

[30] P. J. Sydow. *Optimization Guide.* CRAY Research, Mendota Heights, 1983. CRAY Computer Systems Technical Note.

[31] S. Chapman and T. G. Cowling. *The Mathematical Theory of Non-Uniform Gases.* Cambridge University Press, Cambridge, 1970.

[32] T. P. Coffee and J. M. Heimerl. Transport Algorithms for Premixed Laminar Steady-State Flames. *Combust. Flame*, 43:273–289, 1981.

[33] J. O. Hirschfelder, C. F. Curtiss, and R. B. Bird. *Molecular Theory of Gases and Liquids.* John Wiley, New York, 1954.

[34] T. R. Marrero and E. A. Mason. Gaseous Diffusion Coefficients. *J. Phy. Chem. Ref. Data*, 1:3–118, 1972.

[35] C. F. Curtis and J. O. HIrschfelder. Transport Properties of Multicomponent Gas Mixtures. *J. Chem. Phys.*, 17:550, 1949.

[36] R. B. Bird, W. E. Stewart, and E. N. Lightfoot. *Transport Phenomena.* John Wiley, New York, 1960.

[37] K. J. Laskey. *Numerical Study of Diffusion and Premixed Flames.* PhD thesis, Department of Mechanical Engineering, Carnegie-Mellon University, Pittsburgh, PA, 1989.

[38] S. Mathur, P. K. Tandon, and S. C. Saxena. Thermal Conductivity of Binary, Ternary, and Quaternary Mixtures of Real Gases. *Mol. Phys.*, 12:569, 1967.

[39] C. R. Wilke. A Viscosity Equation for GAs Mixtures. *J. Chem. Phys.*, 18:517, 1950.

[40] N. N. Yanenko. *The Method of Fractional Steps.* Springer-Verlag, Ney York, 1971.

[41] K. Kailasanath, G. Patnaik, and E. S. Oran. Effect of Gravity on Multi-Dimensional Laminar Premixed Flame Structure. IAF Paper 88-354, IAF, Paris, 1988.

[42] G. Patnaik, K. Kailasanath, and E. S. Oran. Effect of Gravity on Flame Instabilities in Premixed Gases. AIAA Paper 89-0502, AIAA, Washington, DC, 1989.

[43] J. L. Ellzey, K. J. Laskey, and E. S. Oran. Study of Low-Speed Diffusion Flames. In preparation, 1988.

Appendix B

Effects of Curvature and Dilution on Flame Propagation

Effect of Curvature and Dilution on Unsteady, Premixed, Laminar Flame Propagation

K. Kailasanath and E.S. Oran

Reprinted from **Dynamics of Reactive Systems Part I: Flames and Configurations,** edited by J.R. Bowen, J.-C. Leyer, and R.I. Soloukhin, Vol. 105 of Progress in Astronautics and Aeronautics series. Published in 1986 by the American Institute of Aeronautics and Astronautics, Inc., 1633 Broadway, N.Y. 10019, 423 pp., 6×9, illus., ISBN 0-930403-14-2, $69.00 Member, $119.00 List.

Effect of Curvature and Dilution on Unsteady, Premixed, Laminar Flame Propagation

K. Kailasanath* and E.S. Oran†
Naval Research Laboratory, Washington, D.C.

Abstract

A time-dependent, one-dimensional, Lagrangian model was used to study laminar flames in stoichiometric hydrogen-oxygen mixtures diluted with nitrogen. For stoichiometric hydrogen-air mixtures we have seen that a spherically expanding flame first decelerates until the velocity reaches a minimum value, and then it accelerates. For large radii, the burning velocity approaches the planar burning velocity. These same trends are also observed as the amount of diluent is increased. With increasing dilution, the flames reach their minimum velocities at later times and larger radii. These observations are explained on the basis of flame stretch. The spherical geometry results are compared with the results from another set of calculations in planar geometry. These show that the minimum burning velocity reached by a spherical flame is less than that of a planar flame in the same mixture. In both planar and spherical geometries, the effect of increasing the dilution is to lower the burning velocities. Since the burning velocity is smaller in the spherical geometry, the flame can be extinguished (or quenched) with less dilution in the spherical geometry than in the planar geometry. We also discuss the implications of these results to laminar flame quenching and flammability limits.

Presented at the 10th ICDERS, Berkeley, California, August 4-9, 1985.

*Research Scientist, Laboratory for Computational Physics.
†Senior Scientist, Laboratory for Computational Physics.

Introduction

In this paper, we present and discuss time-dependent calculations of one-dimensional laminar flames in stoichiometric hydrogen-oxygen mixtures diluted with nitrogen. We use these calculations to study the effects of curvature (or stretch) and dilution on flame propagation in premixed gases. The results presented also have important applications to laminar flame quenching and flammability limits in the absence of external heat sinks.

Previous work on propane-air mixtures by Strehlow[1] shows that rich mixtures exhibit a higher flame velocity at small radii than at large radii, while lean mixtures show a lower flame velocity at small radii than at large radii. In all cases, for large enough radii the flame velocity relaxes to the appropriate planar flame velocity. Strehlow attributes these effects to preferential diffusion of the lighter species, and this has been verified by Frankel and Shivashinsky[2] using an asymptotic analysis. More recently, Law[3,4] used an asymptotic analysis to explain the behavior of stretched flames in rich and lean mixtures of methane and propane in air. These theoretical analyses are for either fuel-rich or fuel-lean conditions and use a simple phenomenology to represent the chemical kinetics.

This paper presents calculations of planar and spherically expanding flames in stoichiometric hydrogen-oxygen mixtures diluted with nitrogen. The results presented here are obtained from numerical simulations, which use a time-dependent, one-dimensional, Lagrangian model[5]. This numerical model was developed specifically to study the initiation, propagation and quenching of laminar flames. In addition to using a detailed chemical reaction mechanism, the model includes the effects of molecular diffusion, thermal conduction, and thermal diffusion of the individual species considered. Because of the level of detail incorporated in the model, the spatial structure and temporal evolution of the flame structure can be highly resolved.

The Numerical Model

The numerical model solves the time-dependent conservation equations for mass, momentum, and energy[6,7]. The model has been used for a variety of flame studies, including calculations of minimum ignition energies[8,9] quench

volumes[8], and burning velocities[10]. The model has a modular form and permits a wide variety of geometric, initial, boundary, and time varying energy input conditions. The algorithms representing the various chemical and physical processes are integrated separately and then asymptotically coupled by time-step splitting techniques[7]. The convective transport is solved by the algorithm ADINC, a Lagrangian fluid dynamic algorithm that solves implicitly for the pressures[11]. The method gives an accurate representation of material interfaces and allows steep gradients in species and temperature to develop and be maintained. In addition to considering the thermal conduction and molecular diffusion processes in detail, the model also includes thermal diffusion. The chemical interactions are described by a set of nonlinear, coupled ordinary differential equations that are solved using a fully vectorized version of the selected asymptotic integration method CHEMEQ[12,13].

For this study, we have used the hydrogen-oxygen reaction scheme[14], which involves the eight reactive species H_2, O_2, H, O, OH, H_2O, HO_2, H_2O_2 and a diluent, chosen to be nitrogen. The thermochemical properties of the various species involved are taken from the *JANAF* tables[14]. The chemical reaction mechanism (given in Kailasanath et al.[5,9]) has been extensively tested and shown to give good results. Burks and Oran[15] showed that the results computed with this mechanism compare well with experimentally observed induction times, second explosion limits, and the

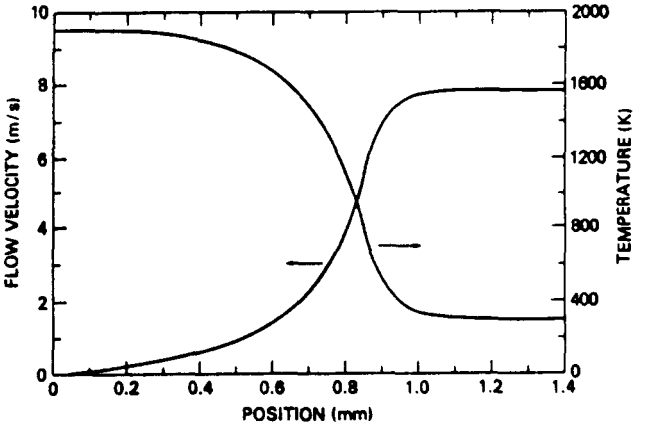

Fig.1 The flow velocity and temperature profiles in a planar flame propagating in a $H_2:O_2:N_2/2:1:4$ mixture.

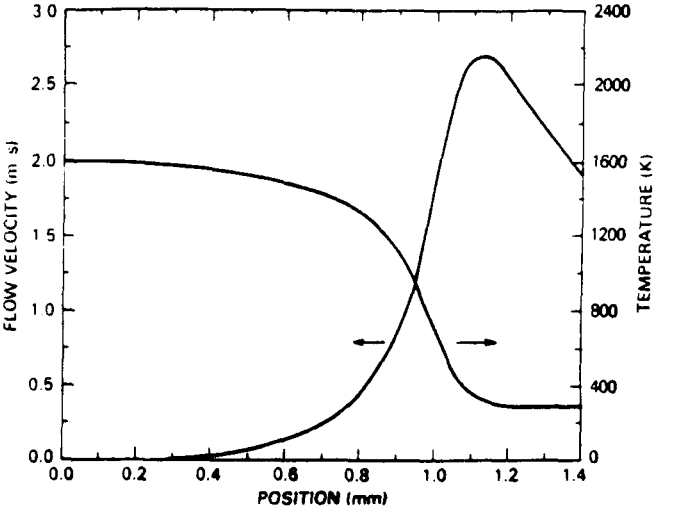

Fig.2 The flow velocity and temperature profiles at a particular time in a spherically expanding flame in a $H_2:O_2:N_2/2:1:4$ mixture.

temporal behavior of reactive species. Oran et al.[16] have shown that the mechanism coupled to a convective transport algorithm gives good results in the simulation of the conditions behind a reflected shock. The laminar burning velocities calculated using the mechanism are in agreement with experimental data[10].

For the calculations presented below, the model was configured with an open boundary at one end to simulate an unconfined system. Most of the calculations were done in a spherically symmetric one-dimensional geometry. Other calculations were done assuming a planar configuration. All the calculations are for stoichiometric mixtures of hydrogen and oxygen at an initial temperature and pressure of 298 K and 1 atm, respectively. The amount of nitrogen was varied, thereby varying the dilution.

Results and Discussion

Estimation of Burning Velocity

For either thin or planar flames, the instantaneous normal burning velocity can be calculated from the flame velocity if we know the velocity of the unburnt gases ahead of the flame. For planar flames, the velocity of the unburnt gases ahead of the flame is constant, as shown in Fig. 1, where the spatial variation of the flow velocity and the temperature across the flame is shown for a

hydrogen-air mixture. Hence the burning velocity can be unambiguously determined as the difference between the flame velocity and the flow velocity ahead of the flame,

$$V_b = V_f - V_{flow}$$

For a thin flame, a similar definition is adequate. However, when the flame has a finite thickness and is curved (as for a spherically expanding flame), the appropriate definitions for the location of the flame front and the fluid velocity of the unburnt gases are ambiguous. This can be seen in Fig. 2, in which the spatial variation of the flow velocity and the temperature across a spherical flame in a hydrogen-air mixture is shown. The fluid velocity reaches a maximum within the flame and then decreases ahead of the flame.

For the flames studied in this paper, two reference fluid velocities have been chosen for estimating the burning velocity. One of them is the maximum fluid velocity V_{max} in the system, and the other is the fluid velocity of the unburnt gases V_{300} corresponding to the first location ahead of the flame with temperature of 300 K. The lower estimate for the burning velocity is obtained as $V_f - V_{max}$ and the upper estimate as $V_f - V_{300}$. For a planar flame in which the fluid velocity ahead of the flame is constant and the same as the maximum fluid velocity, the two estimates for the burning velocity are identical.

Effects of Curvature

In the first set of calculations, a spherically expanding flame in a stoichiometric hydrogen-air (actually, $H_2:O_2:N_2/2:1:4$) mixture was studied. In these simulations, energy was deposited linearly over a fixed period of time at the center of a spherically symmetric system. The radius of energy deposition was larger than the quench-radius[9] and was held constant. We then tracked the spatial location of the flame kernal as a function of time and used this to calculate the apparent flame velocity as a function of time. The results of such a calculation are shown in Fig. 3. The flame velocity V_f initially decreases with time until it reaches a minimum value, and then it increases. The figure also shows the maximum fluid velocity V_{max} of the system and the fluid velocity of the unburnt gases V_{300} corresponding to the first location ahead of the flame with temperature of 300 K. With in-

creasing radii, the difference between the two fluid velocities decreases. For very large radii (not shown in the figure), there is an unambiguous burning velocity, since the two fluid velocities approach the same value. This estimated burning velocity approaches both the experimental value and the value determined from a separate planar one-dimensional calculation.

Effects of Dilution

We also performed a series of calculations in which the amount of diluent was varied. The results of one such calculation, for the H_2:O_2:N_2/2:1:7 mixture, are shown in Fig. 4. Increasing the amount of diluent does not change the observed trends: The flame velocity and the burning velocity decrease with increasing radii, attain a minimum value, and then increase with increasing radii. This calculation and the results shown in Fig. 5 for the 2:1:10 case show that it takes longer for the flame to reach the minimum flame velocity as dilution increases. For the 2:1:10 mixture, we expect the flame velocity to increase again at larger radius, following the trend seen in the other two mixtures. For this mixture, the burning velocity corresponding to the minimum flame velocity is 0.30 - 0.35 m/s, whereas the calculated burning velocity for a

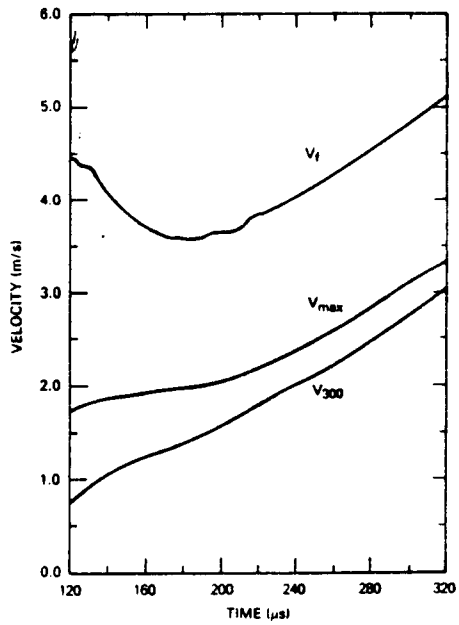

Fig. 3 Time history of the propagation of a spherically expanding flame in a H_2:O_2:N_2/2:1:4 mixture. The flame velocity is denoted V_f, the maximum fluid velocity is V_{max}, and the velocity of the first position ahead of the flame with a temperature of 300 K is V_{300}.

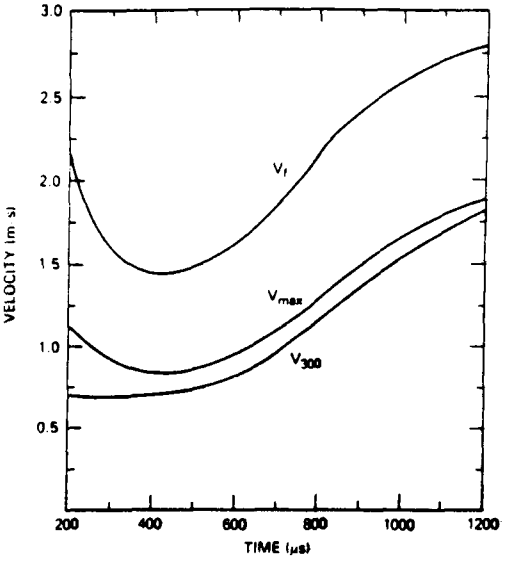

Fig. 4 Time history of the propagation of a spherically expanding flame in H_2:O_2:N_2/2:1:7 mixture. (See Fig. 3 for legends.)

planar flame in the same mixture is 0.85 - 0.90 m/s. Thus the burning velocity of a spherical flame corresponding to the minimum value of the flame velocity is smaller than that of a planar flame in the same mixture. We have observed this trend in all of the stoichiometric mixtures we have studied.

Some of the more dilute mixtures studied do not support spherical flame propagation. One such case is the H_2:O_2:N_2/2:1:13 mixture, in which the flame velocity does not level off but continues to decrease until the flame dies. Figure 6 shows V_f, V_{max}, and V_{300} as a function of time for this case. We varied the radius of energy deposition, the amount of energy input, and the mode of energy input. In all cases, the flame died after propagating for a short time.

When we modeled flame propagation in the planar geometry, we observed significiant burning velocities for a wider range of mixtures than in the spherical geometry. For example, the burning velocity was between 0.34 and 0.40 m/s for the H_2:O_2:N_2/2:1:13 mixture. As mentioned above, this mixture did not support spherical flame propagation.

We have used the term "spherical flame" to mean a flame whose radius of curvature is comparable to its thickness. A flame of very large radius (typically, an order of magnitude larger than the flame thickness) behaves like a

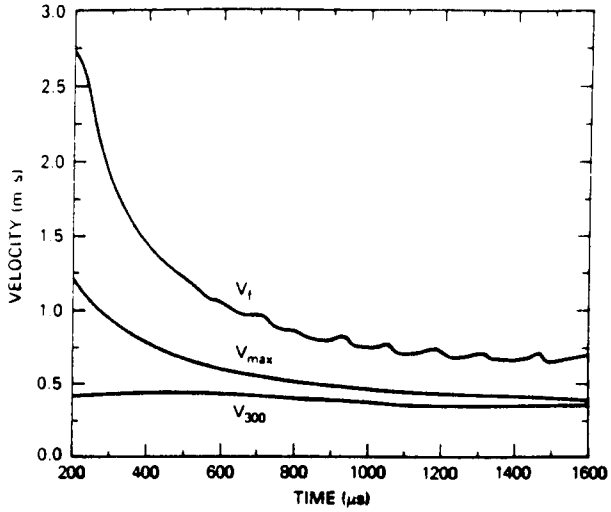

Fig.5 Time history of the propagation of a spherically expanding flame in H_2:O_2:N_2/2:1:10 mixture. (See Fig. 3 for legends.)

planar flame, and can propagate in the H_2:O_2:N_2/2:1:13 mixture. Such a flame can be initiated by depositing a large amount of energy over a very large spherical volume of gas.

Effects of Stretch

The observed time histories of the flame velocity can be explained on the basis of stretch (due to flow divergence) and chemical kinetics. First, consider the initial deceleration of V_f in spherical geometry. Initially, due to flow divergence, the energy released in chemical reactions does not balance the energy conducted and diffused into the unreacted mixture. Because of this, the flame velocity and temperature decrease as the flame expands. The decrease in the flame temperature decreases the energy release rate, which leads to a lower flame velocity, and so on. However, this process does not continue indefinitely, because the stretch effect decreases with increasing radii. Because of this effect a minimum flame velocity is observed in spherical flame propagation. As the radius of the flame increases further, the energy released in chemical reactions is larger than the energy conducted and diffused into the unburnt mixture. Now the flame velocity increases with increasing radii until a balance is attained between the energy released by chemical reactions and the energy conducted and diffused into

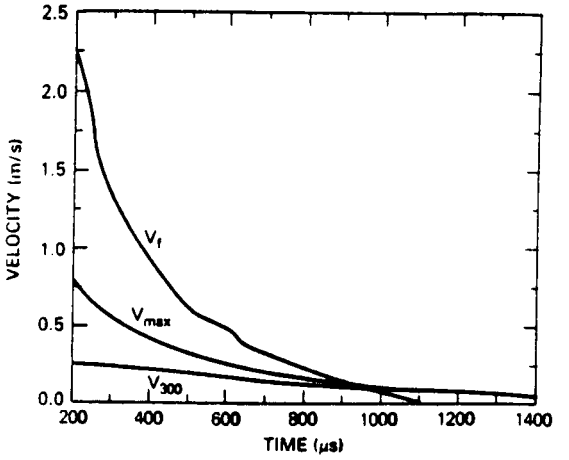

Fig.6 Time history of the propagation of a spherically expanding flame in a H_2:O_2:N_2/2:1:13 mixture. (See Fig. 3 for legends.)

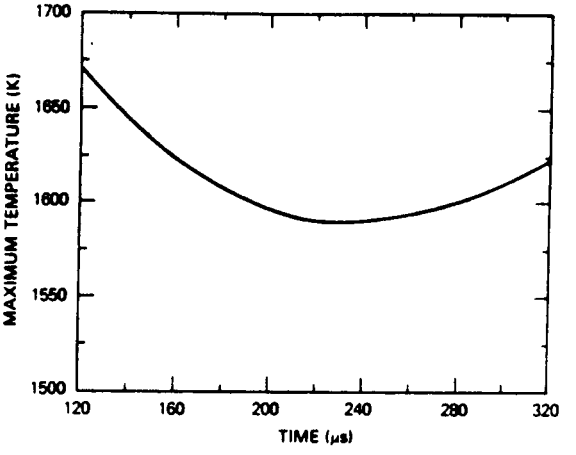

Fig.7 Time history of the maximum temperature of a spherically expanding flame in a H_2:O_2:N_2/2:1:4 mixture.

the unburnt mixture ahead of the flame. Such a balance occurs for large radii, and then the flame propagates as if it were planar.

The above observations are verified by the temperatures calculated in the numerical simulations. The time history of the maximum temperature in a spherically expanding flame in a hydrogen-air mixture is shown in Fig. 7. The maximum temperature corresponding to the minimum velocity spherical flame is significantly lower than that of

a planar flame in the same mixture. After reaching a minimum, the flame temperature increases and tends toward the temperature corresponding to a planar flame in the same mixture.

The actual radius at which the minimum flame velocity occurs and the radius at which the effect of stretch becomes negligible depend on the flame thicknesss. Since the flame thickness increases with increasing dilution, a flame in a more dilute mixture will have to propagate to a larger radius in order to overcome the effects of stretch. This explains the observation made above, which showed that the minimum flame velocity is reached at a later time (and a larger radius) as dilution is increased. Not only is the minimum flame velocity reached later, but the magnitude of the velocity and the flame temperature are smaller. Therefore, by increasing the dilution, one can obtain a mixture which will be quenched by endothermic reactions before it can overcome the effects of stretch. This appears to be the case with the $H_2:O_2:N_2/2:1:13$ mixture.

Summary and Conclusions

We have studied flames in stoichiometric hydrogen-oxygen mixtures diluted by nitrogen in spherical and planar geometries using time-dependent , one-dimensional numerical simulations. The model includes a full description of the eight reactive species involved in hydrogen-oxygen kinetics, plus detailed models for the chemical kinetics, thermal conduction, and thermal and molecular diffusion processes. These studies have led to a number of interesting observations and important questions on flame behavior.

We have seen that in a stoichiometric hydrogen-air mixture, the flame velocity of spherically expanding flames first decreases with increasing radii and then increases. For large radii, the burning velocity approaches the planar burning velocity. These same trends are observed when the amount of diluent is increased. However, with increase in dilution, the minimum flame velocity is reached at a later time and at a larger radius. Comparing these spherical geometry results with another set of calculations in planar geometry shows that the minimum burning velocity of a spherical flame is less than that of a planar flame in the same mixture.

In both planar and spherical geometries, the effect of increasing the dilution is to lower the burning velocities. Since the burning velocity is smaller in the spherical geometry, the flame can be extinguished (or quenched) with less dilution in the spherical geometry than in the planar geometry. The existence of a quench-radius and a minimum ignition energy in the absence of heat or radical loss to walls or other external sinks has already been demonstrated[9] . The results presented here indicate that such "self-quenching" also depends on the geometry or curvature.

The time histories of the flame velocity are controlled by stretch (due to flow divergence) and energy release by chemical reactions. The maximum temperature of a spherically expanding flame exhibits the same trends as the flame velocity. The actual radius at which the minimum flame velocity occurs and the radius at which the effect of stretch becomes less important depends on the thickness of the flame. The thickness of the flame increases with increasing dilution. Therefore, a more dilute flame will have to propagate to a larger radius in order to overcome the effects of stretch. The minimum flame velocity and the flame temperature decrease with increasing dilution. Therefore, by increasing the dilution, one can obtain a mixture which will be quenched by endothermic reactions before it can overcome the effects of stretch. This appears to be the case with the H_2:O_2:N_2/2:1:13 mixture, which does not support spherical flame propagation.

It has been shown experimentally that the addition of inert gases to confined fuel-air mixtures can cause the flammability limits to become narrower . That is, by adding sufficient amounts of an inert gas, we can obtain a mixture that does not support flame propagation. Our calculations support this conclusion even though we do not include any heat or radical loss to the confining walls. The actual limits obtained might, however, depend on parameters such as the method of initiation, the duration of energy deposition, and the geometry of the system. By systematically varying these parameters as well as the stoichiometry, the numerical simulations can be used to help answer questions regarding the existence of fundamental flammability limits.

Acknowledgments

This work was sponsored by the Office of Naval Research through the Naval Research Laboratory. The authors

would like to thank Jay Boris for the many fruitful discussions we have had on the ignition, quenching, and propagation of flames.

References

[1]Strehlow, R.A. (1984) Combustion Fundamentals. McGraw-Hill, New York.

[2]Frankel, M.L. and Shivashinsky, G.I. (1983) On effects due to thermal expansion and Lewis number in spherical flame propagation. Combust. Sci. Technol. 31, 131-138.

[3]Law, C.K. (1984) Heat and mass transfer in combustion: Fundamental concepts and analytical techniques. Prog. Energy Combust. Sci. 10, 295-318.

[4]Law, C.K. (1984) Dynamics of stretched flames. Abstracts of the Eastern Section of the Combustion Institute, Fall 1984 Technical Meeting, pp. C1-C11. The Combustion Institute, Pittsburgh, Pa.

[5]Kailasanath, K., Oran, E.S., and Boris, J.P. (1982) A one-dimensional time-dependent model for flame initiation, propagation and quenching. NRL Memorandum Report No. 4910, Naval Research Laboratory, Washington, D.C.

[6]Williams, F.A. (1965) Combustion Theory, p. 2. Addison-Wesley, Reading, Mass.

[7]Oran, E.S. and Boris, J.P. (1981) Detailed modelling of combustion processes. Prog. Energy Combust. Sci. 7, 1-71.

[8]Oran, E.S. and Boris, J.P. (1981) Theoretical and computational approach to modeling flame ignition. Prog. Astronaut. Aeronaut. 76, 154-171.

[9]Kailasanath, K., Oran, E.S., and Boris, J.P. (1982) A theoretical study of the ignition of premixed gases. Combust. Flame 47, 173-190.

[10] Kailasanath, K., Oran, E.S., and Boris, J.P. (1982) Time-dependent simulation of flames in hydrogen-oxygen-nitrogen mixtures. Numerical Methods in Laminar Flame Propagation, p. 152. Friedr. Vieweg & Sohn, Wiesbaden, West Germany.

[11]Boris, J.P. (1979) ADINC: An implicit Lagrangian hydrodynamics code. NRL Memorandum Report 4022, Naval Research Laboratory, Washington, D.C.

[12]Young, T.R. and Boris, J.P. (1977) A numerical technique for solving stiff ordinary differential equations associated with chemical kinetics of reactive-flows problems. J. Phys. Chem. 81, 2424-2427.

[13]Young, T.R. (1980) CHEMEQ - A subroutine for solving stiff ordinary differential equations. NRL Memorandum Report 4091, Naval Research Laboratory, Washington, D.C.

[14]Stull, D.R. and Prophet, H. (1971) JANAF Thermochemical Tables, NSRDS-NBS 37, 2nd ed., National Bureau of Standards, Gaithersburg, Md.

[15]Burke, T.L. and Oran, E.S. (1981) A computational study of the chemical kinetics of hydrogen combustion. NRL Memorandum Report 4446, Naval Research Laboratory, Washington, D.C.

[16]Oran, E.S., Young, T.R., Boris, J.P. and Cohen, A. (1982) Weak and strong ignition. I. Numerical simulations of shock tube experiments. Combust. Flame 48, 135-148.

[17]Zabetakis, M.G. (1965) Flammability characteristics of combustible gases and vapors. U.S. Bureau of Mines Bulletin 627, Pittsburgh, Pa.

Appendix C

Flame Propagation and Extinction in Fuel-Rich Mixtures

TIME-DEPENDENT SIMULATIONS OF LAMINAR FLAMES IN HYDROGEN-AIR MIXTURES

1. Introduction

In this paper, we present results of detailed numerical simulations of laminar flames in hydrogen-air mixtures. We use these simulations to discuss two major problems: (1) the relative importance of various diffusive transport processes on flame propagation in fuel-lean, stoichiometric, and fuel-rich mixtures, and (2) the time-dependent behavior of flames near the rich flammability limit.

Various numerical simulation techniques have been applied to study a wide variety of problems involving the ignition, propagation and quenching of hydrogen flames. However, there have not been many attempts to use the detailed modeling approach to study quantitatively the relative importance of various physical mechanisms involved in flame propagation. In one such effort [1], numerical simulations were used to evaluate the relative importance of thermal conduction and diffusion of species in specific methane and methanol flames. The calculations seemed to indicate that flame propagation is not governed primarily by diffusion of radicals but diffusion of fuel which subsequently affects the chemical reactions. More recently, we [2] showed that neither diffusion of species nor thermal conduction alone could give the correct burning velocity for a stoichiometric hydrogen-oxygen-nitrogen mixture. In the first part of this paper, we present a systematic study of the relative importance of various diffusive transport processes to flame propagation in fuel-lean, stoichiometric and fuel-rich hydrogen-air mixtures.

In an earlier study on the effects of curvature and dilution on flame propagation [3], we showed that a flame can be extinguished with less dilution in one geometry than in another, even in the absence of external heat losses and buoyancy effects. Specifically, we showed that a planar flame can propagate steadily in a dilute mixture which does not support a spherically expanding flame. Because this behavior is related to the effects of flame stretch, it raises the fundamental question of whether there is an extinguishment limit in the absence of stretch effects. This question can be addressed by carefully studying the behavior of planar flames in the absence of external heat losses and gravitational effects. Both lean and dilute hydrogen-oxygen-nitrogen mixtures are subject to flame instabilities.

Manuscript approved January 13, 1987.

Therefore, we restrict ourselves to the extinguishment behavior of fuel-rich hydrogen-air flames in the second part of this paper.

2. The Numerical Model

The results presented in this paper are derived from numerical simulations using FLAME1D, a one-dimensional, Lagrangian model [4,5]. The model solves the time-dependent conservation equations for mass, momentum and energy [6,7]. The model has been used for a variety of flame studies, including calculations of burning velocities [5], minimum ignition energies [8] and quench volumes [8]. The model has a modular form and permits a wide variety of geometric, initial, boundary, and time varying energy input conditions.

The convective transport is solved by ADINC, a Lagrangian algorithm which solves implicitly for the pressure [9]. Because the method is Lagrangian and there is no numerical diffusion due to convective transport, the method gives an accurate representation of material interfaces and allows steep gradients in species and temperature to develop and be maintained. An adaptive Lagrangian regridding algorithm refines the grid ahead of the flame-front so that the flame zone remains well resolved throughout the calculation. Thermal conduction, ordinary diffusion, and thermal diffusion processes are included for each chemical species. The chemical interactions are described by a set of nonlinear, coupled ordinary differential equations which are solved using a fully vectorized version of the selected asymptotic integration method CHEMEQ [10,11]. The algorithms representing the various chemical and physical processes are integrated separately and then asymptotically coupled by timestep-splitting techniques [7].

For this study we have used the hydrogen-oxygen reaction scheme [12] which involves the eight reactive species H_2, O_2, H, O, OH, H_2O, HO_2, H_2O_2, and the diluent, N_2. The thermochemical properties of the various species involved are taken from the JANAF tables [13]. The chemical reaction mechanism [4,8,12], consisting of about fifty steps has been extensively tested and shown to give good results. Burks and Oran [12] showed that the results computed with this mechanism compared well with experimentally observed induction times, second explosion limits and the temporal behavior of reactive species. Oran et al. [14] have shown that when coupled to a convective transport algorithm, the mechanism gives good results in the simulation of the conditions behind a reflected shock. The laminar burning velocities calculated using the mechanism are in agreement with experimental data [5].

In the calculations presented below, the model was configured with an open boundary at one end to simulate an unconfined system. All the calculations were performed in a planar

(Cartesian) geometry. The initial temperature and pressure of the mixtures considered were 298 K and 1 atm, respectively.

The calculations were initialized with a Gaussian temperature profile. The central temperature and width were chosen so that the added initial energy was above the minimum ignition energy for the mixture. That is, it was ensured that the initial conditions provided enough energy for the flame to evolve to a steady profile.

For either thin or planar flames, the instantaneous normal burning velocity can be calculated from the flame velocity if we know the velocity of the unburnt gases ahead of the flame. As shown in Fig. 1, for planar flames the velocity of the unburnt gases ahead of the flame is constant. Hence the burning velocity can be unambiguously determined as the difference betweeen the flame velocity and the flow velocity ahead of the flame,

$$V_{burn} = V_{flame} - V_{fluid} \ .$$

We have discussed this definition and its application to curved flames elsewhere [3].

3. Relative Effects of Various Diffusive Transport Processes

A series of calculations have been performed to study the effects of the individual diffusive transport processes on flame propagation in hydrogen-air mixtures. The three different diffusive transport processes we consider are 1) thermal conduction, 2) ordinary diffusion, and 3) thermal diffusion. In order to isolate the relative importance of each, we have performed calculations with different combinations of these processes turned on. We repeated the same sequence of calculations for three mixtures:

Fuel-lean: H_2:O_2:N_2 / 0.65:1:3.76

Stoichiometric: H_2:O_2:N_2 / 2:1:3.76

Fuel-rich: H_2:O_2:N_2 / 15:1:3.76.

Table 1 summarizes the calculated burning velocities from this series of calculations. For each of the three mixtures considered we show four different cases:

(a) All three diffusive transport processes are on;

(b) Thermal diffusion is off, and thermal conduction and ordinary diffusion are on;

(c) Thermal conduction is on, and thermal diffusion and ordinary diffusion are off;

(d) Thermal conduction off, and ordinary and thermal diffusion are on.

Several interesting trends in burning velocities appear from looking at this table. First, we see that the relative importance of thermal diffusion does not change from lean to rich mixtures. However, the relative importance of thermal conduction and ordinary diffusion are different for lean, stoichiometric, and rich mixtures.

3.1 The Effect of Thermal Diffusion on Burning Velocities

By comparing cases (a) and (b) in Table 1, we see that the effect of thermal diffusion is to lower the burning velocities by 6–10% in all three mixtures. The effects of thermal diffusion in hydrogen-air mixtures have been studied earlier [4,15,16].

Hydrogen atoms are the fastest moving, most easily diffused species in the system. Their diffusion behavior dominates the diffusion properties of the hydrogen-air system. Hydrogen atoms are formed in the high-temperature region of the flamefront, and are then diffused into the cold mixture by ordinary diffusion. Earlier studies have shown that thermal diffusion tends to diffuse hydrogen atoms from the lower temperature region to the higher temperature region [4,15]. Thus these two processes have the opposite effect with respect to moving hydrogen atoms. The increase in burning velocity when there is no thermal diffusion occurs because thermal diffusion inhibits the diffusion of hydrogen radicals into the cold, unburnt mixture ahead of the flamefront.

3.2 Stoichiometric Mixture

For the stoichiometric mixture, thermal conduction and ordinary diffusion are almost equally important in determining the burning velocity of the flame. Without thermal conduction, the burning velocity is reduced to 62% of its standard value, i.e., the value of the burning velocity with all of the diffusive transport processes turned on. Without ordinary diffusion, it is reduced to 46% of its standard value. Figure 2 shows the behavior of the flame and burning velocities as a function of time. The initial condition causes a large initial velocity which eventually relaxes to a steady flame velocity.

3.3 Fuel-Lean Mixture

For the lean mixture, Table 1 shows that turning off either thermal conduction or ordinary diffusion lowers the burning velocity. In particular, we note that thermal conduction is much more important than ordinary diffusion in determining whether or not the flame propagates. When the thermal conduction is turned off, the flame does not reach a steady burning velocity at all.

Figure 3 shows the calculated flame velocity and fluid velocity as a function of time for case (d), where the flame appears to die. The flame velocity decreases with time, and becomes practically identical to the fluid velocity. The result is a negligible burning velocity. Using a time-dependent model to study burning velocities allows us to see the flame die out in time. No changes in the initial conditions which we tried could keep this flame from eventually "dying out" in the way shown in the figure.

For this lean flame, radicals can diffuse ahead of the flame front, but without thermal conduction, the temperature ahead of the flame never becomes high enough to sustain the reaction. The fuel deficit also means a deficit of hydrogen radicals, which hinders the reaction process. Thermal conduction alone, however, carries forward enough heat to create new radicals and sustain the process. Figure 4 shows the difference in the hydrogen radical profiles for cases (a), (c) and (d) at typical times in the calculation.

3.4 Fuel-Rich Mixture

For the fuel-rich mixture, ordinary diffusion is the most important process in determining the burning velocity. In contrast to the fuel-lean flame, the fuel-rich flame does not propagate without ordinary diffusion. In the fuel-rich case, not enough heat can be transferred by conduction alone to sustain the reactions. However, because of the excess of hydrogen radicals, ordinary diffusion alone can spread enough radicals ahead of the front to initiate chemical reactions and sustain the flame.

4. Flames in Fuel-rich Mixtures

In the second set of calculations we restricted ourselves to flames in fuel-rich hydrogen-air mixtures. In these calculations all the diffusive transport processes discussed above were included. The amount of hydrogen in the mixture was systematically increased and with each concentration of hydrogen, the calculations were carried out untill a steadily propagating flame (if any) was observed. The burning velocities were calculated as discusssed earlier. The burning velocity and the temperature of the burned gases (flame temperature) for the various mixtures are summarized in Table 2. As expected, the burning velocity and the flame temperature decrease with increasing fuel concentration. However, a couple of interesting observations can be made from the data presented in the table.

First of all, for a 80.8% hydrogen-air mixture (H_2:O_2:N_2 / 20:1:3.76), we obtain a steady burning velocity of about 8 cm/s. This mixture is beyond the experimentally observed rich-flammability limit under normal gravity conditions. This difference between the numerical and experimental observations may be due to the effects of gravity, heat losses to the confining walls in the experiments or multidimensional effects. As mentioned earlier, these effects have not been included in these numerical simulations. For example, we know from previous calculations [3] that curvature (or stretch) can reduce the burning velocity.

The second interesting observation from the numerical simulations is that a 82.2% hydrogen-air mixture (H_2:O_2:N_2 / 22:1:3.76) does not support a steadily propagating flame. We tried different ignition sources but in all cases the burning velocity decreased to zero. The behavior of the transient flame was qualitatively similar to that shown in Fig. 3 for a dying flame. The simulations indicate that there is a flammability limit even in the absence

of stretch, buoyancy and external heat losses. Furthermore this limit is higher than that observed in the standard flammability limit tube under normal gravity conditions.

A possible reason for this flammability limit can be seen in the trend of flame temperatures shown in Table 2. The flame temperature for a 20:1:3.76 mixture is just 970 K. With increase in fuel concentration the temperature would decrease further. At these temperatures, it is possible that the H atoms are consumed faster in chain terminating reactions than produced in chain branching reactions. This would result in a depletion of H atoms and a decrease in temperature. This could eventually lead to a situation where the energy released in exothermic reactions is not sufficient to balance the energy diffused by the transport processes and hence a steady flame is not possible. This possibility is currently being investigated.

5. Summary and Conclusions

We have examined two fundamental problems in premixed laminar flames using a detailed one-dimensional model. The model is time-dependent and can calculate the evolution to a steady-state, propagating flame from an initial energy source. Because it is time-dependent, the absence of a steady-state can also be revealed by it.

In the first problem, we examined the relative importance of thermal conduction, thermal diffusion, and ordinary diffusion in determining the burning velocities of laminar hydrogen-air flames. Three cases were examined in detail: a fuel-lean mixture, a stoichiometric mixture, and a fuel-rich mixture. For the fuel-lean and fuel-rich mixtures, care was taken to ensure that the mixture considered was far enough from the limit to have a finite, but relatively low, burning velocity. The results are summarized in Table 1, which shows the burning velocities calculated for the three mixtures.

The effect of thermal diffusion is to decrease the burning velocity by 5–10%, in agreement with previous calculations [4,15,16]. This can be explained by noting that the effect of thermal diffusion is to diffuse hydrogen radicals in towards the hot region of the flame, instead of out towards the unburned region. It has the opposite effect of ordinary diffusion and thus inhibits the flame-propagation process.

For the stoichiometric mixture, both thermal conduction and ordinary diffusion make important contributions to sustaining the flame. When thermal conduction was turned off, the burning velocity was reduced to 62% of its standard value. When ordinary diffusion was turned off, the burning velocity decreased to 46% of its standard value. These results were qualitatively as expected.

The more surprising results were for the fuel-rich and the fuel-lean mixtures. For the fuel-lean mixture, the flame would not propagate when thermal conduction was turned off.

That is, ordinary diffusion alone could not sustain the flame. However, the burning velocity was only 69% of its standard value with just thermal conduction.

In contrast to the fuel-lean behavior, the fuel-rich mixture could not sustain a flame when ordinary diffusion was turned off. That is, thermal conduction alone could not sustain the flame. With just ordinary and thermal diffusion, the burning velocity was 86% of its standard value.

Our general conclusion from this study is that both ordinary diffusion and thermal conduction are necessary to quantitatively describe flame propagation in a hydrogen-air mixture. Their relative importance, however, varies as we go from fuel-lean to fuel-rich hydrogen-air mixtures. It is not clear that these conclusions hold for hydrocarbon combustion, since there are other, heavier radicals that might change the balance between thermal conduction and ordinary diffusion. An implication of this work to flame modelling efforts is that it may be possible to neglect thermal diffusion, but both molecular diffusion and thermal conduction must be included in the model.

In the second part of this paper we considered the behavior of flames in fuel rich hydrogen-air mixtures near the experimentally observed flammability limit. The effects of gravity, stretch and external heat losses were eliminated in the numerical simulations. The results suggest wider flammability limits than those observed experimentally under normal gravity conditions. The simulations indicate that there may be a limit due to chemical kinetic considerations alone. Further details of a possible chemical-kinetic limit are currently under investigation. The simulations also suggest that multi-dimensional calculations under normal gravity conditions and experiments under reduced gravity conditions are needed to better understand flames near the standard flammability limits.

6. Acknowledgements

This work was sponsored by the Office of Naval Research through the Naval Research Laboratory and by the National Aeronautics and Space Administration through the Microgravity Combustion Program. We would like to thank Jay Boris, Paul Ronney, Howard Ross, and Kurt Sacksteder for their encouragement and many helpful discussions and Alexandra Fields for her help with the calculations and graphics.

References

1. J.R. Creighton: 1980 Fall Technical Meeting of the Eastern Section of the Combustion Institute, Princeton, NJ, Paper No. 53 (The Combustion Institute 1980)
2. K. Kailasanath, E.S. Oran: 1985 Fall Technical Meeting of the Eastern Section of the Combustion Institute, Philadelphia, PA, Paper No. 10 (The Combustion Institute 1985)

3. K. Kailasanath, E.S. Oran: Effects of Curvature and Dilution on Unsteady, Premixed, Laminar Flame Propagation, NRL Memorandum Report 5659, (Naval Research Laboratory, Washington, D.C. 1985). Also in Dynamics of Reactive Systems, Prog. Astro. Aero., Vol.105, Part 1, (American Institute of Aeronautics and Astronautics, New York 1986) p. 167

4. K. Kailasanath, E.S. Oran, J.P. Boris: A One-dimensional Time-dependent Model for Flame Initiation, Propagation and Quenching, NRL Memorandum Report No. 4910, (Naval Research Laboratory, Washington, D.C. 1982)

5. K. Kailasanath, E.S. Oran, J.P. Boris: In Numerical Methods in Laminar Flame Propagation, ed. by N. Peters and J. Warnatz, (Friedr. Vieweg & Sohn, Braunschweig 1982) p. 152

6. F.A. Williams: Combustion Theory, p. 2, (Addison-Wesley, Reading 1965)

7. Oran, E.S. and Boris, J.P.: Prog. Energy Comb. Sci. 7, 1 (1982)

8. K. Kailasanath, E.S. Oran, J.P. Boris: Combust. Flame. 47, 173 (1982)

9. J.P. Boris: ADINC: An Implicit Lagrangian Hydrodynamics Code, NRL Memorandum Report 4022, (Naval Research Laboratory, Washington, D.C. 1979)

10. T.R. Young, J.P. Boris: J. Phys. Chem. 81, 2424 (1977)

11. T.R. Young: CHEMEQ - A Subroutine for Solving Stiff Ordinary Differential Equations, NRL Memorandum Report 4091, (Naval Research Laboratory, Washington, D.C. 1980)

12. T.L. Burks, E.S. Oran: A Computational Study of the Chemical Kinetics of Hydrogen Combustion, NRL Memorandum Report 4446, (Naval Research Laboratory, Washington, D.C. 1981)

13. D.R. Stull, H. Prophet: JANAF Thermochemical Tables, NSRDS-NBS 37, 2nd Ed., (National Bureau of Standards, Gaithersburg 1971)

14. E.S. Oran, T.R. Young, J.P. Boris, A. Cohen: Combust. Flame 48, 135 (1982)

15. G. Dixon-Lewis: Phil. Trans. Roc. Soc. A 292, 45 (1979).

16. J. Warnatz: In Numerical Methods in Laminar Flame Propagation, ed. by N. Peters and J. Warnatz, (Friedr. Vieweg & Sohn, Braunschweig 1982) p. 94

Table 1. – Burning Velocities of H_2-Air Mixtures

Case	Processes On	Lean	Stoichiometric	Rich
(a)	All	36 cm/s	185 cm/s	44 cm/s
(b)	Thermal Conduction Ordinary Diffusion	40	195	48
(c)	Thermal Conduction	25	85	0
(d)	Ordinary Diffusion Thermal Diffusion	0	115	38

Table 2. – Flames in Fuel-Rich Mixtures

Mixture $H_2 : O_2 : N_2$	Burning Velocity (cm/s)	Flame Temperature (K)
16:1:3.76	38	1180
17:1:3.76	30	1108
18:1:3.76	23	1046
19:1:3.76	16	1002
20:1:3.76	8	970
22:1:3.76	—	<970

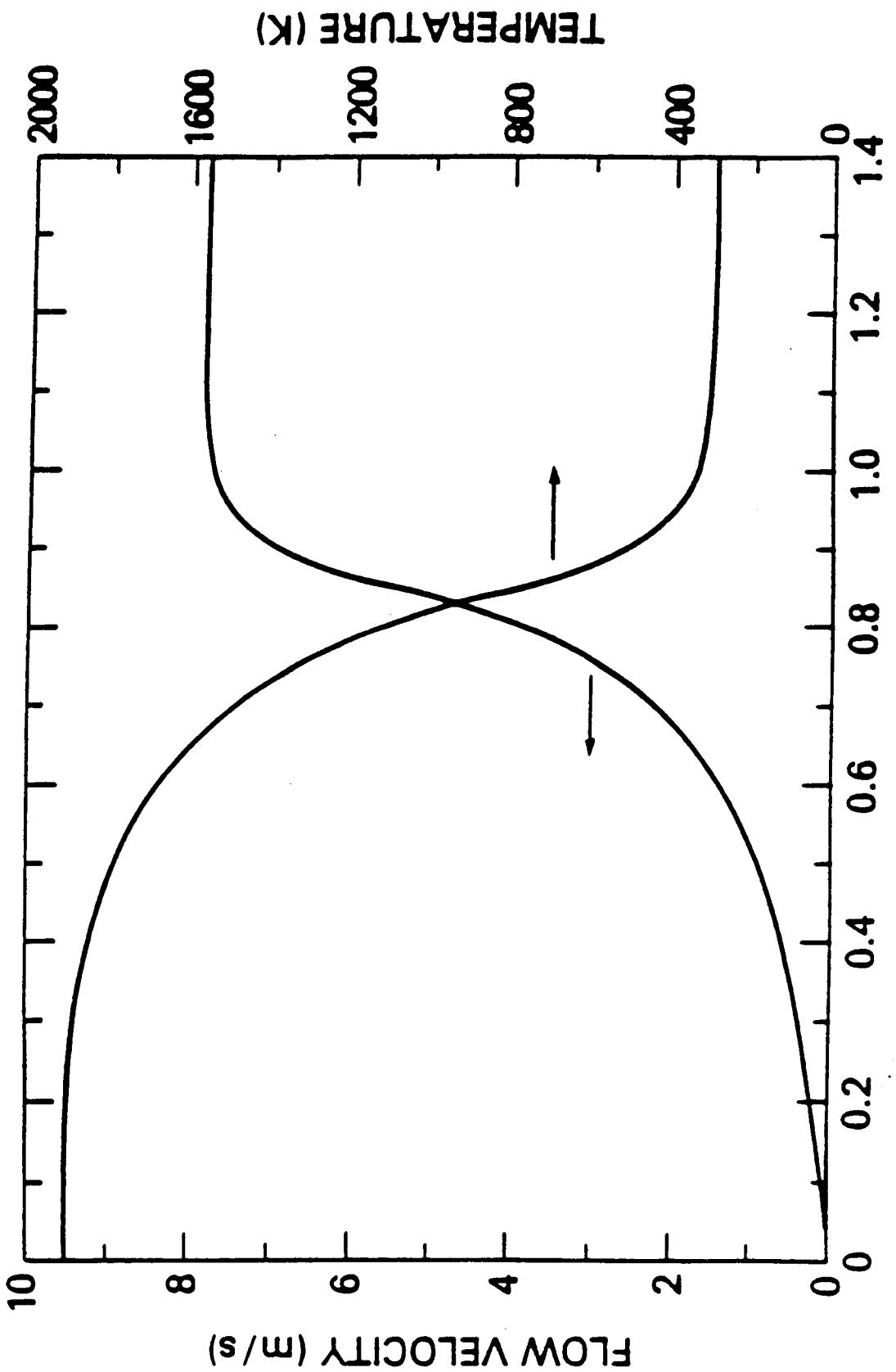

Fig. 1 — Velocity and temperature profiles in a planar flames propagating in an H_2:O_2:N_2/2:14 mixture.

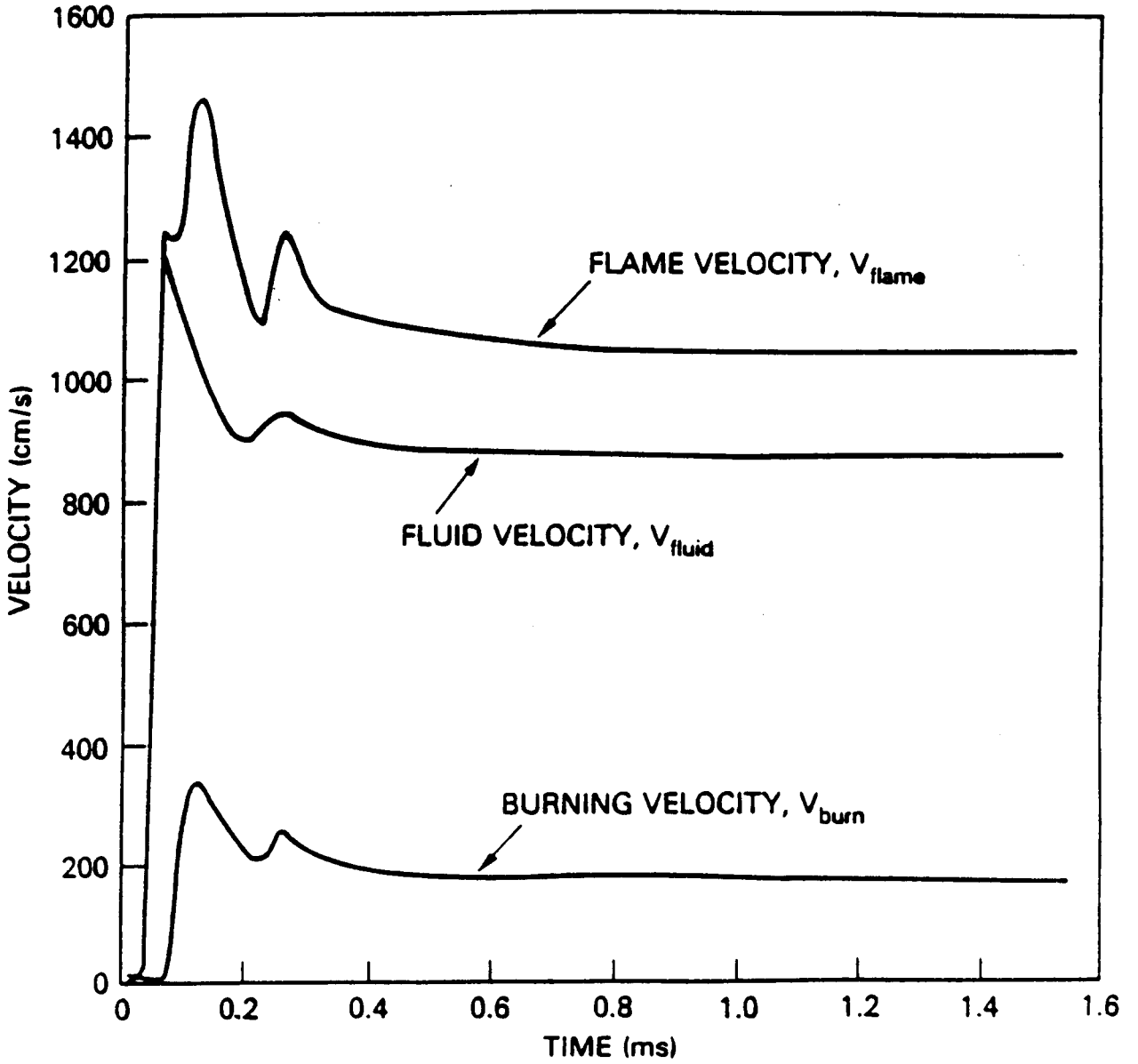

Fig. 2 — Calculated fluid, flame, and burning velocities as a function of time for the mixture H_2:O_2N_2/2:1:3.76 at 298 K and 1 atm.

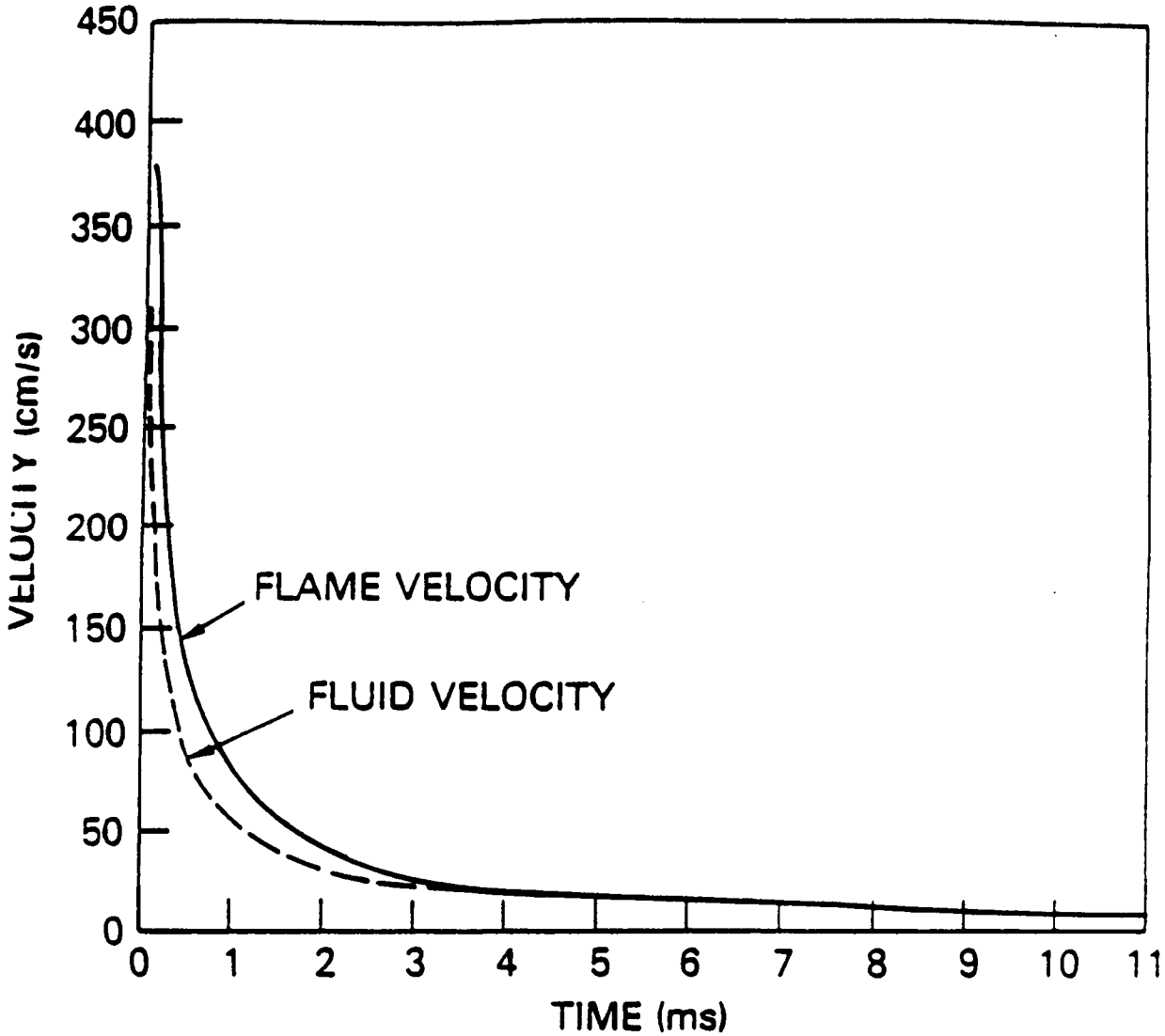

Fig. 3 — Calculated flame and fluid velocities as a function of time for the H_2:O_2:N_2/0.65:1:3.76 mixture.

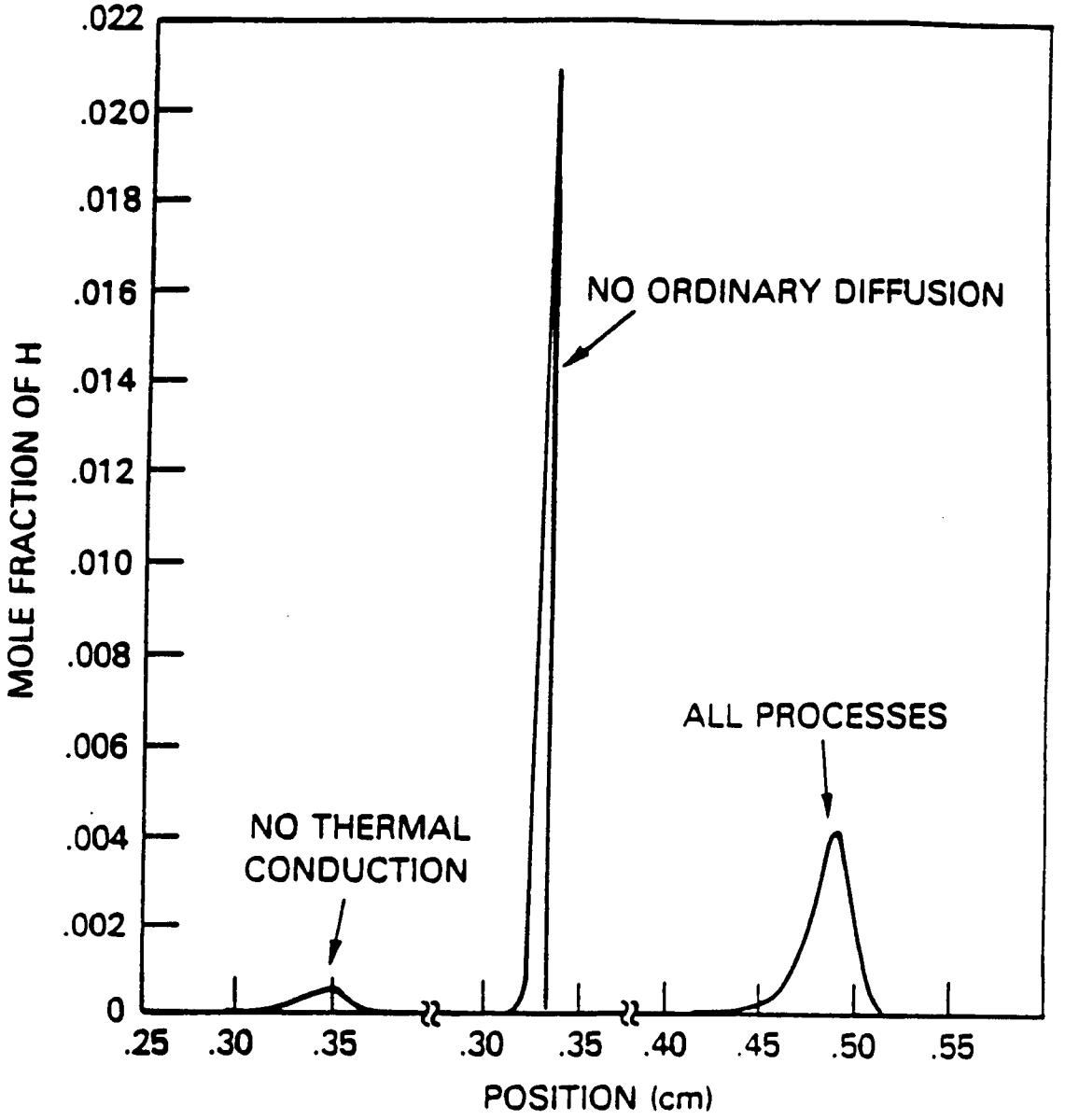

Fig. 4 — Hydrogen radical number densities at typical times in the calculation for the lean H_2:O_2:N_2/0.65:1:3.76 mixture.

Appendix D

Detailed Numerical Simulations of Cellular Flames

DETAILED NUMERICAL SIMULATIONS OF CELLULAR FLAMES

G. Patnaik*, K. Kailasanath, K.J. Laskey†, and E.S. Oran

Center for Reactive Flow and Dynamical Systems
Laboratory for Computational Physics and Fluid Dynamics
Naval Research Laboratory
Washington, D.C. 20375

* Berkeley Research Associates, Springfield, VA 22150
† Carnegie-Mellon University, Pittsburgh, PA 15213

Abstract

Time-dependent two-dimensional simulations of perturbed premixed laminar flames have been used to study the development of cellular structures in rich and lean hydrogen flames. The model includes a detailed reaction mechanism for hydrogen-oxygen combustion consisting of 25 elementary reactions among eight reactive species and a nitrogen diluent, molecular diffusion between all of the species, thermal conduction, and convection. Calculations of the evolution of a perturbed lean hydrogen flame showed that the flame was unstable at the front, and the structure that evolved resembled the cellular structures observed in experiments. The same perturbation applied to a rich hydrogen flame showed that the perturbation died out and cellular structures did not appear. Tests of the importance of molecular diffusion were carried out by varying the binary diffusion coefficients. First, the binary diffusion coefficient of molecular hydrogen was set equal to that of molecular oxygen, in which case the perturbation died out. Then, the binary diffusion coefficient of molecular oxygen was set equal to that of molecular hydrogen, in which case the instability persisted. The results of the simulations support the diffusional-thermal theory of flame instability.

I. Introduction

Previous one-dimensional, time-dependent numerical simulations of laminar premixed flames have given physical insights and quantitative information on the effects of parameters such as stretch, curvature, and dilution on flame initiation and propagation, as well as qualitative information on flammability limits[1,2]. The structure of flames, especially near the flammability limits, is usually multidimensional. To investigate such multidimensional effects, we have developed a detailed time-dependent two-dimensional model that can be used to simulate either premixed or diffusion flames. In this paper, we present results of calculations that used this model to study premixed laminar flames in rich and lean hydrogen-oxygen mixtures diluted with nitrogen. The results of these simulations are discussed in terms of current theories of flame stability and the formation of cellular structures. The validity of two prominent theories of cellular instability is investigated.

Early experimental observations showed that cellular flames occur in lean hydrogen-air as well as in rich hydrocarbon-air mixtures such as propane and ethane[3,4]. Cellular flames have generally been observed in lean fuel-air mixtures when the fuel is lighter than air and in rich fuel-air mixtures when the fuel is heavier than air[4,5]. These observations suggest that the relative diffusivities of fuel and air play a crucial role in determining the sensitivity of a mixture to cellular instability and lead to the formulation of the preferential diffusion theory[5]. According to this theory, preferential diffusion of the lighter reactant will create regions of

varying stoichiometry in front of a non-planar flame. This in turn causes portions of the flame to move at different speeds, making the flame front either less or more planar. This theory, however, does not explain all of the observations of cellular flames. For example, ethane and ethylene have molecular weights close to but less than that of oxygen, and yet they show cellular structure in rich mixtures.

Another theory of cellular flames is the diffusional-thermal theory[6,7]. In this theory, an abundance of the excess component was assumed, so that the reaction is controlled only by the deficient component. Then for the simple case of a one-step reaction, in what is effectively a single reactant system, this theory predicts that cellular instability occurs when the thermal diffusivity of the mixture is sufficiently small compared to the mass diffusivity of the reactant. For lean hydrogen-air mixtures, hydrogen is the limiting reactant and its mass diffusivity significantly exceeds the thermal diffusivity of the mixture. In rich hydrogen-air mixtures, oxygen is the limiting reactant and its mass diffusivity is nearly the same as the mixture thermal diffusivity. Hence the theory agrees with the early experimental predictions that lean hydrogen-air mixtures are unstable and rich mixtures are stable.

A limitation of the diffusional-thermal theory is that it assumes that the density of the fluid is a constant, and hence the effects of thermal expansion are neglected. Furthermore, according to this theory, the cell size increases indefinitely as the Lewis number goes to its critical value. More recent experimental observations[8,9] have shown cellular instabilities in some rich and near stoichiometric hydrogen-air mixtures, in contrast to the predictions of both the preferential diffusion as well as the diffusional-thermal theories. The diffusional-thermal theory is strictly valid only for strongly non-stoichiometric mixtures, although it has been extended[10,11] to near stoichiometric mixtures by considering both the deficient and abundant components. According to this two-reactant theory, the stability behavior depends on the stoichiometry of the mixture, the difference between the Lewis numbers of the two components, and the reaction orders of each reactant. This observation suggests that in multicomponent systems, the Lewis numbers of many of the components and detailed chemical kinetics might play a role. The modified diffusional-thermal theory also neglects the thermal expansion of the combustion products.

The simulations of multidimensional flame structure presented here include a multi-reaction mechanism for hydrogen combustion, molecular diffusion between the reactants, intermediates,

and products, thermal conduction, and convection. Such a detailed model should allow us to investigate the tendency of mixtures to show cellular instability, to evaluate the importance of various contributing physical processes, and to evaluate the predictions of the various theories. For example, previous explanations of cellular instability have considered the fuel and oxidizer, but the instability may also depend on the diffusivities of intermediate radicals. In addition, the effects of the fluid dynamics and therefore the variable gas density can be evaluated. Below we describe the numerical model, show the results of using this model to simulate a series of hydrogen-oxygen flames with different stoichiometries, and then relate these results to the predictions of two theories of flame instability.

II. Multidimensional Flame Model

A detailed model of a flame must contain accurate representations of the convective, diffusive, and chemical processes. The individual importance of these processes varies from rich to lean flames, and is especially notable near the flammability limits[2] where the exact behavior of these flames depends on a delicate balance among the processes. In this section we briefly describe the algorithms and input data used to model and couple the effects.

The fluid convection algorithm must be able to maintain the sharp gradients present in flames. Numerically this means that any important numerical diffusion in the calculation must be considerably less than any physical diffusion effect. Many explicit algorithms now exist that treat sharp discontinuities in flow variables accurately, but these methods are extremely inefficient at the very low velocities associated with laminar flames. The Barely Implicit Correction Flux-Corrected Transport (BIC-FCT) algorithm[12] was developed specifically to solve low-speed flow problems with high accuracy. BIC-FCT solves the coupled continuity equations for a variable density flow. BIC-FCT combines an explicit high-order, nonlinear FCT method[13,14] with an implicit correction process. This combination maintains high-order accuracy and yet removes the timestep limit imposed by the speed of sound. By using FCT for the explicit step, BIC-FCT is accurate enough to compute with sharp gradients without overshoots and undershoots. Thus spurious numerical oscillations that would lead to unphysical chemical reactions do not occur. The computational cost per timestep needed for BIC-FCT is about the same as for the standard explicit FCT method[12], which is an amazing gain considering that BIC-FCT

is implicit and the standard FCT is explicit.

Thermal conductivity of the individual species is modeled by a polynomial fit in temperature to existing experimental data. Individual conductivities are then averaged using a mixture rule[15,16] to get the thermal conductivity coefficient of the gas mixture. A similar process is used to obtain the mixture viscosity from individual viscosities. Heat and momentum diffusion are then calculated explicitly using these coefficients. In the problem considered in this paper, the timestep restriction of an explicit method for the diffusion terms does not cause any loss in efficiency.

Mass diffusion also plays a major role in determining the properties of laminar flames. Binary mass diffusion coefficients are represented by an exponential fit to experimental data, and the individual species diffusion coefficients are obtained by applying mixture rules[15]. The individual species diffusion velocities are solved for explicitly by applying Fick's law followed by a correction procedure to ensure zero net flux[16]. This procedure is equivalent to using the iterative algorithm DFLUX[17] which solves the multi-component diffusion equations exactly. This method is substantially faster than one that uses matrix inversions and is well suited for a vector computer. This algorithm is also explicit, but because the effective Lewis number of the mixture is close to one, the timestep suitable for heat conduction is adequate for mass diffusion as well.

Chemistry of the hydrogen–oxygen flame is modeled by a set of 24 reversible reactions describing the interaction of eight reacting species, H_2, O_2, H, O, OH, HO_2, H_2O_2, H_2O, and N_2 as a non-reacting diluent[18]. This reaction set is solved at each timestep with a vectorized version of CHEMEQ, an integrator for stiff ordinary differential equations[19]. Because of the complexity of the reaction scheme and the large number of cells in a two-dimensional calculation, the solution of the chemical rate equations takes a large fraction of the total computational time. A special version of CHEMEQ called TBA was developed to exploit the special hardware features of the CRAY X-MP vector computer. The full potential of new computer architectures can only be tapped at the expense of portability of programs to other machines.

All of the chemical and physical processes are solved sequentially and then are coupled asymptotically by timestep splitting[20]. This modular approach greatly simplifies the model and makes it easier to test and change the model. Individual modules were tested against

known analytic and other previously verified numerical solutions. One-dimensional predictions of the complete model were compared to those from the Lagrangian model FLAME1D which has been benchmarked extensively against theory and experiment[15]. The exact values of the input data for a hydrogen-oxygen flame, for example, the chemical reaction rates, thermodynamic parameters, and molecular diffusion coefficients, have been described in detail in previous papers[15], and therefore for brevity are only referenced here.

III. Tests of Mechanisms of Laminar Flame Instability

Initial conditions for the two-dimensional calculations were taken from one-dimensional calculations run to give the conditions for steady, propagating flames. Figure 1 describes the configuration under study and gives the boundary conditions of the computational domain. Fresh unburnt gas flows in from the left, and the products of chemical reaction at the flame front flow out at the right. If the inlet velocity is set to the burning velocity of the flame, the flame zone is fixed in space and a steady solution is obtained. Thus, the transient effects arising from the ignition process can be eliminated and the one-dimensional solution provides the initial condition for the two-dimensional calculation. The two-dimensional computational domain was 2.0 cm × 4.5 cm, which was resolved by a 56 × 96 variably spaced grid. Fine zones, 0.36 mm × 0.15 mm, were clustered around the flame front.

Flames in a Hydrogen-Lean Mixture

The first calculation is of a flame in a fuel-lean mixture of hydrogen and oxygen diluted with nitrogen, H_2:O_2:N_2 / 1.5:1:10, a flame that was clearly multidimensional in the experiments by Mitani and Williams[9]. The initial condition described by Fig. 1 is perturbed by displacing the center portion of the flame in the direction of the flow. The frames in Fig. 2 show isotherms just after the perturbation and then their evolution at subsequent times. The isotherms indicate that the temperature increases in the center portion of the flame which is convex to the flow and decreases in the the two adjacent concave regions. This indicates that the reaction progresses more vigorously in the convex region. This conclusion is corroborated by the atomic hydrogen number density contours in Fig. 3. The concentration of atomic hydrogen increases in the convex region and decreases in the concave regions. Also, the burning velocity in the convex region appears to be slightly higher than in a planar region, and in the concave regions the

burning velocity has noticeably decreased. We conclude that this lean one-dimensional flame is unstable, and a pattern resembling a cellular structure has appeared by the time the calculation was terminated.

Flames in a Hydrogen-Rich Mixture

The second case considered the evolution of a disturbance in a fuel-rich mixture of hydrogen and oxygen, H_2:O_2:N_2 / 3.0:1:16. This mixture is stable in the experiments of Mitani and Williams[9], and also in our calculations. The initial disturbance is quickly damped, restoring the flame profile to its one-dimensional shape. The frames in Fig. 4 show the evolution of temperature contours for the rich flame. The perturbed center section rapidly straightens out, indicating that the flame speed here is lower than in the planar sections. Figure 5 gives the atomic hydrogen contours for the rich flame. The number density of atomic hydrogen is lower in the center, indicating a weaker reaction and hence a lower burning velocity. This is the opposite of the behavior we observed in the lean flame calculations.

These two results are in agreement with experiments and with both the theory of preferential diffusion and the diffusional-thermal theory. In the next two studies, the diffusion coefficients of the reactants (H_2 and O_2) were changed in a systematic manner in order to determine the correct role of mass diffusion. All other variables were held the same as in the fuel-lean case (H_2:O_2:N_2 / 1.5:1:10).

The Role of Mass Diffusion

By setting the diffusion coefficient of hydrogen equal to that of oxygen, the light reactant no longer moves faster than the heavier reactant. This change in the model resulted in a stable one-dimensional flame. Figure 6 shows that the isotherms straighten out and slowly return to the unperturbed planar condition. A lower concentration of atomic hydrogen was found in the center section of the flame front, which agrees with the observed stability of the flame.

The fact that the modified lean flame described above is stable supports the theory of preferential diffusion. Because the diffusion coefficient of hydrogen equals that of oxygen, there can be no preferential diffusion of hydrogen to cause the instability. The remaining stabilizing factors, such as heat conduction, restore the flame to its unperturbed position. However, these results are also in agreement with the diffusional-thermal theory. Since the Lewis number of

the reactants in the modified lean flame is close to unity, the diffusional-thermal mechanism for instability is greatly reduced. The stabilizing factors overcome any tendency to instability.

A further test was needed to distinguish between these two mechanisms. In this test, the diffusion coefficients of the oxygen molecule were set to that of the hydrogen molecule. Now there are two fast species. All other conditions were unchanged from the lean flame test. This case again eliminates preferential diffusion and thus if preferential diffusion is indeed the mechanism, this flame should be stable. However, as Fig. 7 indicates, the flame is unstable and closely resembles the standard lean-flame result shown in Fig. 4. This result contradicts the predictions of the preferential diffusion theory. The diffusional-thermal theory, on the other hand, predicts that because the mass diffusion of the deficient species, molecular hydrogen, remains high, this flame will be unstable. Thus the series of numerical simulations presented here support the diffusional-thermal theory of cellular instability.

IV. Conclusion

A new time-dependent two-dimensional model has been used to study the stability of rich and lean premixed laminar hydrogen-oxygen flames diluted with nitrogen. The model included a detailed chemical reaction scheme consisting of 24 reversible reactions among eight species, thermal conductivity, and the individual species diffusion velocities. Four tests were presented which showed the evolution of perturbed two-dimensional flames:

1. A lean flame, H_2:O_2:N_2 / 1.5:1:10,
2. A rich flame, H_2:O_2:N_2 / 3.0:1:16,
3. The lean flame with the H_2 diffusion coefficients set equal to the O_2 diffusion coefficients, and
4. The lean flame with the O_2 diffusion coefficients set equal to the H_2 diffusion coefficients.

The numerical simulations show that the one-dimensional lean flame is unstable, and by the time the calculation is terminated, evolves into a pattern that resembles a cellular flame. The rich flame, however, is stable, and the perturbation dies in time. Both of these results agree with those in the experiments of Mitani and Williams[9] for mixtures with the same stoichiometry.

We then ask if we can use the simulation to determine the mechanism controlling the

instability. This is addressed by the third and fourth calculations, which focus on the mass diffusion of the reactants, H_2 and O_2. In the third calculation, the mass diffusivity of hydrogen was set equal to oxygen. This eliminates the preferential diffusion effect, and means that the light fuel will not move faster than the other reactant. If the mechanism of instability were preferential diffusion, the lean flame would be stable. This is in fact the result: the lean flame in the calculation with this change of relative diffusivities was stable.

This result supports both the preferential diffusion theory and the diffusional-thermal theory. A further calculation was performed in which the mass diffusivity of oxygen was set equal to that of hydrogen. In this case, the flame was unstable, which disagrees with the prediction of preferential diffusion. However, the diffusional-thermal theory does predict that this flame is unstable. Thus for these hydrogen flames studied, the results agree with the predictions of the diffusional-thermal theory proposed by Barenblatt[6] and Sivashinsky[7].

This series of calculations has also raised a number of computational issues. First, there were limitations on the calculations which it would be interesting to eliminate. We would in fact like the computational domain to be larger with the same or even better resolution. A larger domain would allow the central parts of the calculation to be less influenced by the boundary conditions, and it would be interesting to see if more cells form and how they change in time. It would be useful to redo these calculations with other kinds of perturbation at the front, for example, vary the wavelength of the perturbation. This would be used to address questions such as what is the necessary width of the perturbation relative to the flame thickness to cause the lean flame to go unstable, and what is the effect of long versus short wavelength perturbations on the growth and type of instability that results.

The computations were very expensive. The cost of each one was between four or five hours of CRAY X-MP 2/4 time, which translates to 0.5 ms per pointstep. Because the computations were so expensive, calculations were terminated even though it would have been interesting to follow them longer. For example, we would like to address the question of whether the cellular structure in Fig. 2 will split into more cells. None of the computations were bound by the memory limitation of the computer, but rather were CPU bound, with most of the time spent in integrating the extensive chemical reaction mechanism. One approach we could take, now that we have been able to reproduce the types of results that are observed experimentally,

is to consider a model system with a greatly simplified chemical reaction mechanism. This appears justified for the study of the mechanism of cellular structure because chemistry does not appear to play a major role in the instability. Then the numerical model would be relatively inexpensive to run, and could be used to test selected theoretical concepts much less expensively and perhaps less ambiguously.

There are, however, certain advantages to having the full simulation model. For example, other phenomena we wish to investigate, that occur near the flammability limits, might be very sensitive to the details of the chemical reactions. The mass diffusivities of light intermediate species such as atomic hydrogen might also play a role in determining stability. At this juncture, now that the model exists, it is possible to move in either direction.

Acknowledgements

This work was sponsored by NASA in the Microgravity Science Program, the Office of Naval Research through the Naval Research Laboratory, and the Pittsburgh Supercomputing Center. The authors would like to acknowledge a useful and interesting discussion with Professor C.K. Law.

References

1. Kailasanath, K. and Oran, E. S.: *Prog. Astro. Aero.* **105**, Part 1, 167 (1986).
2. Kailasanath, K. and Oran, E. S.: *Time-Dependent Simulations of Laminar Flames in Hydrogen-Air Mixtures*, Naval Research Laboratory Memorandum Report 5965, 1987.
3. Markstein, G. H.: *J. Aero. Sci.* **3**, 18 (1951).
4. Markstein, G. H.: Non-Steady Flame Propagation, p. 78, Pergamon, 1964.
5. Strehlow, R. A.: Fundamentals of Combustion, p. 221, R.E. Kreiger, 1979.
6. Barenblatt, G. I., Zeldovich, Y. B. and Istratov, A. G.: *Zh. Prikl. Mekh. Tekh. Fiz.* 4, 21 (1962).
7. Sivashinsky, G. I.: *Combust. Sci. Tech.* **15**, 137 (1977).
8. Bregon, B., Gordon, A. S. and Williams, F.A.: *Combust. Flame.* **33**, 33 (1978).
9. Mitani, T. and Williams, F. A.: *Combust. Flame* **39**, 169 (1980).
10. Joulan, G. and Mitani, T.: *Combust. Flame* **40**, 235 (1980).
11. Sivashinsky, G. I.: *SIAM J. Appl. Math.* **39**, 67 (1980).
12. Patnaik, G., Guirguis, R. H., Boris, J. P. and Oran, E. S.: *J. Comput. Phys.* **71**, 1 (1987).
13. Boris, J. P. and Book, D. L.: *Meth. Comput. Phys.* **16**, 85 (1976).
14. Boris, J.P.: *Flux-Corrected Transport Modules for Solving Generalized Continuity Equations*, Naval Research Laboratory Memorandum Report 3237, 1976.
15. Kailasanath, K., Oran, E. S. and Boris, J. P.: *A One-Dimensional Time-Dependent Model for Flame Initiation, Propagation, and Quenching*, Naval Research Laboratory Memorandum Report 4910, 1982.
16. Kee, R. J., Dixon-Lewis, G., Warnatz, J., Coltrin, M.E. and Miller, J. A.: *A FORTRAN Computer Code Package for the Evaluation of Gas-Phase Multi-Component Transport Properties*, Sandia National Laboratories Report SAND86-8246, 1986.
17. Jones, W. W. and Boris, J. P.: *Comp. Chem.* **5**, 139 (1981).
18. Burks, T.L. and Oran, E. S.: *A Computational Study of the Chemical Kinetics of Hydrogen Combustion* Naval Research Laboratory Memorandum Report 4446, 1981.
19. Young, T. R. and Boris, J. P.: *J. Phys. Chem.* **81**, 2424 (1977).
20. Oran, E. S. and Boris, J. P.: Numerical Simulation of Reactive Flow, p. 130, Elsevier, 1987.

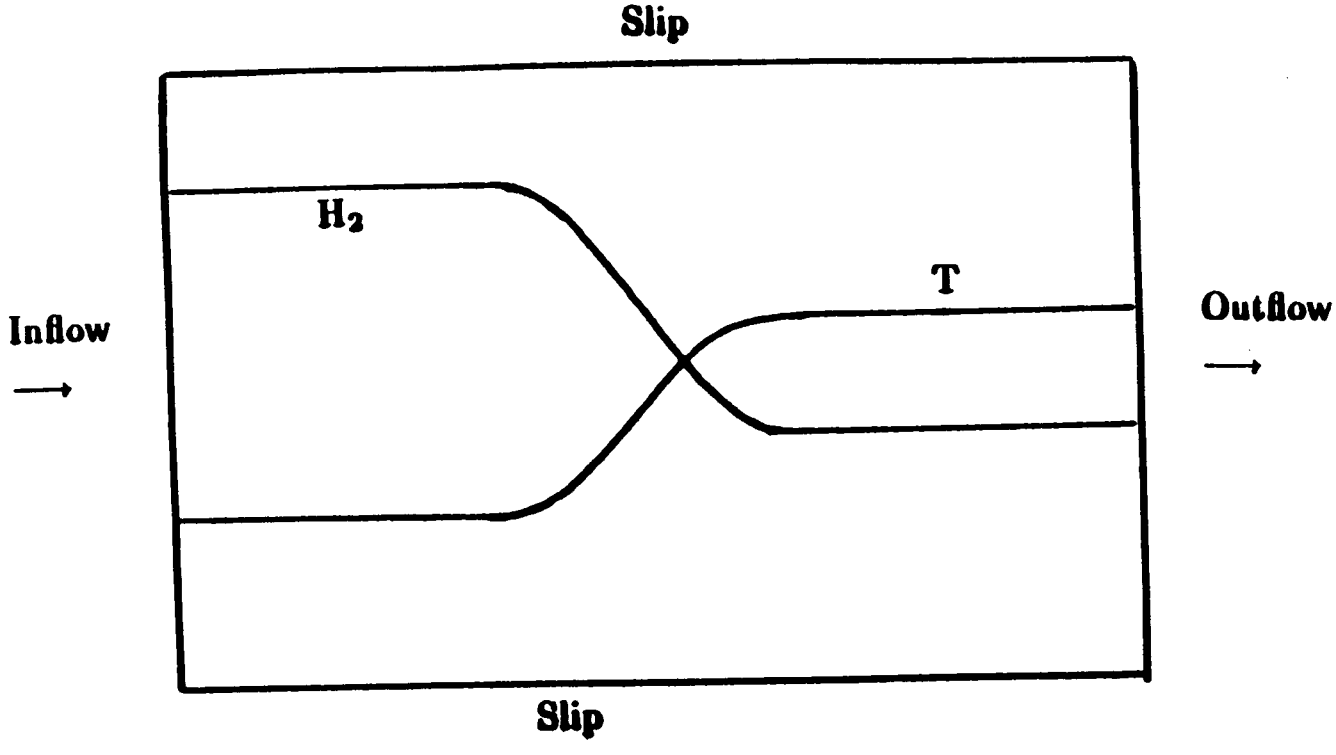

Figure 1. Initial and boundary conditions for the two-dimensional flame calculations.

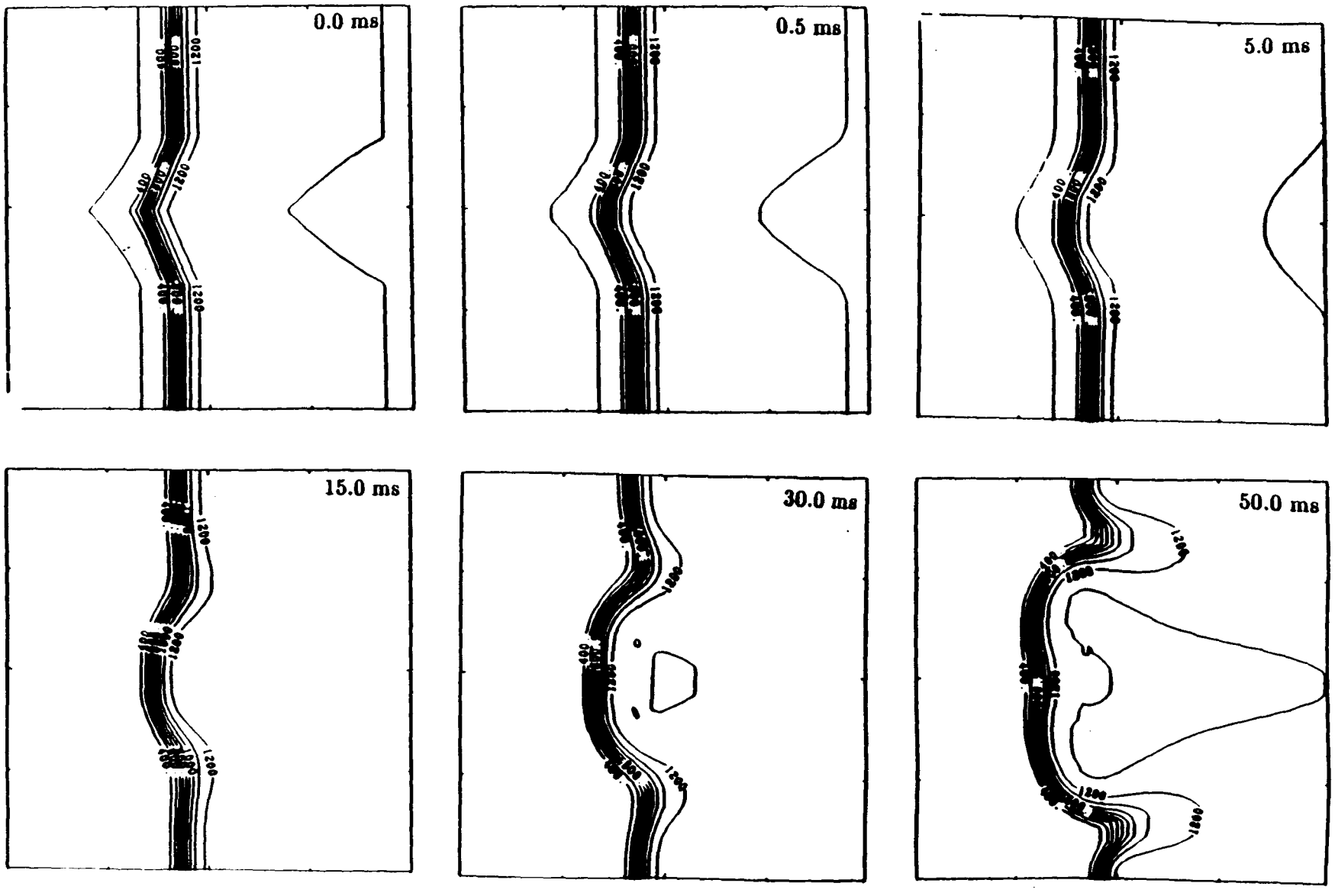

Figure 2. Evolution of isotherms in a fuel-lean hydrogen flame.

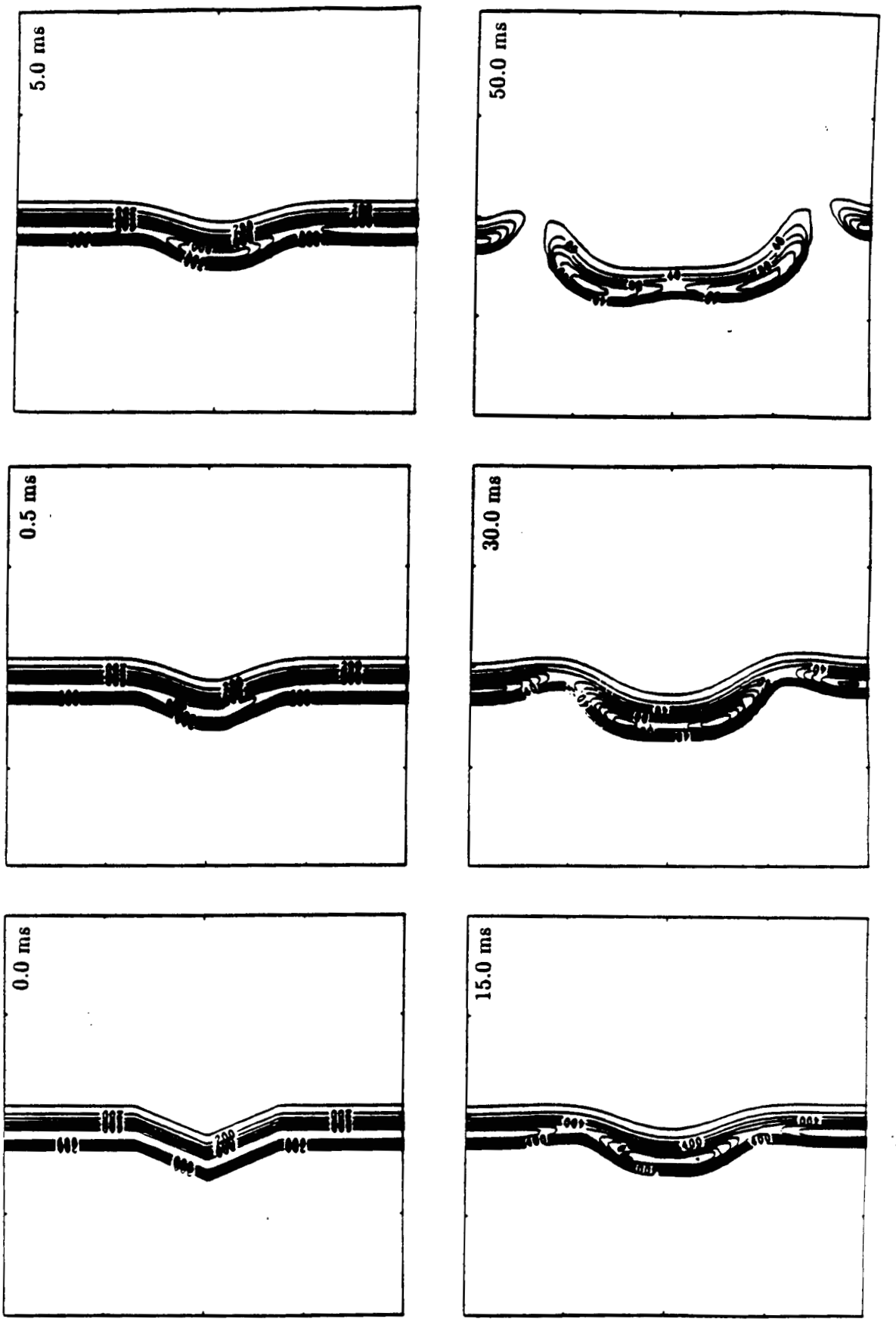

Figure 3. Evolution of hydrogen atom number density contours in a lean flame, values scaled by 10^{-14}.

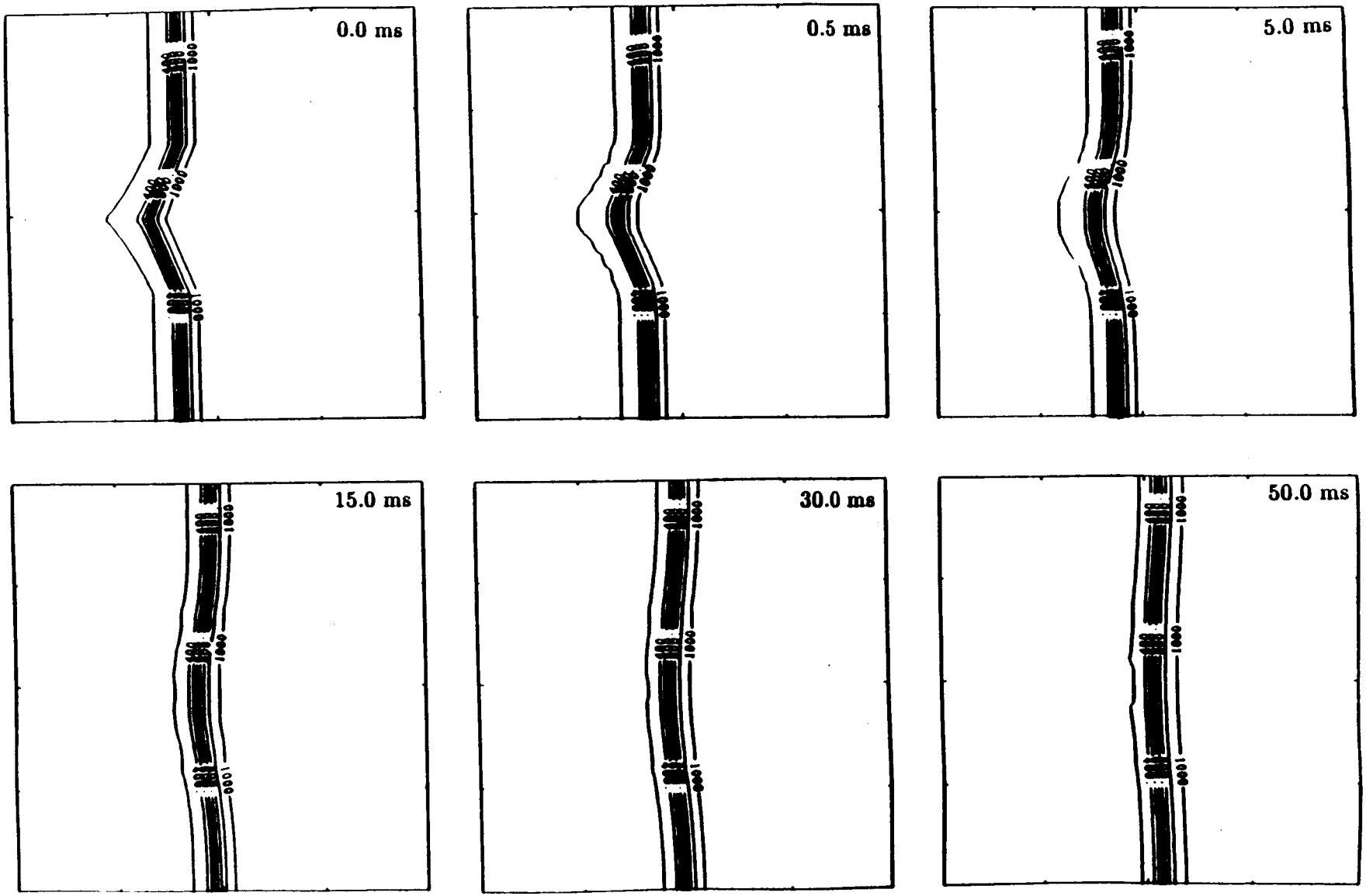

Figure 4. Evolution of isotherms in a fuel-rich hydrogen flame.

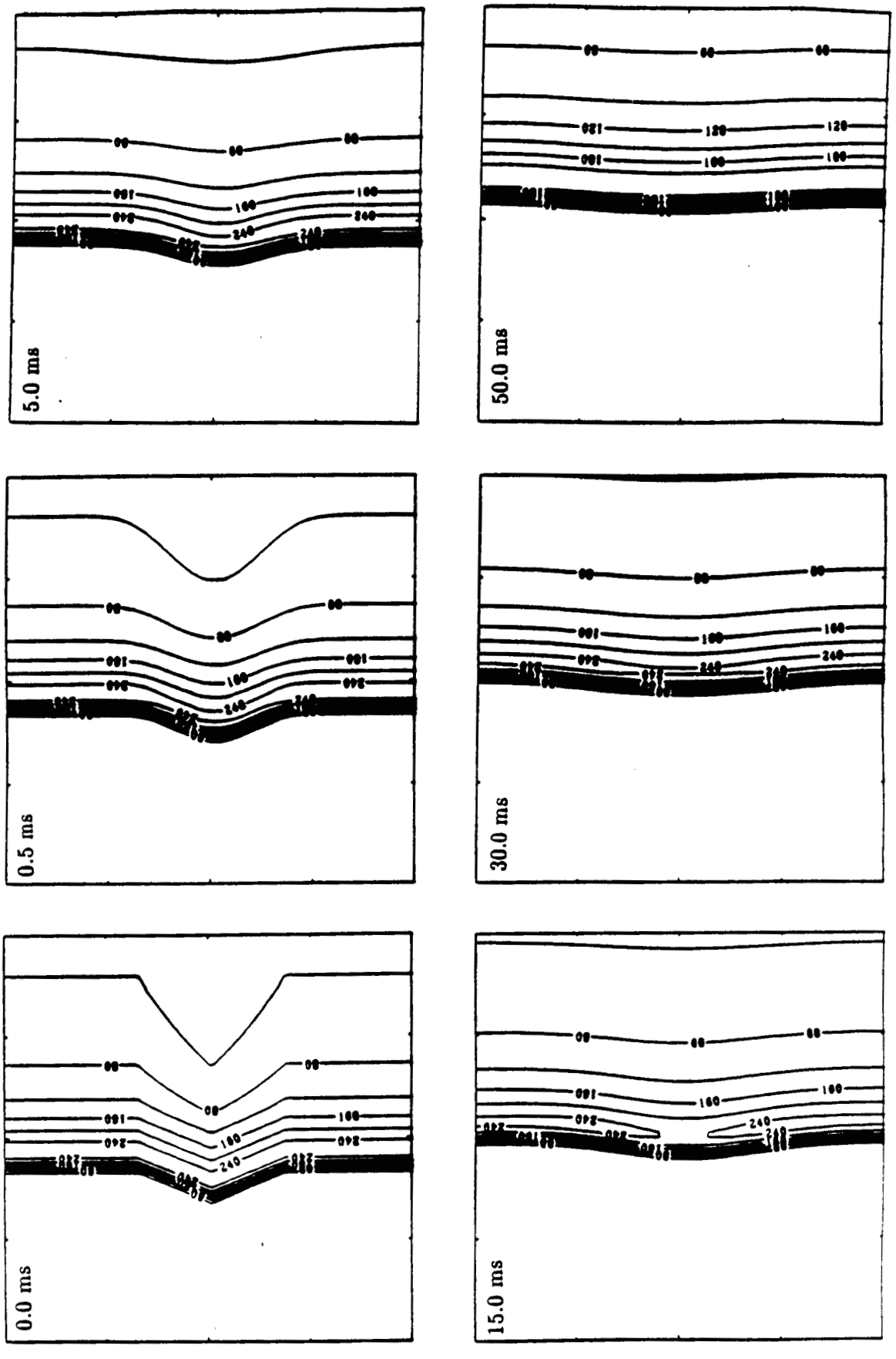

Figure 5. Evolution of hydrogen atom number density contours in a rich flame, values scaled by 10^{-14}.

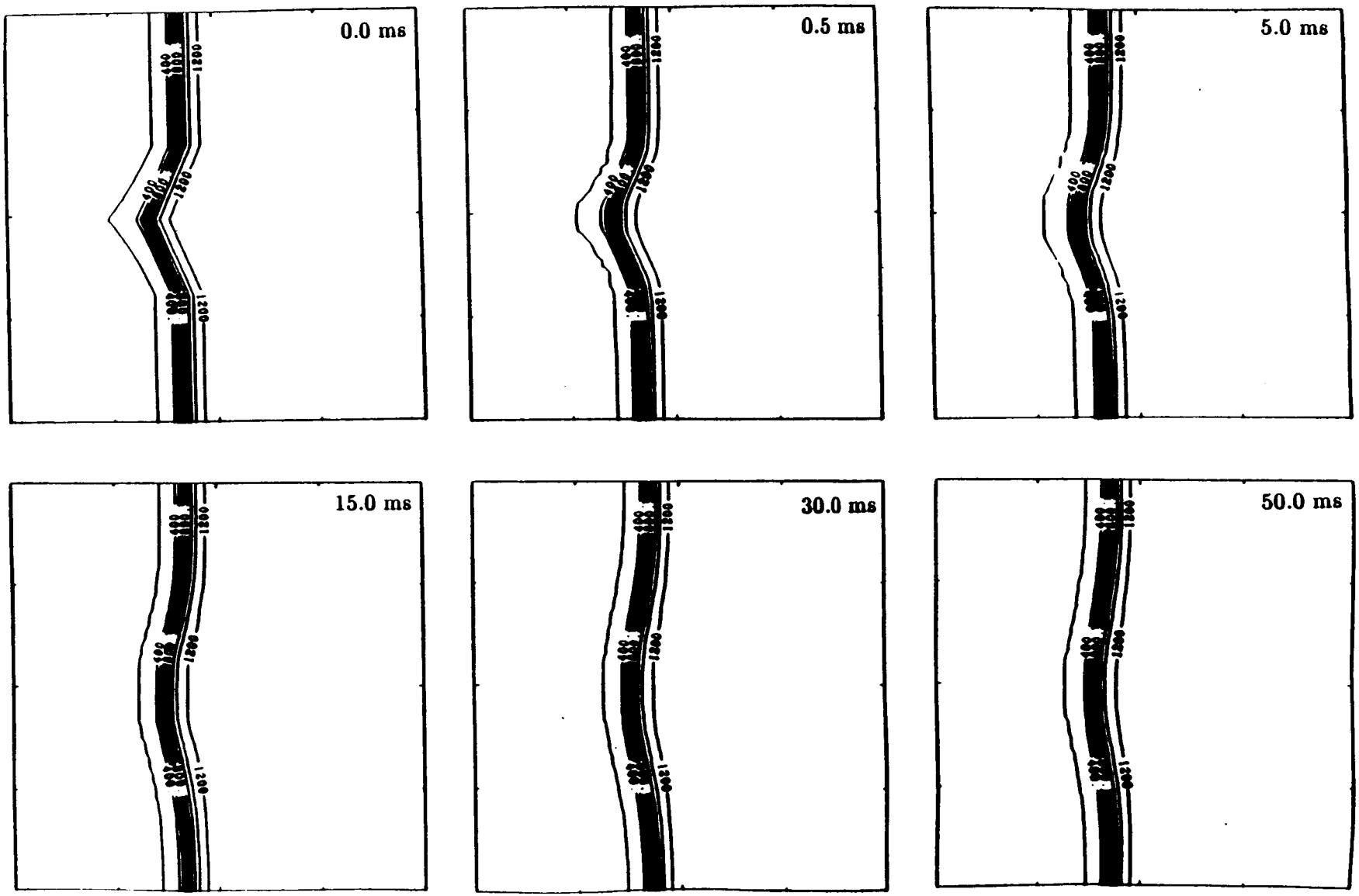

Figure 6. Evolution of isotherms, diffusion coefficients of H_2 equal to O_2.

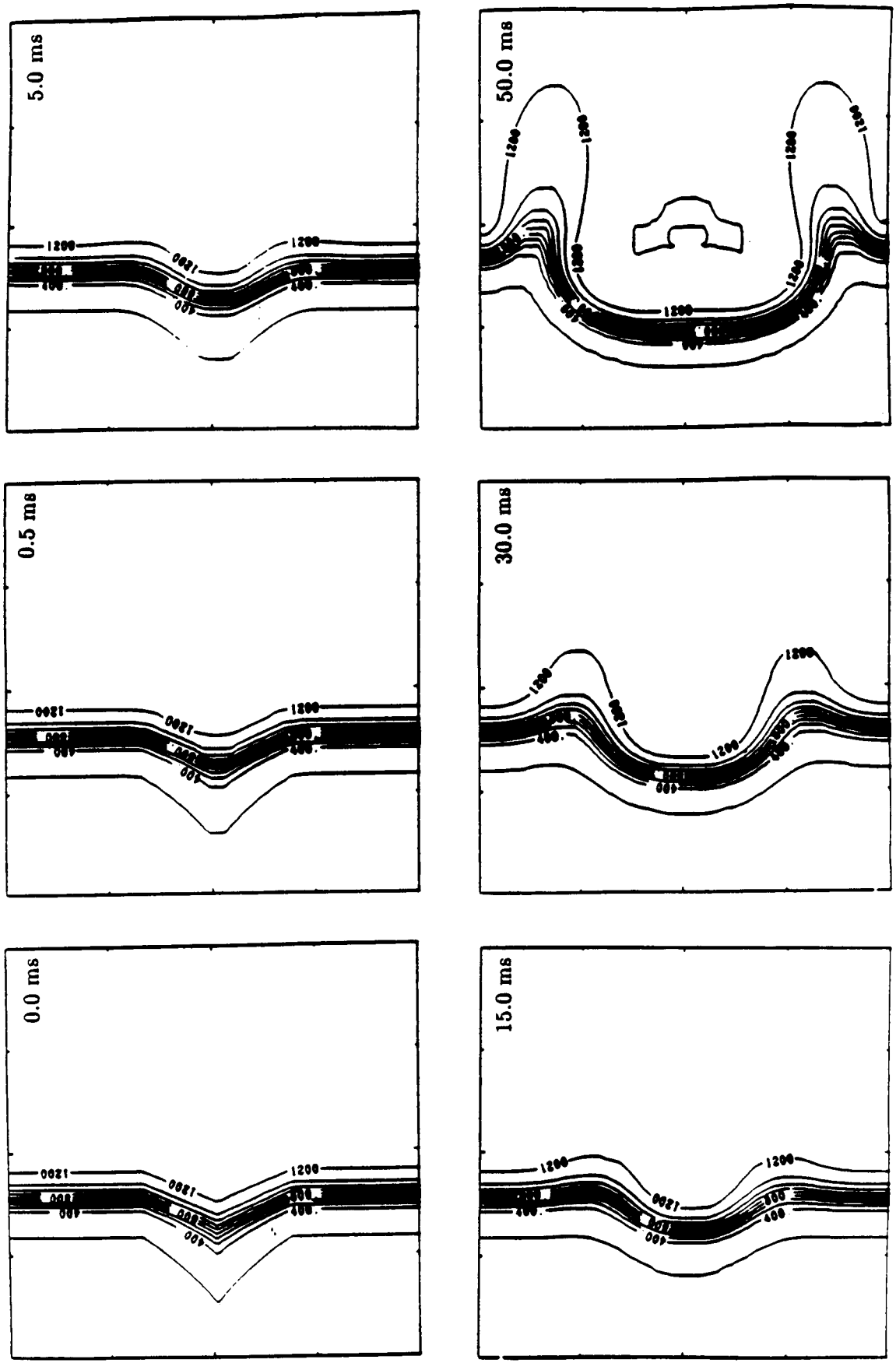

Figure 7. Evolution of isotherms, diffusion coefficients of O_2 equal to H_2.

Appendix E

Effects of Gravity on Multidimensional Flame Structure

NASA
National Aeronautics and Space Administration

Report Documentation Page

1. Report No.	2. Government Accession No.	3. Recipient's Catalog No.
NASA CR-182298		

4. Title and Subtitle
Time-Dependent Computational Studies of Flames in Microgravity

5. Report Date
June 1989

6. Performing Organization Code

7. Author(s)
Elaine S. Oran and K. Kailasanath

8. Performing Organization Report No.
None

10. Work Unit No.
674-22-05

9. Performing Organization Name and Address
The Center for Reactive Flow and Dynamical Systems
The Laboratory for Computational Physics and Fluid Dynamics
Naval Research Laboratory, Code 4410
Washington, D.C. 20375

11. Contract or Grant No.
C-80001-G

13. Type of Report and Period Covered
Contractor Report
Final

12. Sponsoring Agency Name and Address
National Aeronautics and Space Administration
Lewis Research Center
Cleveland, Ohio 44135-3191

14. Sponsoring Agency Code

15. Supplementary Notes

Project Manager, Howard D. Ross, Space Experiments Division, NASA Lewis Research Center. Appendix A—FLIC-A Detailed, Two-Dimensional Flame Model by G. Patnaik, K.J. Laskey, K. Kailasanath, E.S. Oran, and T.A. Brun. Appendix D—Detailed Numerical Simulations of Cellular Flames by G. Patnaik, K. Kilasanath, K.J. Laskey, and E.S. Oran. Appendix E— Effects of Gravity on Multidimensional Flame Structure by K. Kailasanath, G. Patnaik, and E.S. Oran.

16. Abstract

This report describes the research performed at the Center for Reactive Flow and Dynamical Systems in the Laboratory for Computational Physics and Fluid Dynamics, at the Naval Research Laboratory, in support of the NASA Microgravity Science and Applications Program. The primary focus of this research was on investigating fundamental questions concerning the propagation and extinction of premixed flames in Earth gravity and in microgravity environments. Our approach was to use detailed time-dependent, multispecies, numerical models as tools to simulate flames in different gravity environments. The models include a detailed chemical kinetics mechanism consisting of elementary reactions among the eight reactive species involved in hydrogen combustion, coupled to algorithms for convection, thermal conduction, viscosity, molecular and thermal diffusion, and external forces. The external force, gravity, can be put in any direction relative to flame propagation and can have a range of values. A combination of one-dimensional and two-dimensional simulations has been used to investigate the effects of curvature and dilution on ignition and propagation of flames, to help resolve fundamental questions on the existence of flammability limits when there are no external losses or buoyancy forces in the system, to understand the mechanism leading to cellular instability, and to study the effects of gravity on the transition to cellular structure. These studies have shown that a flame in a microgravity environment can be extinguished without external losses and that the mechanism leading to cellular structure is not preferential diffusion but a thermo-diffusive instability. The simulations have also lead to a better understanding of the interactions between buoyancy forces and the processes leading to thermo-diffusive instability. When a flame which exhibits a cellular structure in a zero-gravity environment is subjected to Earth gravity, it evolves into either a bubble rising upwards in a tube or a flame oscillating between convex and concave curvatures in the case of downward propagation. The effect of gravity is minimal on flames in mixtures which are far from flammability limits.

17. Key Words (Suggested by Author(s))	18. Distribution Statement
Microgravity combustion Premixed gas Cellular flames Flammability limits	Unclassified – Unlimited Subject Category 29

19. Security Classif. (of this report)	20. Security Classif. (of this page)	21. No of pages	22. Price*
Unclassified	Unclassified		

*For sale by the National Technical Information Service, Springfield, Virginia 22161